U N I V E R S I T Y O F N A P L E S F E D E R I C O I I

DEPARTMENT OF PHARMACY

Ph.D thesis in

PHARMACEUTICAL SCIENCE

XXX CYCLE 2014 - 2017

Preclinical development of anticancer Ru-based nanoaggregates in breast cancer models

Candidate: Dr Marialuisa Piccolo

Tutor: Prof. Carlo Irace

Coordinator: Prof. Maria Valeria D'Auria

INDEX

ABSTRACT

Cancer, a growing health problem around the world, affects millions of people every year, so that innovative anticancer drugs with specific molecular mechanisms of action are essential in chemotherapeutic treatment to kill specific cancer types, and to overcome toxic side effects as well as chemoresistance. Impaired apoptosis and autophagy seem to play a central role in cancer development and constantly limit the efficacy of conventional cytotoxic therapies. Indeed, current research efforts are focused on a deeper understanding of the cellular response and/or resistance to anticancer treatments, including the role of cell death pathways activation by metallochemotherapeutics such as novel ruthenium-based drugs, proposed as safe and effective potential drugs. Moreover, in the last few years nanostructures have gained considerable interest for the safe delivery of therapeutic agents.

In these fields, we have recently developed a novel approach for the *in vivo* delivery of novel Ru(III) complexes, preparing stable nucleolipidic-based formulations endowed with considerable antiproliferative activity. In particular, aiming at improving the suitability of Ru(III) complexes in biological environment - specifically of AziRu, a pyridine NAMI-A analog - as well as their advantages for biomedical applications, we have designed innovative nanoaggregates by means of high-functionalized nucleolipidic Ru(III) complexes, *ad hoc* mixed with zwitterionic or cationic lipids to provide stable and biocompatible liposome formulations for cancer therapy.

Hence, in line with this project and by *in vitro* bioscreens in the frame of preclinical studies, we have focused on the ability of nucleolipidic ruthenium-containing liposomes to inhibit cancer proliferation in selected human breast cancer models *in vitro*, possibly by predisposing cells to programmed cell death. In the case, breast cancer is the second most common cancer worldwide after lung cancer, the fifth most common cause of cancer death, and the leading cause of cancer death in women. The global weight of breast cancer exceeds all other cancers and the incidence rates of breast cancer are increasing. Luckily, the total survival rates of most cancers have been prolonged due to the energies of both clinicians and scientists. Behind an in-depth microstructural characterization, we have herein

demonstrated that the most efficient ruthenium-containing cationic nanoaggregates we have hitherto developed are able to elicit both extrinsic and intrinsic apoptosis, as well as autophagy. Using especially designed fluorescent formulations and confocal microscopy approaches for targeted studies of intracellular localization, in addition to subcellular fractionation and inductively coupled plasma-mass spectrometry (ICP-MS) to assess cellular accumulation, we have detected, unlike the naked AziRu, a wide both cytosolic and nuclear distribution of the active Ru(III) complex. This would allow the ruthenium to interact with both mitochondrial and nuclear molecular targets, accounting for its ability to inhibit breast cancer cell proliferation by the activation of multiple cell death pathways, possibly *via* mitochondrial perturbations involving Bcl-2 family members, and Ru(III) ions incorporation into double-stranded DNA. To limit chemoresistance and counteract uncontrolled proliferation, multiple cell death pathways activation is a promising strategy for targeted therapy development, especially in aggressive cancer diseases such as triple-negative breast cancer with limited treatment options. The heterogeneity of breast cancers makes them both a fascinating and difficult solid tumour to diagnose and treat. Triple-negative breast cancers in particular are difficult to define lacking Her2 expression, estrogen and progesterone receptor, and do not respond to hormonal therapies or Her2-targeted therapies; hence, new systemic therapies are desperately needed. The oncology community needs for a new dawn of innovative and creative means to overcome these challenges so we can witness further breakthroughs. Moreover, allowing for the importance of the tumour microenvironment as well as of the stromal components playing both critical role in the tumourigenic process, the function of cancer-associated immune cell system and their cellular secrets were also investigated, in order to achieve a deeper understanding of the typical molecular pathways involved in the cross-talk between tumour components and stromal cells; this would allow to properly act on tumour microenvironment in order to further improve the efficacy of chemotherapy. In this case, the EPO/ESA treatment – commonly used in therapy for anaemia – can induce tumour progression and growth, because of its impact on the anti-cancer immune response.

So overall these outcomes discharge original knowledge in the field of anticancer therapy and on ruthenium-based candidate drugs, thus providing new insights for future optimized cancer treatment protocols.

TUMOUR AND NEW THERAPEUTIC PERSPECTIVES

1.1 Cancer: incidence and mortality patterns

The term “cancer” indicates a group of diseases where abnormal cells divide without control and can invade neighboring tissues. Cancer cells can also spread to other parts of the body through the blood and lymphoma system.

Cancer is an important condition, both in terms of the number of people affected and of the impacts on those people and people close to them. Millions new cancers are diagnosed annually worldwide, across over a lot of different cancer types. Each of these cancer types has different presenting features, though there may be overlap. Although there have been large advances in treatment and survival, with a half of cancer sufferers now living at least ten years after diagnosis, it remains the case that more than a quarter of all people alive now will die of cancer.

Based on the EUCAN estimates (Foucher et al., 2014), more than 3.4 million new cases of cancer (excluding non-melanoma skin cancer) were diagnosed in Europe in 2012; almost 80% of them in the European Union. The most common cancers were those of breast, large bowel, prostate and lung, all of which represented more than 1.7 million cases annually. The cancer with the largest number of incident and prevalent cases was breast cancer (464,000 cases), while by far the largest number of deaths was due to lung cancer (353,000 deaths) (Ferlay et al., 2012).

For women, there was a clear southeast-northwest gradient in incidence of all cancers (Figure 1) with the highest incidence in Denmark (European age-standardized rate, ASR(E) 454 per 100,000) and the lowest in Greece (ASR(E) 192 per 100,000). There was a similar but less consistent pattern for males (Figure 2) with the highest incidence in France (ASR(E) 551 per 100,000) and the lowest in Bosnia-Herzegovina (ASR(E) 254 per 100,000). A comprehensive overview of cancer patterns in Europe is provided elsewhere.

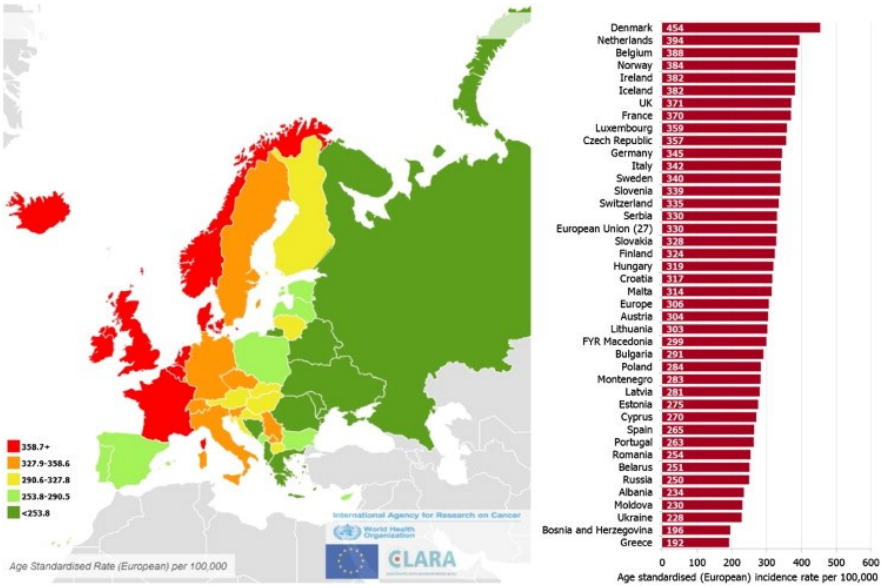

Figure 1. Estimated incidence of all cancers excluding non-melanoma skin, females, Europe 2012 (Ferlay et al., 2012).

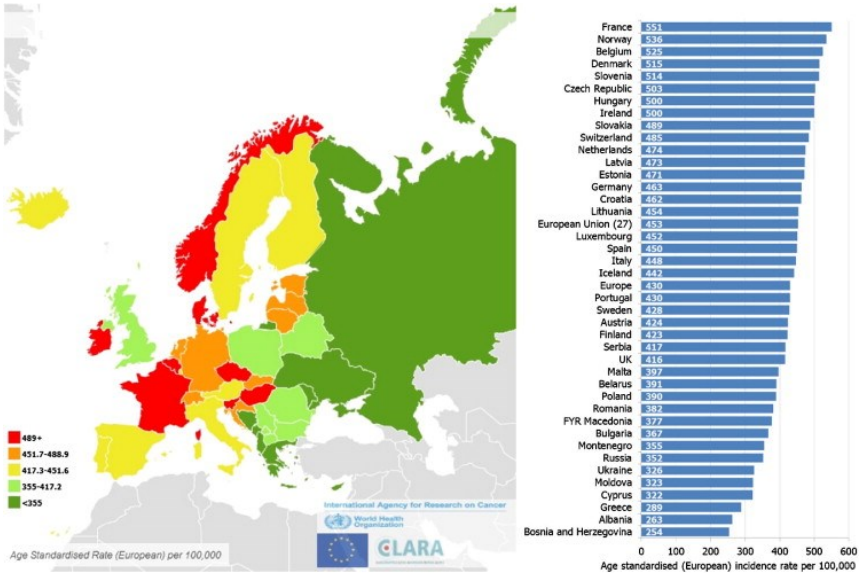

Figure 2. Estimated incidence of all cancers excluding non-melanoma skin, males, Europe 2012 (Ferlay et al., 2012).

1.2 Most common therapeutic approaches

The "surgery therapy" is the oldest and most effective strategy to eradicate the tumour, but its limits were clear in view of the small size of the tumour and its inaccessibility, or the extent of invasion, the presence of metastasis and, above all, the involvement of important organism structures (such as vases and nerves). Also, the radiation therapy is more efficient if the tumour is not largely diffused. Often it is used in combination with chemotherapy and/ or surgery.

A more recent approach is the Immunotherapy, which consists in stimulating the immune sistem by administering a vaccine containing an antigen derived from tumours able to stimulate the production of antibodies or by direct somministration of antibodies monoclonal cells directed towards a precise type of tumour antigen.

The use of chemotherapeutic agents is certainly the most widely used approach to reduce metastases as well as primary tumour, which is particularly important since the mortality of cancer patients is often attributable to the proliferation of metastases rather than the development of the primary tumour.

In fact, if this can be surgically removed, drug therapy is the only choice for the treatment of metastases, which often develop before the tumour is diagnosed.

It has spread from the second half of the twentieth century when research has led to the creation of a wide range of drugs that block tumour cell DNA replication by various mechanisms of action such as DNA alkylating agents to form a covalent bond with the purine or pyrimidine bases of the DNA), antimetabolites (such as folic acid analogs, pyrimidine analogs and purine analogs), antimitotes, blocking the cell division phase, topoisomerase inhibitors.

1.3 Breast cancer: clinical classification and standard of care

Breast cancer is the most common type of diagnosed malignancy and the second leading cause of cancer death in women worldwide (Ferlay et al., 2015). Nowadays, most breast cancers are diagnosed early enough to be successfully treated with surgery, chemotherapy, radiotherapy, or a combination thereof. However, despite the success of screening programs and the development of adjuvant therapies, a significant percentage of breast cancer patients will suffer a metastatic disease that, to this day, remains incurable and justifies the search of new therapeutic strategies. Among the new therapies that have been developed in recent years, the emergence of targeted therapies has been a milestone in the fight against cancer (García-Aranda and Redondo, 2017).

Clinically, breast cancer can be divided into distinct subtypes that have prognostic and therapeutic implications. Thanks to the deep sequencing of breast cancer genome and transcriptome, this heterogeneous disease has been classified into four major molecular subtypes of invasive breast cancer (HER2-enriched, luminal A, luminal B and basal-like) (Tamimi et al., 2012), with different prognosis and treatment response (Miller et al., 2017; Tamimi et al., 2012; García-Aranda and Redondo, 2017).

- HER2-Enriched

Human epidermal growth factor receptor 2 (HER2)-enriched mammary tumors have been extensively studied and are well described. Together with HER1 (EGFR/ErbB-1), HER3 (ErbB-3), and HER4 (ErbB-4), HER2 (ErbB2/neu) is a member of the ErbB membrane tyrosine kinase receptors family, closely related to the transcription of signaling pathways leading to cell proliferation, differentiation and inhibition of apoptosis pathways (Segovia-Mendoza et al., 2015). HER2 is constitutively activated in approximately 20-30% of breast cancers (Segovia-Mendoza et al., 2015). Given that HER2 overexpression is widely known to dysregulate cell proliferation in the aggressive HER2-positive breast cancers, this

protein represents an important therapeutic target for patients with this breast cancer subtype. Moreover, knowing that the presence of tumour-infiltrating lymphocytes was associated with favorable outcomes in HER2-positive and triple-negative breast cancer, immunotherapy (with immune checkpoint blockade) induced long-lasting responses and improved survival in hard-to-treat malignancies (ie, melanoma and non-small cell lung cancer), changing treatment paradigms in a variety of neoplastic diseases (Lambertini et al., 2017).

The approved therapy is the humanized monoclonal antibody trastuzumab (Herceptin) that is able to blocks the extracellular domain of HER2. Although trastuzumab has dramatically improved the outcome for patients with this type of cancer, appearance of resistance is a frequent problem that has motivated the search of alternative therapies targeting this tyrosine kinase receptor. In this context, small kinase inhibitors like lapatinib/Tykeb, neratinib (Prove et al., 2016), gefitinib (Segovia-Mendoza et al., 2015), or afatinib (Zhang et al., 2014), have shown preclinical and clinical evidence in the treatment of HER2-enriched tumors.

However, identification of patients who are most likely to benefit from immune checkpoint blockade remains challenging, with many patients not responding to treatments and a significant financial cost. The combination of immune checkpoint blockade with conventional cancer treatments such as chemotherapy, radiotherapy, targeted therapies or with other immunotherapies is a promising strategy to potentiate its efficacy in breast cancer although further research is required to effectively identify who will respond to these immunotherapies (Solinas et al., 2017).

- Hormone Receptor Positive (Luminal-A, Luminal-B)

Both luminal-A and luminal-B breast cancer subtypes, which account for up to 75% of breast tumor cases (Zhang et al., 2015), are hormone receptor-positive (HR-positive), and,

therefore, they express estrogen receptors (ER), progesterone receptors (PR), and/or estrogen-responsive and ER-dependent gene products (Chang et al., 2012). As the estrogen hormone (17 β-estradiol) plays an important role during different hallmarks of cancer, luminal-A and luminal-B breast carcinomas are, theoretically, sensitive to hormone-targeted treatments. Indeed, Tamoxifen (TMX, Nolvadex) is the most common drug used in clinical practice over the past decades as first-line treatment in pre- and post-menopausal women with ER-positive breast cancer (Carlson et al., 2003). However, although this competitive ER-receptor antagonist has shown a significant reduction of reappearance (40–50%), and the risk of death from breast cancer (30–35%), the existence of an important number of cases with natural or acquired resistance to tamoxifen along with long-term toxicities has motivated the search for new approaches for HER2-enriched breast cancer patients (García-Aranda and Redondo, 2017).

- Basal-Like

Basal-like breast tumors are characterized by a gene-expression profile similar to that of the basal-myoepithelial layer of the normal breast along, with the absence of HER2 overexpression and the absence or low levels of estrogen receptor expression (Foulkes et al., 2010). The triple negative breast cancer (TNBC) subtype, which constitutes approximately 80% of the basal-like tumors, accounts for approximately 10–15% of breast carcinomas, and is characterized by the lack of expression of both hormone receptors (estrogen and progesterone) and HER2-receptor over-expression (Dawood et al., 2010). For these reasons, both TNBC and basal-like breast cancers usually lead to an aggressive disease, with a high probability of metastasis (Foulkes et al., 2010), and with poor prognosis, which is due, in part, to the absence of an existing effective targeted therapy (García-Aranda and Redondo, 2017).

1.4 Several types of cell death induced by chemotherapeutics

Cell death is the last fate of the life cycle of cells. In physiological condition, such as during development, accurate patterns of cell death determine the size and shape of limbs and other tissues (Ngabire and Kim, 2017). Cells can also die when they become damage or infected. In these and many other cases - in particular for cancer cells - cell death is not a random process but occurs by a programmed sequence of molecular events, in which the cell systematically destroys itself from within and is then eaten by other cells, without trace. Different pathways involved in cell death are known to date, and are mostly represented by apoptosis, autophagy and necrosis. Cells dying by apoptosis undergo characteristic morphological changes, such as shrinkage and condensation, cytoskeleton shock, the disassembling of nuclear envelope as well as condensation of nuclear chromatin. In this way, and also for the autophagy pathway, the cell dies neatly and is rapidly cleared away, without causing a damaging inflammatory response. In contrast, necrotic cells swell and burst, spilling their contents over their neighbors and eliciting an inflammatory response.

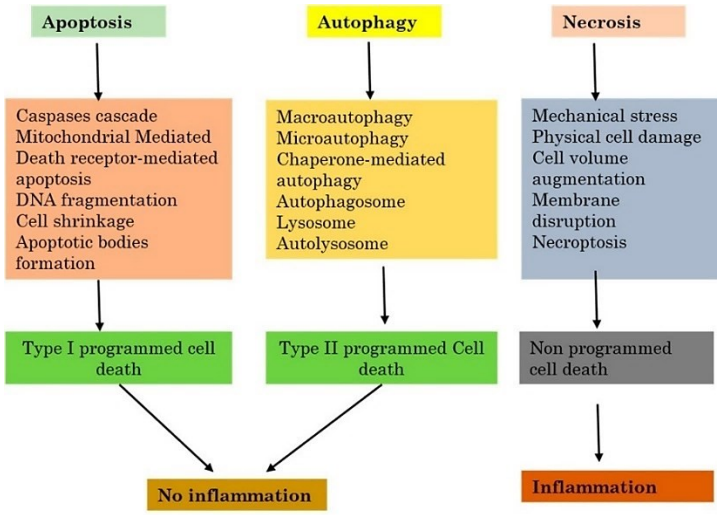

Figure 3. The three major cell death pathways. (Ngabire and Kim, 2017)

1.4.1 Necrosis

Necrosis regroups a considerable variety of cell death pathways that share their loss of physiological structure of the cellular cytoplasmic membrane to which follows the dispersion of cytoplasmic elements. It can arise as a result of many events that affect cellular homeostasis or repeated extensive damage and both will cause cell death with loss of cellular integrity. Some examples are high temperature, repeated freeze/thaw series, or during other stressful situations. In these cases, necrosis can be considered as a passive process because there is not activation of specific pathways of proteins. Cytoplasmic cell membrane rupture may also be considered in the late steps of apoptotic or autophagic deaths, especially when phagocytosis does not suppress dead cell from circulation. As no signaling pathway is here implicated, it is mainly called secondary necrosis, to differentiate it from other programmed deaths such as apoptosis, necroptosis or autophagy. Necrosis is not entirely a result of pure risk or passive processes, since it can group well-organized successive events (Ngabire and Kim, 2017). In most cases, necrosis is linkely to be caused by energy depletion, which leads to metabolic defects and loss of the ionic gradients that normally exist across the cell membrane. One form of necrosis, called “necroptosis” (Yuan and Kroemer, 2010), is a form of programmed cell death that is triggered by a specific regulatory signal from other cells and dependent on a receptor-interacting protein kinase (RIP). This process demands the kinase activity of RIP3, and can lead to a quick cell death with characteristics specific to necrosis (Towers and Thorburn, 2016).

1.4.2 Apoptosis

The process of programmed cell death, or apoptosis, is generally characterized by distinct morphological characteristics and energy-dependent biochemical mechanisms. It is considered a vital factor of several processes including normal cell turnover, correct development and functioning of the immune system, hormone-dependent atrophy, embryonic development and chemical-induced cell death. While inappropriate apoptosis, is a factor in many human conditions including neurodegenerative diseases, autoimmune disorders, ischemic damage as well as different types of tumour, where it is a mechanism typically dysregulated.

Apoptosis is triggered by members of a specialized intracellular family proteases, which cleave specific sequences in numerous proteins inside the cell. These proteases, called caspases, have a cysteine residue at their active site and cleave their target proteins at specific aspartic acids residues. Caspases are synthetized in the cell as inactive precursors and are activated only during apoptosis. There are three major classes of apoptotic caspases: initiator caspases (caspase-2, -8, -9, -10), effectors or executioner caspases (caspase-3, -6, -7) and inflammatory caspases (caspase-1, -4, -5) (Cohen, 1997; Rai et al., 2005). Initiator caspases, as their name implies, begin the apoptotic process. In fact, an apoptotic signal causes the assembly of large protein platforms that bring multiple initiator caspases together into large complexes. Within these complexes, pairs of caspases associated to form dimers, resulting in protease activation. The principal role of the initiator caspases is the activation of the executioner caspases. As the former ones, also these latter ones exist as inactive dimers which rearrange to an active conformation after cleavage. One initiator caspase complex can activate many executioner caspases resulting in an amplifying proteolytic cascade. To date, research indicates that there are two main apoptotic pathways: the extrinsic - or death receptor pathway - and the intrinsic - or mitochondrial pathway (Elmore, 2007).

Furthermore, there is now clear evidence that the two pathways are linked and that molecules in one pathway can influence the other (Igney and Krammer, 2002).

The intrinsic pathway is activated by a numerous of stress signals, such as DNA damage caused by chemo- and radiotherapies. Upon cellular stresses, a signal is transmitted to the mitochondria, leading to the mitochondrial outer membrane permeabilization (MOMP) and the release of apoptotic proteins. This crucial event in the intrinsic apoptosis pathway, is controlled by B cell lymphoma 2 (Bcl-2) family proapoptotic effector proteins Bax and Bak, which are activated by proapoptotic BH3-only Bcl-2 family proteins and antagonized by antiapoptotic Bcl-2 family proteins (i.e., Bcl-2, Bcl-XL, Bcl-B).

Moreover, recent studies suggested the presence of an additional pathway that implies T-cell mediated cytotoxicity and perforin-granzyme-dependent killing of the cell (Figure 4) (Elmore, 2007).

All the pathways converge on the same execution pathway. This pathway starts by the cleavage of caspase-3 and ends in several events, such as DNA fragmentation, degradation of cytoskeletal and nuclear proteins, cross-linking of proteins, formation of apoptotic bodies, expression of ligands for phagocytic cell receptors and finally uptake by phagocytic cells. However, the granzyme A pathway can activate a parallel, caspase-independent cell death pathway via single stranded DNA damage (Martinvalet et al., 2005).

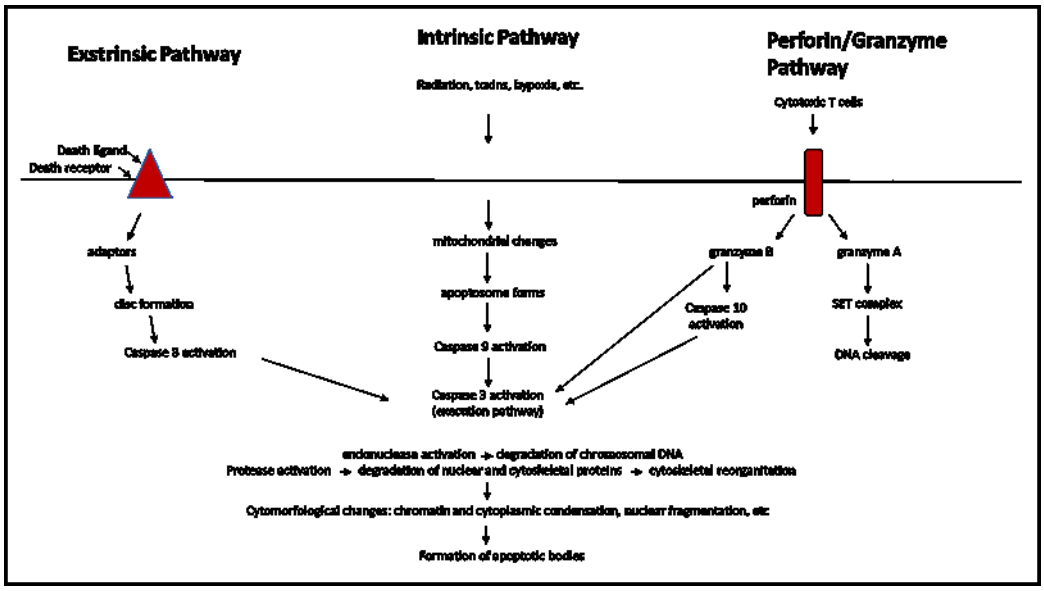

Figure 4. Schematic illustration of apoptotic events. The two main pathways of apoptosis are extrinsic and intrinsic as well as a perforin/granzyme pathway. Each requires specific triggering signals to begin an energy-dependent cascade of molecular events. Each pathway activates its own initiator caspase (8, 9, 10) which in turn will activate the executioner caspase-3. However, granzyme A works in a caspase-independent fashion. The execution pathway results in characteristic cytomorphological features including cell shrinkage, chromatin condensation, formation of cytoplasmic blebs and apoptotic bodies and finally phagocytosis of the apoptotic bodies by adjacent parenchymal cells, neoplastic cells or macrophages (Elmore, 2007).

Dysfunction of apoptosis pathways can confer cancer-treatment resistance, as most conventional chemotherapies as well as radiotherapy depend on their ability to provoke apoptotic cell death in cancer cells. Therefore, apoptosis pathways can be therapeutically exploited for cancer treatment.

Apoptosis is tightly regulated by the balance between pro- and anti-apoptotic proteins and becomes dysregulated when the balance between pro- and antiapoptotic proteins is altered. In human cancers, overexpression of antiapoptotic proteins is frequently observed and has been linked to tumour progression, treatment resistance, and poor prognosis. Therefore, targeting antiapoptotic proteins with the goal to recreate the apoptotic response has been considered as a promising cancer therapeutic strategy in the past decade (Bai and Wang, 2013).

1.4.3 Autophagy

Autophagy is an evolutionarily conserved lysosomal pathway involved in the turnover of long-lived proteins and organelles (Klionsky and Ohsumi, 1999; Meijer and Codogno, 2004). To date, three forms of autophagy are known—chaperone-mediated autophagy, microautophagy, and macroautophagy (Ngabire and Kim, 2017). The latter one is the most referred to when autophagy is mentioned. Both differ from each other due to their initiation, the mechanisms involved and the mode of destruction during delivery to the lysosome. Autophagy is one of the most preserved cell death pathways, characterized by the elimination of large parts of cytoplasmic components after being consumed by a multilayer-membrane-bound vesicle called an autophagosome. The autophagosomal membrane is derived from a pre-autophagosomal structure of uncertain origin (Mizushima et al., 2011; Mizushima and Komatsu, 2011). In mammalian cells, a structure called the phagophore contributes to the formation of the autophagosome (Fengsrud et al., 1995). A first step towards the formation of the autophagosome is the expansion of the pre-autophagosomal membrane. This step is dependent upon signaling molecules that modulate the activity and the expression of some “autophagy genes”. About cellular homeostasis, autophagy plays a dual role promoting both cell survival and cell death (Kang et al., 2007). Furthermore, in cancer cells, autophagy plays a major role -triggered in response to cellular stress, such as nutrient and growth factor starvation or hypoxia - acting as either tumour suppressor or tumour promoter (Kang et al., 2007). Such diverse role of autophagy largely depends on the type and genetic background of cancer cells (Elmore, 2007). In the tumour microenvironment, it is able to regulate the differentiation of macrophages into tumour-associated macrophages (TAMs) and fibroblasts into cancer-associated fibroblasts (CAFs), the most abundantly components present in the tumour microenvironment.

Although autophagy is linked to multiple cancer-related pathways, the most relevant and best studied is phosphatidylinositol 3-kinase/protein kinase B/mammalian target of rapamycin (PI3kinase/Akt/mTOR) signaling pathway. In fact, this signaling pathway plays a major role in transmitting autophagic stimuli because of its ability to sense nutrient, metabolic and hormonal signals. In addition, autophagy, just because characterized by a flux of membrane from the formation of the autophagosome to the fusion with the lysosome, is regulated by GTPases, similarly to the vesicular transport along the exocytic/endocytic pathway (Meijer and Codogno, 2004).

Microtubule-associated protein 1A/1B-light chain 3 (LC3) is a soluble protein, distributed ubiquitously in mammalian tissues and cultured cells, that plays an important role in the autophagy process. During autophagy, autophagosomes engulf cytoplasmic components, including cytosolic proteins and organelles. Concomitantly, a cytosolic form of LC3 (LC3-I) is conjugated to phosphatidylethanolamine (PE) to form LC3-phosphatidylethanolamine conjugate (LC3-II), which is recruited to autophagosomal membranes. This newly formed complex, LC3-II, is very important for the fusion of autophagosomes with lysosomes. As soon as this step is terminated, the autophagosome fuses with lysosomes, and from the fusion, will result in one double membrane vesicle called autolysosome. Simultaneously, LC3-II in autolysosomal lumen is degraded. Thus, lysosomal turnover of the autophagosomal marker LC3-II reflects starvation-induced autophagic activity, and detecting LC3 by immunoblotting or immunofluorescence has become a reliable method for monitoring autophagy and autophagy-related processes, including autophagic cell death (Tanida et al., 2008).

Inadequate autophagy can be deleterious, as can be exorbitant activation, therefore autophagy in a cell must be strictly controlled. The induction together with the regulation of

autophagy has been well investigated, mostly in yeast, in mammalian cells, and in Drosophila. The formation and maturation of the autophagosome in the cytoplasm are controlled and regulated by a set of multiple proteins both related to autophagy (ATG proteins) (Figure 5). The preinitiation complex is formed first, and is made of different proteins (such as ULK1, FIP200 protein, and ATG13). Two major proteins regulate this complex: the mammalian target of rapamycin complex 1 (mTORC1) from the PI3k-Akt pathway which inhibits autophagy, and adenosine monophosphate (AMP)-activated protein kinase (AMPK) that inhibits mammalian target of rapamycin complex 1 (mTORC1) (Kim et al., 2011). This step marks the autophagy initiation phase. When ATP molecules are being consumed and not successfully replaced, AMP together with adenosine diphosphate (ADP) accumulate and activate AMPK. The activated AMPK initiates indirectly autophagy by suppressing the activity of mTORC1. Thus, the preinitiation complex plays a major role in the inhibition of mTORC1 and/or activation of AMPK. The preinitiation complex attracts and then activates another initiative complex with Beclin-1, a protein in the class III PI3K (Vps34), and a kinase protein Vps15. In addition, Beclin-1 is confined by antiapoptotic proteins like Bcl2 and Bcl-XL (Luo et al., 2010), and therefore inhibits the activity of the initiation complex.

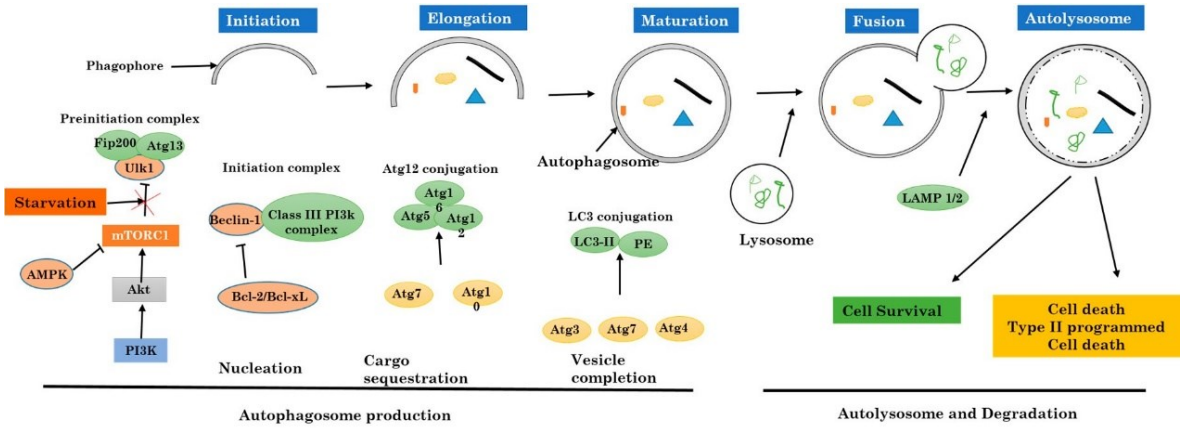

Figure 5. Activation and regulation of autophagy (Ngabire and Kim, 2017).

1.4.3.a) Apoptosis and autophagy: their molecular crosstalk

Apoptosis and autophagy are in a complex crosstalk sharing molecular components that directly regulate them and can be triggered by common upstream signals (Fimia and Piacentini, 2010). Both processes can either induce cell death in a coordinated manner, or the cell can switch between the two responses in a mutually exclusive way. Consequently, autophagy can antagonize apoptotic cell death by promoting cell survival, and apoptosis-associated caspase activation can disrupt the autophagic process. Understanding the interplay between these key processes in cancer and other diseases is fundamental for the development of successful therapy. In fact, the manipulation of autophagy for therapeutic purposes is crucial to recognize its role in both cytoprotection and cytotoxicity, since interfering with one type of cell death may activate another cell-damaging pathway.

1.5 Anticancer metal-based therapy: ruthenium complexes as a new class of chemotherapeutics

In recent years, research efforts are focused on a deeper investigate and development of antineoplastic agents. Among these, metallodrugs represent a very important class of chemotherapeutics, exhibiting a wide range of interesting biological activities (McQuitty, 2014).

Cisplatin and its analogues have hitherto dominated the field of metal-based compounds endowed with high importance in cancer treatment, so that platinum-based drugs are currently the most widely used chemotherapeutics (Petrelli et al., 2016). Activation of cellular apoptosis caused by DNA targeting seems to be the most factor in causing bioactivity of cisplatin and its derivatives (Dasari and Tchounwou, 2014). Thanks to the evident clinical applications of these platinum-based drugs, in the field of inorganic biochemistry the number of researches to find other metallodrugs - that can be used for cancer therapy - has significantly increased. Although anticancer platinum compounds continue to be designed and synthesized through numerous different approaches in order to improve the therapeutic effects as well as to overcome their limitations, the use of transition metal compounds different to platinum has also attracted attention (Komeda and Casini, 2012). In particular, ruthenium-based drugs have attracted great interest due to their lower toxicity, often associated with the ability to overcome the resistance encountered with platinum drugs. In fact, they possess several favorable chemical properties marking them as strong antitumour candidates in a rational drug discovery approach (Mühlgassner et al., 2012). The major advantages of ruthenium complexes are related to their peculiar features, as for example: i) the facility to exchange O- with N-donor ligands similarly to platinum-based drugs; ii) their octahedral geometry, which offers unique possibilities for the binding to nucleic acids; iii) the high versatility in terms of oxidation states, including II, III and

perhaps IV in the biological fluids; iv) the possibility to be transformed into poorly reactive prodrugs, with the ruthenium ion in the +3 oxidation state that can be reduced, and thus activated, selectively in solid tumour masses as a result of their low oxygen content (Mazuryk et al., 2012).

Since the early 80's, Alessio, Sava and co-workers have been pioneers in studying transition-metal complexes in a biomedical perspective as potential anticancer agents, developing, among others, the very active Ru(III) complex ImH^+ [*trans*-$RuCl_4(DMSO)Im^-$] called NAMI-A (Sava et al., 2002; Rademaker-Lakhai et al., 2004). This compound, with indazolium *trans*-[tetrachlorobis(1H-indazole)ruthenate(III)] (KP1019) and [Ru(η^6-p-cymene)Cl_2(pta)](pta is 1,3,5-triaza-7-phosphaadamantane) (RAPTA-C), successfully completed phase I, has been introduced into advanced clinical trials currently (Sava et al., 1999; Hartinger et al., 2008; Berndsen et al., 2017). Despite of their structural similarities (Figure 6), these Ru derivatives exhibit distinctly different anticancer effects (Frasca et al., 1996; Mazuryk et al., 2012). In fact, while NAMI-A shows a remarkable and selective activity against cancer metastases, mostly of solid lung tumours, KP1019 present a high cytotoxic effect on primary cancers (Kapitza et al., 2005).

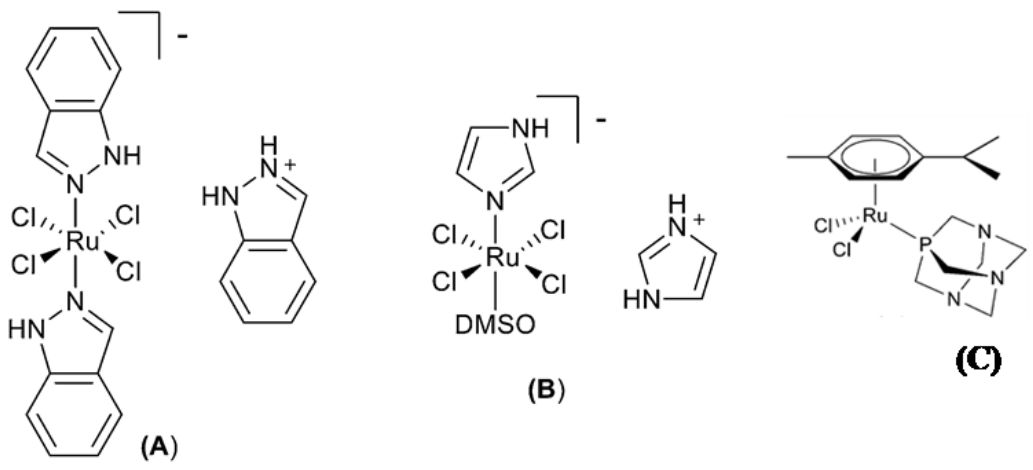

Figure 6. Molecular structure of KP1019 (A), NAMI-A (B) and RAPTA-C (C) (Ranier et al., 2017).

Similar to KP1019 and NAMI-A, which are both based on a Ru III ion, the Ru II complex RAPTA-C also appears to be well tolerated *in vivo* showing less side-effects compared to platinum-based drugs (Weiss et al., 2014). However, RAPTA-C has recently demonstrated to exert a strong anti-angiogenic effect (Nowak-Sliwinska et al., 2011), similar to that of sorafenib, a clinically used anti-angiogenic small molecule drug (Weiss et al., 2014). Moreover, there are characteristics shared by RAPTA-C and NAMI-A, exhibiting limited direct cytotoxic effects on cancer cells *in vitro* as well as anti-metastatic behavior *in vivo*. NAMI-A has also presented an anti-angiogenic activity, demonstrated by its ability to induce and activate apoptosis cell death pathway in a spontaneously transformed human endothelial cell line (ECV304) through the inhibition of MEK/ERK signaling (Sanna et al., 2002).

In these compounds, similarly to cisplatin, the chloride ligands of the ruthenium complex can be replaced by water molecules or hydroxide ions, leading to partial hydrolysis of the complex and poly-oxo species formation – ultimately responsible for the antimetastatic activity.

Along with ligands release and/or substitution - which occurs rapidly under physiological conditions *in vitro* and *in vivo* - the biological reduction of ruthenium III complexes is a possible process, especially in high proliferating cells, thereby promoting a unique activation process of this kind of metal-based drug in tumour tissues (Ravera et al., 2004). Nevertheless, in the general uncertainty concerning their mechanism of action, it cannot be excluded that Ru III complexes, properly transported into tumour cells, can interact in their original redox status with potential molecular targets. Furthermore, the possibility to be transported by the transferrin/transferrin receptor (Tf/TfR) network in place of iron, might allow for a natural ruthenium accumulation within cancer cells, typically requiring high iron amounts to accommodate for their rapid proliferation (Pessoa et al., 2010; Palermo et al., 2016).

Despite the positive outcomes throughout advanced preclinical and clinical evaluations of the anticancer ruthenium(III)-based compounds NAMI-A - the most advanced candidate drug having completed Phase II clinical trials - and KP1019, various drawbacks have been observed, mainly related to their limited stability in physiological conditions, impairing both their general pharmacokinetic and pharmacodynamic profiles (Chen et al., 2007).

1.6 AziRu: a new organometallic ruthenium complex analogue of NAMI-A

In 2012, almost concurrently, two different research groups – Walsby et al. (Webb et al., 2012) and Paduano et al. (Vaccaro et al., 2009; Simeone et al., 2012) – revisited a pyridine analogue of NAMI-A, called NAMI-Pyr by the first group and AziRu by the second. In comparison with NAMI-A, AziRu has a pyridine ligand replacing the imidazole one, and sodium replacing imidazolium as the counterion (Figure 7).

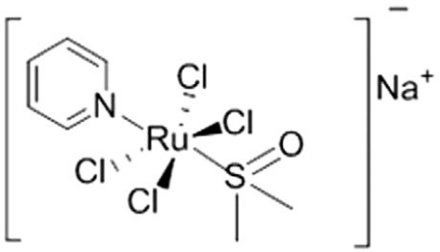

Figure 7. Molecular structure of AziRu (Mangiapia et al., 2012).

NAMI-A and AziRu have great similarities as far as their behavior in aqueous solutions and in vitro bioactivity are concerned. In particular, both rapidly replace chloride and DMSO ligands with water molecules or hydroxide ions. Biological experiments *in vitro* have shown very low cytotoxicity for AziRu on different cancer cell lines. Although AziRu showed a moderate cytotoxicity against human cancer cells, it is interesting to note that its IC_{50} value is half that of NAMI-A towards MCF-7 breast cancer cells (Table 1) (Mangiapia et al., 2012). One possible reason for this difference lies in the presence of a pyridine ligand to replace the imidazole, giving greater lipophilicity to AziRu, improving cellular uptake efficiency. Additionally, the ligands may also play an important role in biomolecular interactions and recognition processes. Indeed, hydrophobicity, cellular uptake efficiency and cytotoxic effects of anti-proliferative drugs on cancer cells are often strictly correlated. Since the AziRu and NAMI-A mechanism of action should be the same, this finding emphasizes the importance of the transition-metal complex physical and chemical properties which can play a critical role in the vehiculation of the active metal to the molecular targets, thus modulating its bioavailability.

	MCF-7	WiDr	C6
NAMI-A	620±30		
AziRu	305±16	441±20	318±12

Table 1. IC_{50} values (μM) relative to NAMI-A and AziRu in the indicate cancer cell lines after 48h of incubation (Mangiapia et al., 2012).

As mentioned above, these Ru(III) compounds behave as valid prodrugs with somehow limited side-effects (Dragutan et al., 2015), being likely activated to the more reactive and

cytotoxic Ru(II) derivatives within the reducing microenvironment of solid tumours (Ravera et al., 2004). Furthermore, it has been proposed for Ru(III) complexes that their lower toxicity to healthy tissues may be precisely attributed to the so-called "activation by reduction" mechanism.

This kind of mechanism is also shared by other types of compounds (Ravera et al., 2004) which, after a reduction, are able to procedure a more active form.

1.7 The importance of tumour microenvironment and the impact of the immune system on tumour progression

For many years, cancer studies and cancer-related research were focused only on cancer as being limited just to cancer cells, ignoring the environment created in the tumour, believing it as just a disease characterized by a cell-autonomous process. However, it has been acknowledged that tumours are heterogeneous organs, made of a various number of stromal components which are crucial players and not just participants in the tumourigenic process. One of the interests of cell laboratories is to investigate the role of cancer-associated macrophages, tumour-infiltrating lymphocytes (TILs), cancer-associated fibroblasts, and the extracellular matrix components that they secrete (Hui and Chen, 2015). Obtaining a much better understanding of the usual molecular pathways involved in the interactive bi-directional communication between tumour components and stroma cells will help researchers to manipulate the tumour microenvironment.

It is known that it contains innate immune cells (including macrophages, neutrophils, mast cells, myeloid-derived suppressor cells, dendritic cells, and natural killer cells) and adaptive immune cells (T and B lymphocytes) in addition to the cancer cells and their surrounding

stroma (which consists of fibroblasts, endothelial cells, pericytes, and mesenchymal cells). Numerous epidemiological, clinical and experimental studies shown that tumour microenvironment and infiltrating immune cell subsets are important for regulating the process of tumour angiogenesis, classical hallmark of cancer onset. These infiltrates involve the adaptive immune system including several types of lymphocytes (TILs) as well as cells of the innate immunity such as macrophages, neutrophils, eosinophils, mast cells, dendritic cells and natural killer cells (Stockmann et al., 2014). Macrophages are specialized phagocytes that are able to incorporate invaliding cell debris and microbes as well as to secrete different immunomodulatory cytokines. Depending on dynamically changing microenvironments that encounter, they have a unique ability to adapt their phenotype. Generally, monocytes/macrophages can be polarized to M1 or M2 macrophages (Yang and Zhang, 2017; Stockmann et al., 2014). The M1 phenotype, activated by interferon-ɣ and microbial products, is characterized as proinflammatory - since produce proinflammatory and immunostimulatory cytokines - and is involved in helper T cell (Th) 1 responses to infection. M2 macrophages, “alternatively” activated macrophages, exhibit a T-helper-2 cytokine expression pattern and are considered to be rather immunosuppressive. Although most confirmed tumour-promoting cytokines are “M1 cytokines,” TAMs – tumour associated macrophages - are considered to have an M2 phenotype (Grivennikov et al., 2010). Neutrophils represent the largest population of blood leukocytes and are critical for the initial inflammatory reaction to invading microbes. They are particularly plentiful in the invasive part of the tumour (Bellocq et al., 1998) and neutrophils infiltration has been reported in different type of cancer. Moreover, PMN-MDSC population, positive for $Ly6G^{+}CD11b^{+}$ markers, can be found in tumour infiltrate showing tumourigenic activity. Some studies demonstrate that, like TAM, CD11b+/Ly6G+ tumour-associated neutrophils (TAN) also have differential states of activation/differentiation, suggesting a classification

scheme for TAN similar to that of TAM: TAN can thus take an anti-tumourigenic (what we are calling an “N1-phenotype”) versus a pro-tumourigenic (“N2”) phenotype (Fridlender et al., 2009). Also infiltrates of mast cells have been observed in solid tumours as well as hematological malignancies. Mast cells are able to release an array of angiogenic factors, including VEGF and fibroblast growth factor (FGF)-2.

Natural killer cells are cells of the innate immunity characterized by a high cytolytic capacity against transformed cancer cells. In addition to their important role in immunosurveillance, NK cells can contribute to neovascularization.

CD4 T cells play essential roles in the function of the immune system. They help B cells make antibody, enhance and maintain responses of CD8 T cells, regulate macrophage function, orchestrate immune responses against a wide variety of pathogenic microorganisms, and regulate/suppress immune responses both to control autoimmunity and to adjust the magnitude and persistence of responses.

CD4 T cells are important mediators of immunologic memory, and when their numbers are diminished or their functions are lost, the individual becomes susceptible to a wide range of infectious disorders. The initial understanding of the existence of distinctive populations of differentiated CD4 T cells came from the analysis of mouse CD4 T cell clones that were shown by Mosmann and Coffman (Mosmann et al., 1986) and slightly later by Bottomly and her colleagues (Killar et al., 1987) to be divisible into two major groups, designated Th1 and Th2 cells by Mosmann and Coffman. Th1 and Th2 clones could be distinguished mainly by the cytokines produced by the cells, but also through the expression of different patterns of cell surface molecules. About the expression of cytokine, Th1 cells tend to be good IL-2 producers, and many make TNF-α as well. By contrast, Th2 cells fail to produce IFN-γ or lymphotoxin. Their principal cytokines are IL-4, IL-5, and IL-13, but also make TNF-α, and some produce IL-9 (Figure 8).

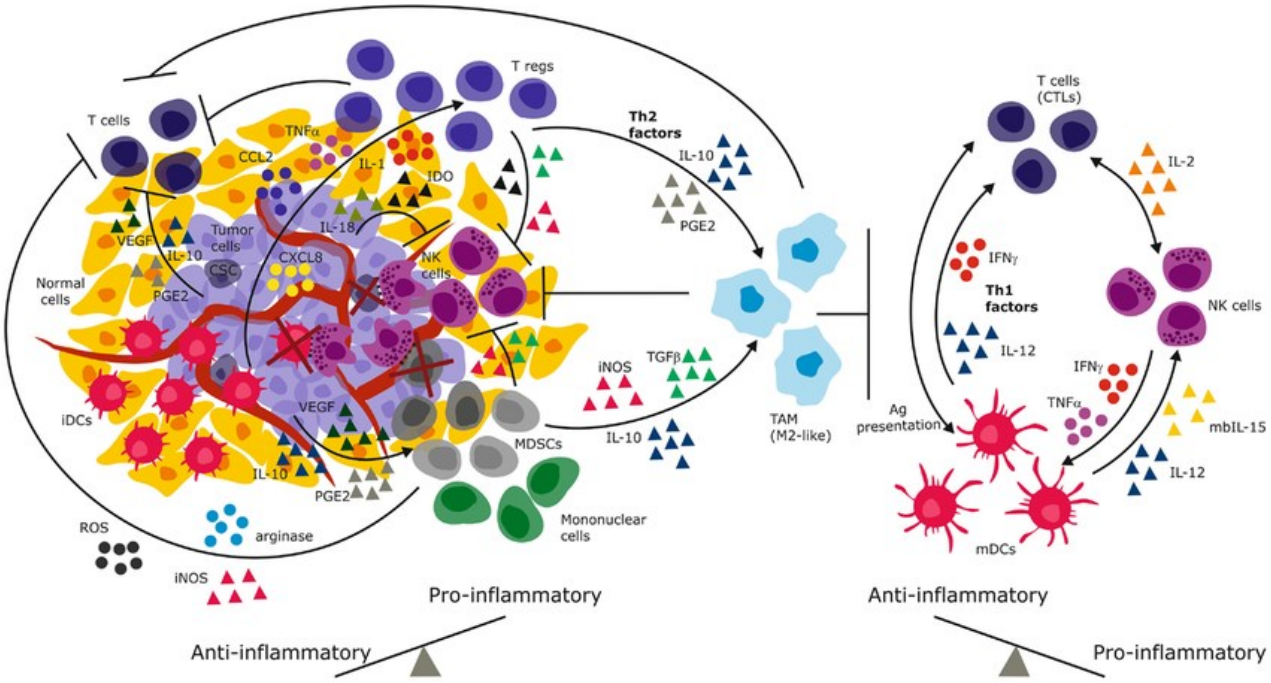

Figure 8. Immune suppressive mechanisms of the solid tumor microenvironment. Tumor-derived immunosuppressive mechanisms include secreted cytokines and chemokines that recruit and sustain immature and suppressive immune cells. These secrete Th2 factors, creating a chronic anti-inflammatory environment which promotes and predominates malignant progression (left). NK cell therapy has the potential to reverse the anti-inflammation to engender dominant pro-inflammatory signaling through secretion of IFN-γ, Th1 cytokines, and activation of both innate and adaptive immune cells (right). By elimination of tumor cells and immature suppressive cells, NK cells have the potential to reverse the anti-inflammatory signals and eliminate tumor progression (Gras Navarro et al., 2015).

Moreover, other types of CD4 T cells were recognized, such as NKT, but also into Th9 or Th17. The latter are mainly observed at the epithelial barriers where they help B and epithelial cells to block entrance of pathogens. Another type of CD4 T cells, T regulators (Treg), are important in the tolerance and secrete cytokine leading to the inhibition of immune cells (Zhu et al., 2010).

1.6.1 Regulation of the immune system

It is known that tumour angiogenesis is critical for tumour development. Although tumour cells were first believed to fuel tumour angiogenesis, numerous studies have shown that the tumour microenvironment and infiltrating immune cell subsets are important for regulating the process of tumour angiogenesis (Stockmann et al., 2014). Besides their known immune function, these infiltrating cells are now recognized for their crucial role in regulating the formation and the remodeling of blood vessels in the tumour as well as the growth and development of tumour.

Because of their activity, immune system cells could represent a possible target for cancer therapy. Many factors can act on the cells of the immune system and therefore interfere with the way the immune response functions, such as stress and ageing now consistently appear in the literature as factors that act upon the immune system in the way that is often damaging (Vitlic et al., 2014). Among these, the EPO can act on macrophages, neutrophils, lymphocytes T and B, through a particular receptor.

The renal cytokine hormone erythropoietin (EPO) regulates bone marrow erythrocyte production by stimulating the differentiation and inhibiting the apoptosis of erythroid progenitor cells (De Maria et al., 1999; Liu et al., 2006). The production of EPO is controlled by a classical feedback loop mechanism and its effects are mediated through the cell surface erythropoietin receptors (EpoR). However, EPO also bears extra-hematopoietic properties that are transduced by receptors (EpoRs) expressed on various nonerythroid tissues including immune cells (Brines and Cerami, 2005; Jelkmann, 2007). Taking into consideration the pleiotropic effects of EPO in extraerythroid tissues, the expression of EpoRs on immune cells, and the partial similarities between EPO- and cytokine-mediated signal transduction, we questioned whether EPO may exert putative immune-modulatory effects, which could be of clinical relevance in certain inflammatory diseases. Furthermore, there are provided

evidences that EPO acts as a potent anti-inflammatory immune modulator by specifically targeting NF-κB p65-driven inflammatory effector pathways (Nairz et al., 2011).

Few studies have explored in depth the impact of EPO-delivery on the immune system. Interestingly, immunosuppressive role of EPO in humans has already been described favouring kidney graft survival by decreasing T cell function (Cravedi, 2014). In an auto-immune encephalomyelitis mouse model, this beneficial effect of EPO was attributed to a Th2-polarized immune response. Recently, EPO was described to dampen monocyte/macrophage Th1-cytokine production in a DSS-induced colitis, decreasing inflammation and disease development (Nairz et al., 2017). On another hand, EPO was shown in a mouse model of infection, to inhibit macrophage activation, through NF-κB pathway inhibition, impairing antibacterial function (Nairz et al., 2011). Conversely, other studies reported improved humoral and cellular immune functions against vaccine antigens in CKD patients under ESA supplementation (Cravedi, 2014), which remain unconfirmed since then.

1.6.2 Benefits and drawbacks of using EPO

The circulating red cell mass reflects a dynamic balance between EPO-regulated red cell proliferation and the subsequent loss or destruction of mature erythrocytes. Factors which affect oxygen delivery to the kidney, such as the inspired partial pressure of oxygen or defective cardio-pulmonary function perturbing normal renal perfusion, can increase EPO production and stimulate erythropoiesis. Conversely, increased oxygen supply to the kidney

reduces the stimulus to EPO synthesis. The EPO is able to avoid the risk of viral transmission and also all the immune reactions. However, even if the EPO is extremely well tolerated, some patients can develop anti-EPO neutralizing antibodies.

Since EPO is the primary hormone responsible for the maintenance of the erythroid lineage, anemia - a very common disorder and probably still quite under recognized - may be classified based on levels of this hormone present in the circulation, but also according to mechanisms such as levels of red blood cell production, destruction, or loss, and by parameters of red blood cell morphology, such as the size, color and shape, as well as the red blood cell (RBC) indices, mean corpuscular volume (MCV), mean corpuscular hemoglobin concentration (MCHC) and mean corpuscular hemoglobin (MCH) (Hodges et al., 2007).

Erythropoietin (EPO), the most widely used erythropoiesis-stimulating agent (ESA), is commonly used to promote red blood cell production in the treatment of anemia associated with chronic kidney disease (CKD) (Eschbach et al., 1987) and also in cancer-related anemia, associated with conventional chemotherapy (Littlewood et al., 2002), even if this supportive therapy remains subject of controversy. Indeed, although this condition is considered as an independent prognosis factor in various cancers, such as cervical carcinoma, head and neck cancer, chronic lymphocytic leukemia and Hodgkin disease, ESAs have been reported to further reduce overall survival, increasing cardiovascular and venous thromboembolism risks in cancer patients, as well as inducing tumour progression independently of the type of cancer or the anti-cancer treatment (Bohlius et al., 2009; Henke et al., 2003).

Mechanisms underlying the role of EPO/ESA on tumour proliferation still remain highly controversial. Multiple studies showed that various human tumour cells express EPO-receptor (EpoR) and respond to EPO stimulation by activating specific signaling pathways

and subsequent tumour proliferation (Feldman et al., 2006; Um et al., 2006; Um et al., 2007; Henke et al., 2007). However, it has also been claimed that EpoR detection on tumour cells is due to commercially unspecific anti-EpoR antibodies and absence of EPO activation on tumour cells lacking its receptor has been described (Elliott et al., 2013). Alternatively, EPO's action on tumourigenesis might be mediated, at least in part, by EPO's role in angiogenesis as demonstrated in mouse models (Okazaki et al., 2008), through activation of endothelial cells, which is also a matter of debate (Sinclair et al., 2010).

Keeping in mind what was said before, it was hypothesize that anemia, through both endogenous EPO secretion, and exogenous ESA administration constitute bad prognosis factor in cancer patients as a consequence of the activation of multiple biological pathways, among which the immunological component may be a major one. In this setting, the overall project framework of Professeur Hacein-Bey-Abina's team is the characterization of EPO's treatment impact on the anti-cancer immune response, by using *in vivo* studies.

The 4T1 cell line displays multiple interesting features for this project, such as an aggressive phenotype, being characterized as triple negative tumour cells, a strong metastasis potential similar to human breast cancer (Lelekakis et al., 1999), and the lack of EpoR expression. The latter characteristic allows Hacein-Bey-Abina's team to exclude any direct effect of EPO on tumour-cell proliferation or survival.

They conducted *in vivo* studies to evaluate the immune suppressive role of EPO in this model. For this purpose, 4T1 breast tumour cell lines were intra-dermal injected nearby the mammary gland and followed for tumour growth. Mean tumour volume measured every 2 days was calculated using the following formula: (length × width × thickness)/2.

Preliminary data showed that EPO-treated mice displayed higher tumour volumes compared to control group (Figure 9).

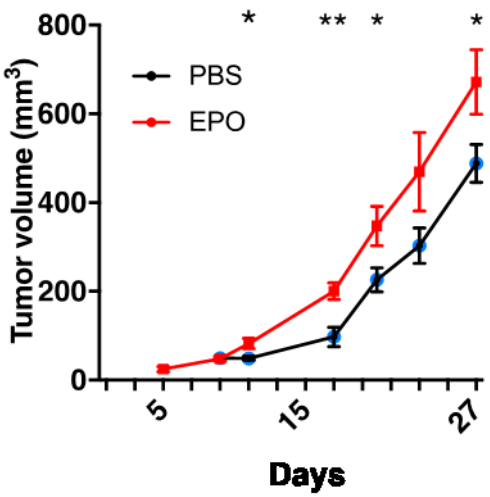

Figure 9. Impact of EPO on tumour establishment and development. Tumour size was measured by a caliper and the volume estimated using the following formula, V=length*Width2/2. Values are expressed as the mean +/- SEM of 2 independent experiments, n=14 mice per group. Statistics: unpaired t test, *p<0.05, **p<0.01, ***<0.001.

Moreover, to gain further insight into the mechanisms involved in the tumourigenic EPO effect, the same team analyzed the infiltration and the activation status of immune cells at the primary tumour site. Interestingly, results showed that the proportion of TIL decreased over time more dramatically in EPO-treated mice as compared to PBS-treated control mice, from D10 to D16 pi, with a higher impact on CD4 T helper cells (CD4 Th) than on CD8 T cells (Figure 10). These differences are maintained throughout the analysis of intra-tumour immune infiltrate.

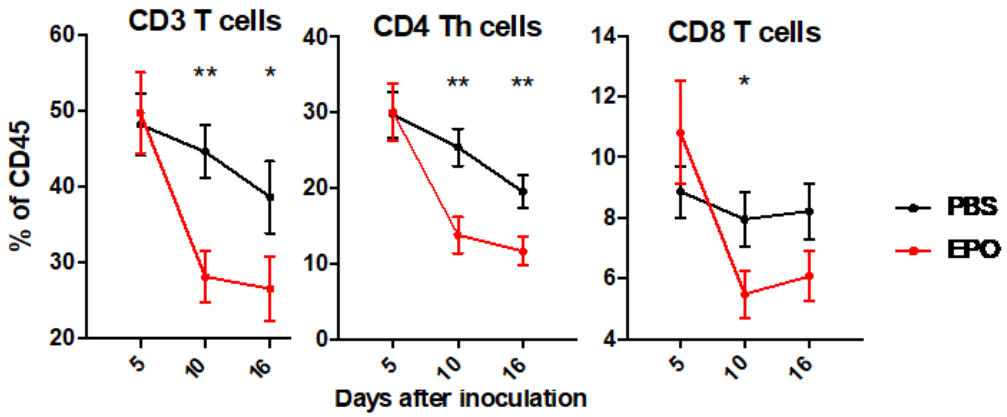

Figure 10. Impact of EPO on TIL proportion. Tumour-infiltrating immune cells were purified using Histopaque gradient and then incubated with specific antibodies □-CD16-32, □-CD45-PE, □-CD3-BV785, □-CD4-BV421, □-CD8□-AF700, during 30 min at 4°C before flow cytometry acquisition (Fortessa). Data are analysed on FlowJo.10. Values are expressed as mean +/- SEM of 3 independent experiments, n=15 mice per group. Statistics: unpaired t test, *p<0.05, **p<0.01, ***<0.001.

Blood analysis revealed comparable kinetics of T cell concentrations between EPO- and PBS-treated mice indicating that EPO effect is not attributable to a systemic action but rather associated to an inhibition of T-cell recruitment within the tumour site. In order to analyze deeply the effect of EPO on adaptive immune response initiation, the team has planned to characterize T-cell activation in draining lymph nodes and polarization toward effector T cell subsets. The same analysis has been also planned for TIL.

INNOVATIVE DRUG DELIVERY SYSTEM

The use of pharmaceutical technologies can be an astute choice for developing innovative therapeutic strategies. The association of nanotechnologies provides new therapeutic possibilities due to the combined properties of different skills. Nanocarriers can localize the drugs administration to the specific target tissue. In addition, drugs encapsulated within or conjugated to nanoparticle vehicles display pharmacokinetics that are markedly different from those of free drugs, in fact nanocarriers can provide additional drug sustained release or different pharmacokinetic and bio distribution profiles, improving the drug therapeutic index. Furthermore, they could facilitate the passive targeting as well as the active one, leading to less side effects.

Liposomes, micelles, liquid and solid lipid nanocapsules, polymeric nanoparticles, dendrimers, and fullerenes are all nanotechnologies which have been recently assessed for medical applications, such as cancer therapy, anesthesia, the treatment of cutaneous and infectious diseases, the administration of antidepressants, and the treatment of unexpected diseases, such as alopecia. Among all, liposomes are the most commonly used vehicles, and most of the currently approved nanoparticle chemotherapy formulations are liposomal (Lee et al., 2017).

2.1 Drug delivery strategies by using nucleolipidic nanovectors

Nucleolipids - hybrid molecules carrying lipid moieties covalently attached to nucleoside scaffolds - have recently attracted great interest, in both the design of artificial molecular devices (Mao et al., 2000; Petitjean et al., 2004; Rosemeyer et al., 2005) and the development of novel therapeutic agents. (Krutzfeldt et al., 2005) In contrast to classical amphiphiles, nucleolipids possess a highly informative polar headgroup (adenine, thymine, guanine,

uracil, or related analogs) with additional H-bonding and p-stacking capacity allowing them to enhance their self-aggregation properties and specifically recognize other nucleobases (Barthelemy et al., 2005; Onda et al., 1996).

Nanostructuring in pseudo-physiological conditions leads to efficient cellular uptake through the phospholipid bilayers as well as confers protection to the drug from extracellular enzymatic degradation. On the other hand, full reversibility—within the cells—of the chemical bonds connecting the nucleoside decorations may be a powerful strategy to prevent toxicity, thus opening the way to a completely new approach for drug delivery.

As mentioned before, even if our low molecular weight Ru complex – AziRu – is more effective that the well-known NAMI-A, it presents some limitations, in particular due to its low stability in physiological environment, in which it can be converted in non-soluble poly-oxo species. Although the formation of poly-oxo species does not seem to significantly hamper the ruthenium bioactivity, at least when tested on some tumour cell lines, an important consequence of these degradation processes is that only a limited amount of the administered drug can be effectively internalized into cells (Sava et al., 1999). Therefore, aiming at improving the stability of the ruthenium(III)-based drugs in biological environment, as well as their suitability for biomedical applications, an innovative strategy for their transport *in vivo* by means of nanobiotechnological tools has recently proposed. In detail, the project is based on the incorporation of AziRu, (Simeone et al., 2011; Montesarchio et al., 2013) used as a core molecular scaffold - into suitable nucleolipidic structures, developing a mini-library of highly functionalized amphiphilic ruthenium(III) complexes, including differently decorated nucleolipids (Figure 11). In particular, three different types of nucleolipids are used:

- **ToThy** : 3- [4-pyridylmethyl] -30-O-oleoyl-50-O (monomethoxy) triethylene glycol-acetyl-thymidine;

- **HoThy** : 3- [4-pyridylmethyl] -30-O-oleyl-50-O (benzyloxy) exaetilen glycol-acetyl-thymidine;
- **DoHu** : 3- [4-pyridylmethyl] 20, 30 of O-oleyl-50-O (benzyloxy) esaetilen glycol-acetyl-uridine

In these structures, the active metal part -AziRu - was attached to the nucleobase of a nucleoside, which was further decorated with one or two long aliphatic chains able to promote the assembly into ordered nanosized aggregates in aqueous solutions and with one oligoethylene glycol chain of variable length, behave as a protective "stealth" agent for the nanoaggregates (Vaccaro et al., 2009; Lasic et al., 1991).

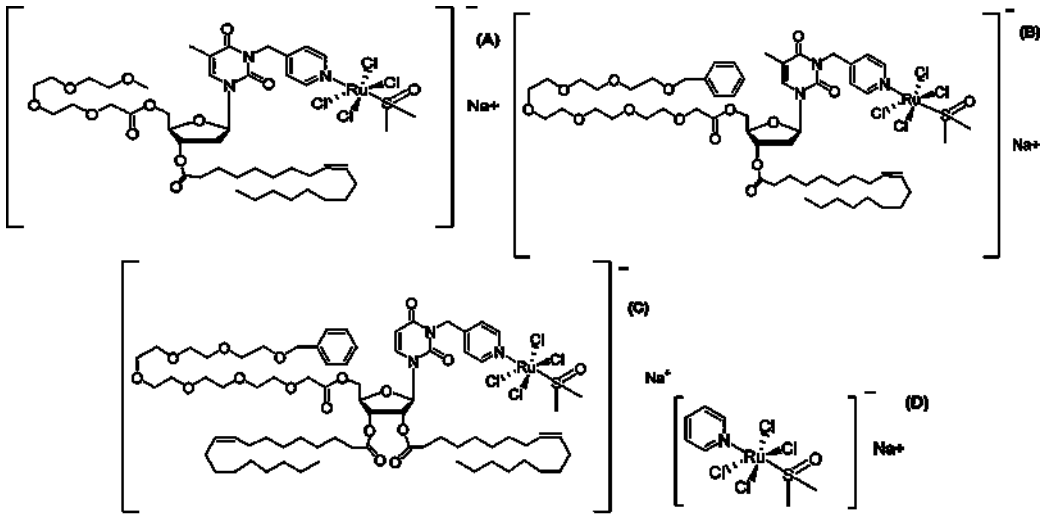

Figure 11. Molecular structures of Ru(III)-containing complexes. The investigated Ru(III) nucleolipidic complexes (A) ToThyRu, (B) HoThyRu and (C) DoHuRu, along with the low molecular weight Ru(III) complex (D) AziRu (Mangiapia et al., 2012).

The resulting nucleolipidic Ru(III) complexes - named ToThyRu, HoThyRu and DoHuRu- are endowed with a marked propensity for self-aggregation in physiological solutions and

high *in vitro* antiproliferative activity against human cancer cells, thus proving to be promising lead compounds for future *in vivo* studies (Irace et al., 2017).

However, knowing that cholesterol (fundamental constituent of organism) plays a critic role in keeping the fluidity of the cell membrane as well as the endocytosis phenomena, Paduano and co-workers focused on the design of bio-mimetic model membranes system that, exploiting the advantages of the similarity to the biological membranes, could be a new strategy for the drug delivery. Thus, the inclusion of cholesterol in membrane models can have different advantages. It increases the rigidity of the lipid bilayer and reduces its instability in the blood, due to the serum protein binding (Mabrey et al., 1978). Furthermore, recognized by receptors of low-density lipoprotein (LDL), it can facilitate the endocytosis (Krieg et al., 1993). In this context, a ruthenium complex, covalently linked to a cholesterol-containing nucleolipid and stabilized by co-aggregation with a biocompatible lipid, has been synthetized. The amphiphilic ruthenium complex, named ToThyCholRu, is intrinsically negatively charged and has been inserted into liposomes formed by the cationic 1,2-dioleyl-3-trimethylammoniumpropane chloride (DOTAP) to hinder the degradation kinetics typically observed for known ruthenium-based antineoplastic agents (Figure 12). These nanovectors, containing up to 30% in moles of the ruthenium complex and stable for several weeks, revealed an important antiproliferative activity and, most remarkably, the highest ability in ruthenium vectorization measured so far (by *in vitro* bioactivity experiments) and fast cellular uptake in human carcinoma cells (by fluorescence microscopy experiments - following the incorporation of rhodamine-B within the ruthenium-loaded liposomes).

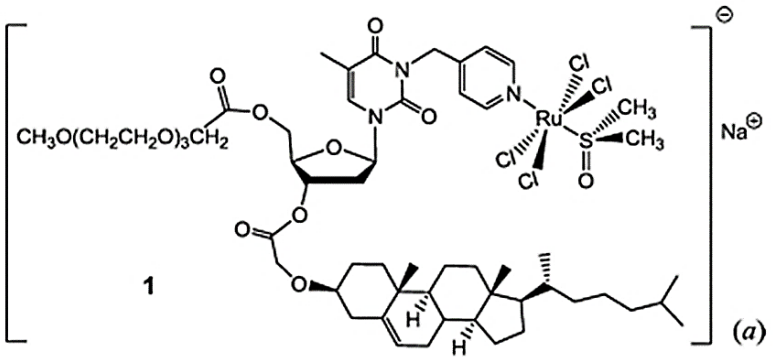

Figure 12. Molecular structure of the nucleolipid ToThyCholRu (Simeone et al., 2012).

In the first series of compounds developed, the pyridine residue – chosen as the privileged ligand for ruthenium – was anchored to the N-3 position of the pyrimidine part. Therefore, in order to take advantage of the recognition abilities of the nucleobases and their potential interactions with nucleic acids via Watson–Crick hydrogen bonds or stacking contacts, these should not be blocked by hindered groups. Then, based on the promising results obtained for the first generation of ruthenium(III) complexes, Paduano and co-workers have designed a novel nucleolipid where the pyridine ligand is not attached at the N-3 but at the C-3′ position on the sugar, identified as a model compound for a second generation of metal-complexed nucleolipids (Montesarchio et al., 2013).

This compound, named **HoUrRu**, has an oleic acid residue at the 2′-position and a heptakis (ethylene glycol) chain at the 5′- position. The peculiarity of this compound is in the presence of the pyridine in the 3′-position (Figure 13), but with preservation of the same decoration present in HoThyRu. All three linked groups – the pyridine moiety and the hydrophilic and the lipophilic chains – are linked to the sugar, so the uracil nucleobase is not hampered in hydrogen-bond formation or in stacking interactions with potential *in vivo* targets.

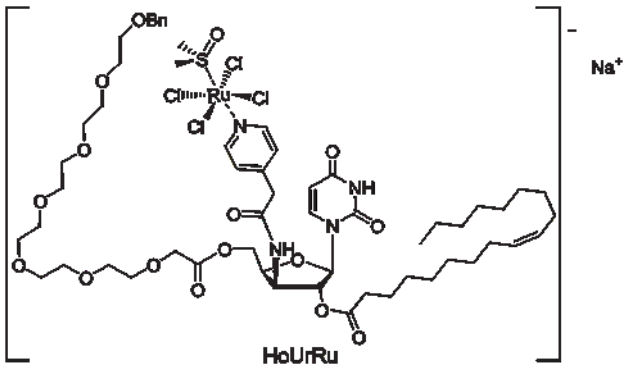

Figure 13. Molecular structure of nucleolipidic ruthenium(III) complex (Bn = benzyl) (Montesarchio et al., 2013).

It is interesting to highlights that, with respect to other amphiphilic Ru-complexes previously investigated, HoUrRu exhibited enhanced capability to co-aggregate with different lipids. *In vitro* bioactivity assays showed (when it's co-aggregated with POPC or DOTAP) a much more inhibition of the human cancer cells MCF-7 and WiDr growth, respect to the reference ruthenium-complex AziRu. Furthermore, compared with previously synthesized analogs HoThyRu, ToThyRu and DoHuRu, HoUrRu showed similar antiproliferative ability on MCF-7 cells - with IC_{50} values in the 10 μM range - and notably, a higher impact on WiDr cells, with IC_{50} values in the 10–20 μM range (Figure 14; Table 2) (Montesarchio et al., 2013).

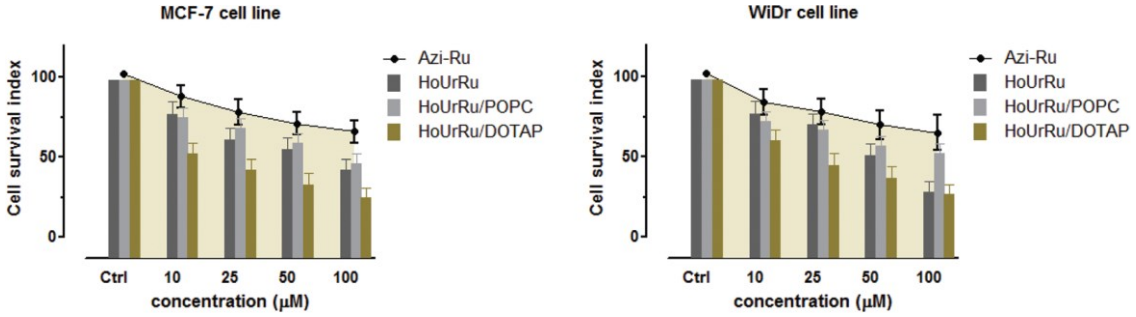

Figure 14. Cell survival index values, evaluated by MTT assay and total cell count, in MCF-7 and WiDr cell lines incubated for 48h with a range of concentrations (10 → 100 μM) of the different Ru-containing formulations and with HoUrRu and AziRu, as indicated in the legend. AziRu, a NAMI-A analog, is here used as a reference drug (Montesarchio et al., 2013).

Cell lines	CDDP	NAMI-A	Azi-Ru	DoHuRu POPC (DOTAP)	HoThyRu POPC (DOTAP)	ToThyRu POPC (DOTAP)	HoUrRu POPC (DOTAP)
MCF-7	25 ± 3	620 ± 30	305 ± 16	71 ± 6 (13 ± 5)	7 ± 4 (15 ± 7)	9 ± 4 (19 ± 8)	14 ± 7 (8 ± 5)
WiDr	—	—	441 ± 20	99 ± 5 (41 ± 10)	40 ± 5 (65 ± 8)	75 ± 4 (50 ± 11)	20 ± 8 (12 ± 5)

Table 2. IC_{50} values (μM) in the indicated cell lines following 48 h of incubation with cisplatin (CDDP), NAMI-A, Azi-Ru and with POPC or DOTAP (in parentheses) formulations of DoHuRu, HoThyRu, ToThyRu and HoUrRu (in bold) amphiphilic ruthenium-complexes (Montesarchio et al., 2013).

So, based on the amazing results obtained, there are many benefits related to the use of nanostructures in metal-based drug delivery, including the potential to transport greater amounts of the metal in the bloodstream, to obtain "stealth" aggregates to produce aggregates selectively captured by specific cancer cell lines by inserting, within the aggregates, targeting molecules specifically recognized by receptors overexpressed in tumour cells (Mangiapia et al., 2012).

2.2 Co-aggregation with biocompatible lipids

Nucleolipids have been selected as scaffold for building up the amphiphilic Ru complexes because of their capability to mime the molecular organizations of the biological systems, as well as for the possibility to form a wide variety of supramolecular systems such as liposomes/vesicles, cubic phases, ribbons, etc. (Barthelemy et al., 2009; Fortini et al., 2004), that have found an increasing application in the biomedical field.

However, as NAMI-A and "naked" AziRu, these amphiphilic ruthenium-complexes described, when left in aqueous solutions, also tend to be unstable, forming insoluble precipitates in a period ranging from few hours, in phosphate buffer, to a few days, when dissolved in pure water.

For that reason, besides enhancing their biostability as well as aiming at biocompatible systems, these nucleolipidic complexes are also co-aggregated with biocompatible lipids, giving rise to stable and biomimetic ruthenium-based nanoaggregates acting as efficient nanovectors. These nanoaggregates - which have been subjected to an in-depth microstructural characterization - are *ad hoc* designed to present high stability in aqueous condition as well as to transport high ruthenium amounts in cells, thereby ensuring more effective metal-based treatments. Nucleolipids, being amphiphilic compounds, offer unique properties of spontaneous self-assembly providing nano-sized nanoaggregates with exquisite tunability in terms of volume and shape (Lainé et al., 2012; Licona et al., 2017).

2.2.1 Zwitterionic lipid POPC

The synthesized molecules have been studied as pure aggregates, as well as in mixture with palmitoyl-2-oleoyl-sn-glycero-3- phosphocholine (POPC) (Mangiapia et al., 2012), at

selected POPC/Ru molar ratios (85:15). Indeed, the combination of Ru complexes with phospholipids can allow a fine tuning of the metal amount to be administered, as well as protection from degradation, since the ruthenium complex is stuck in the liposome bilayer. Among phospholipids, POPC (its structure is shown below) is of particular interest because it is one of the components of natural membranes (Arriaga et al., 2009).

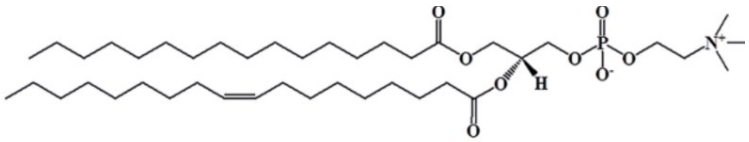

The aggregation behavior of the prepared nanoaggregates has been investigated through an experimental strategy that combines dynamic light scattering (DLS) to estimate aggregate dimensions, small angle neutron scattering (SANS) to analyze the aggregate morphology and to determine their geometrical characteristics, and electron paramagnetic resonance (EPR) to get information on the dynamics of the lipid hydrophobic tail in the bilayer. The evaluation of the "cell survival index" emerging from concentration/effect curves, suggested that these nanocarriers produce a cytotoxic effect substantially similar to that of the "naked" AziRu, although they enclose only 15% of ruthenium in moles. They exhibited IC_{50} values much lower (~6 times) than AziRu (Table 3) and other known organometallic complexes, but on the other hand, they required quite long times (>6 h) to produce relevant cytotoxic effects, probably as a consequence of their slow cell uptake (Mangiapia et al., 2012).

	MCF-7	WiDr	C6
NAMI	620 ± 30		
AziRu	305 ± 16	441 ± 20	318 ± 12
DoHuRu/POPC	71 ± 6	99 ± 5	24 ± 5
HoThyRu/POPC	7 ± 4	40 ± 5	81 ± 7
ToThyRu/POPC	9 ± 4	75 ± 4	36 ± 8

Table 3. IC_{50} values relative to NAMI-A, AziRu and to the effective ruthenium concentration carried by ToThyRu/POPC, HoThyRu/POPC and DoHuRu/POPC liposomes in the indicated cell lines after 48 h of incubation (MCF-7: human breast adenocarcinoma cell line. WiDr: human epithelial colorectal adenocarcinoma cell line. C6: tumour rat glioma cells) (Mangiapia et al., 2012).

2.2.2 Cationic lipid DOTAP

In order to enhance the antineoplastic activity, by increasing the ruthenium content within the aggregates and favoring their cell uptake, the coaggregation of the nucleolipids whit the cationic lipid 1,2-dioleyl-3- trimethylammoniumpropane chloride (DOTAP) (shown below) in the mixture 50:50 has been tested.

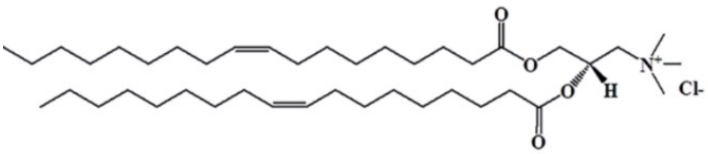

The resulting nanoaggregates are specifically designed to present high stability in biological environment even at high Ru-complex content. The aggregation behavior of the prepared nanoaggregates, as well as their stability in the time, has been investigated through dynamic

light scattering (DLS) to estimate aggregate dimensions, small angle neutron scattering (SANS) to analyze the aggregate morphology and to determine their geometrical characteristics, neutron reflectivity and zeta potential to gain structural information on the bilayer, and electron paramagnetic resonance (EPR) to get information on the dynamics of lipid hydrophobic tails in the bilayer.

Based on the IC_{50} values (Table 4), the three mixed amphiphilic ruthenium complexes/DOTAP nanoaggregates are much more active than the precursor AziRu and also than the analogues nanoaggregates *via* POPC, perhaps due to their faster cellular up-take, that results massive after only 3h (Montesarchio et al., 2013).

	IC50 [μM]		
	MCF-7	**WiDr**	**C6**
AziRu	305 ± 16	441 ± 20	318 ± 12
ToThyRu/DOTAP	19 ± 8	50 ± 11	54 ± 8
HoThyRu/DOTAP	15 ± 7	65 ± 8	43 ± 11
DoHuRu/DOTAP	13 ± 5	41 ± 10	34 ± 9

Table 4. IC_{50} values relative to AziRu and to the effective ruthenium concentration carried by ToThyRu/DOTAP, HoThyRu/DOTAP and DoHuRu/DOTAP liposomes in the indicated cell lines after 48 h of incubation. IC_{50} values are reported as means ± SEM. (MCF-7: human breast adenocarcinoma cell line. WiDr: human epithelial colorectal adenocarcinoma cell line. C6: tumour rat glioma cells.) (Montesarchio et al., 2013).

The cationic liposomes are emerged as valid alternative to the neutral vesicles, and could bring different benefits, such as the major interaction with the cell membranes (Wiethoff et al., 2001).

The positive charge can also enhance the aggregation with the negative one of the nucleolipids forming the amphiphilic ruthenium complex and thus make a more stable liposome (Figure 15).

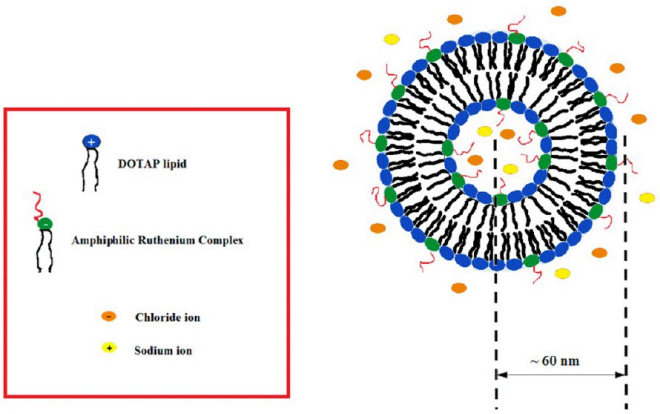

Figure 15. Representation of the amphiphilic ruthenium complex/DOTAP nanoaggregates (Mangiapia et al., 2013).

2.3 Up-take investigations

Because transition metal-based anticancer drugs target DNA in the nuclear cage, the cellular uptake characteristics and the nuclear entry ability have emerged as central factors influencing their antiproliferative efficacy. Thus, in order to evaluate the kinetics of cellular up-take as well as the investigation of the mechanism of action of the synthesized Ru(III) complexes, experiments of fluorescent microscopy were carried out into human MCF-7 cancer cells, by using the fluorescent probes Rhodamine B lipid derivative, 1,2- dioleoyl-sn-glycero-3-phosphoethanolamine-N-(lissamine rhodamine B sulfonyl) ammonium salt - inserted in the liposomal bilayer of DoHuRu/DOTAP - and fluorogenic group of the dansyl – linked to HoThyRu for deeper studying the cell internalization process and metabolic fate.

Thus, the new nucleolipidic Ru(III) complex, named HoThyDansRu, was synthesized. It contains the dansyl group attached through a sulfate bridge in the 2′-position, an oleic acid residue at the 3′-position, an ethylene glycol chain in the 5′-position and a pyridinylmethyl arm at N-3 (Figure 16).

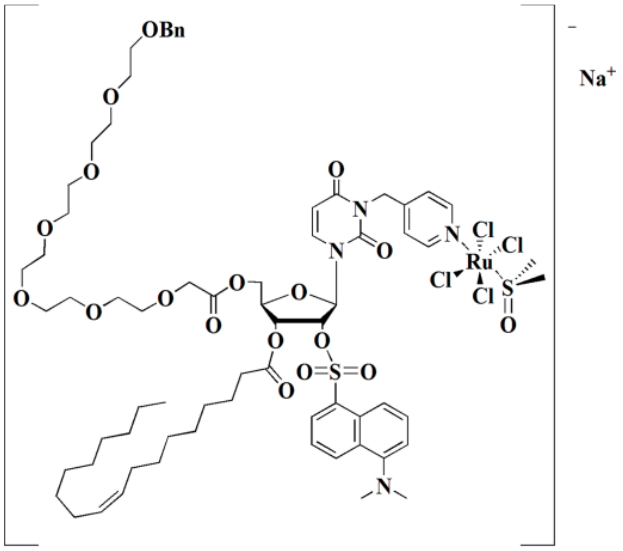

Figure 16. Chemical structure of the fluorescently labelled ruthenium(III) complex HoThyDansRu (Bn = benzyl) (Mangiapia et al., 2013).

About the cell uptake, the fluorescent microphotographs (Figure 17), showed a high propensity of DoHuRu/DOTAP liposomes to cross cell membranes, and the cell entry appears to be a very fast process (Mangiapia et al., 2013). Furthermore, merged images - where fluorophore emission is overlapped at the same location - suggest also a nuclear localization of the aggregates. By means of their lipid properties, it is feasible that the Ru complexes/DOTAP nanoaggregates are taken up by cells directly via membrane fusion and by endocytosis.

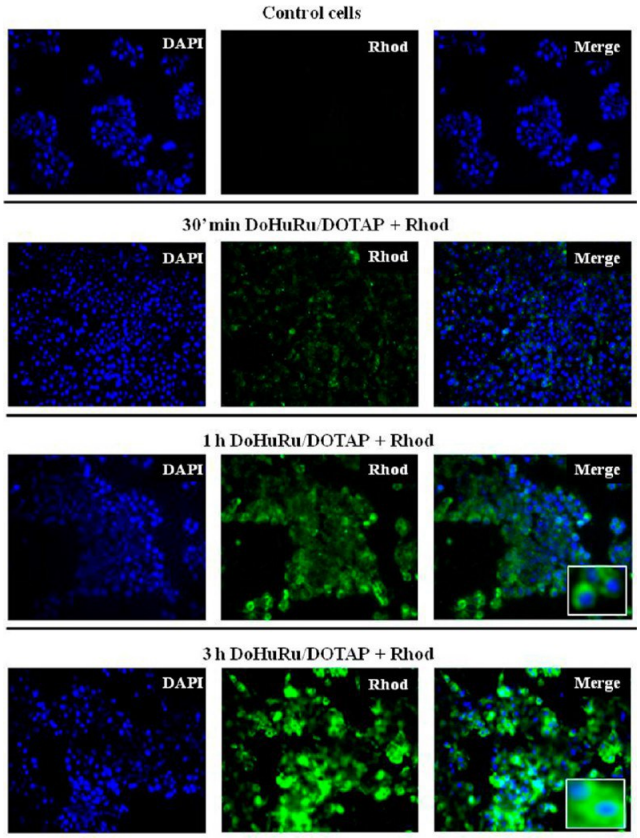

Figure 17. Fluorescent microphotographs of monolayers showing the cellular uptake of liposomes by human MCF-7 breast adenocarcinoma cells. MCF-7 were incubated with 100 μM of the rhodamine-added DoHuRu/DOTAP liposome solution for 30 min, 1 h, and 3 h. DAPI is used as a nuclear stain (shown in blue). Rhodamine-dependent fluorescence (Rhod) of DoHuRu/DOTAP liposomes is shown in green. In merged images (Merge), the two fluorescent emissions are overlapped (Mangiapia et al., 2013).

On the other hand, to assess the fate of the active ruthenium complex, additional *in vitro* fluorescence experiments were performed on MCF-7 cells treated with the dansyl-labeled ruthenium complex HoThyDansRu co-aggregated with DOTAP. In this way, fluorescently labeled HoThyDansRu (Figure 18) localizes rapidly within the cells. The analysis of fluorescent emission also suggests that the complexes lodged in DOTAP liposomes enter the cytoplasm before being predominantly delivered to discrete foci in the perinuclear compartment; moreover, although attenuated by DAPI nuclear staining, dansyl-dependent fluorescence emission is also detectable in the nuclei area. Overall, in addition to demonstrating an effective process of cellular uptake, the fluorescent patterns seem to

suggest an intracellular liposome degradation coupled with the release of the pharmacologically active agent within the cytoplasm. This would explain the prevalent rhodamine-associated fluorescence and the concomitant generation of discrete dansyl-associated spots following cellular uptake and disaggregation of nanocarriers.

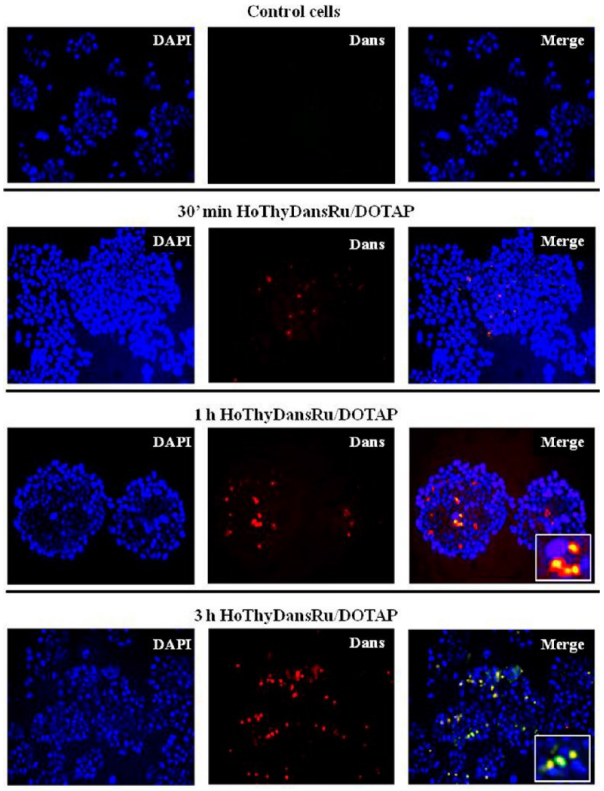

Figure 18. Fluorescent microphotographs of monolayers showing the cellular location of dansylated-HoThyDansRu complex into human MCF-7 breast adenocarcinoma cells subsequent to nanocarriers application. MCF-7 were incubated with 100 μM of the intrinsically fluorescent HoThyDansRu/DOTAP liposome solution for 30 min, 1 h, and 3 h. DAPI is used as a nuclear stain (shown in blue). Dansyl dependent fluorescence (Dans) of HoThyDansRu/DOTAP liposomes is shown in red. In merged images (Merge), the two fluorescent emissions are overlapped (Mangiapia et al., 2013).

AIM OF THE PROJECT

This proposal is part of a broader multidisciplinary research project aimed at the development of biocompatible and stable amphiphilic molecules containing Ru(III) complexes, assembled in selective nanostructures able to improve their efficacy and bioavailability with respect to the well-known NAMI complex, already under clinical trial. The interest toward ruthenium arises from its promising anticancer properties as reported in literature by others and our research team, showing the high antiproliferative activity of novel Ru-complexes. At this stage we have tested the amphiphilic nucleolipid ruthenium-based complexes (named ToThyRu, HoThyRu and DoHuRu), which contain the low molecular weight complex AziRu as "active metal part", and which are co-aggregated with the lipids POPC (1-palmitoil-2oleoil-sn-glycero-3fosfocolina) and DOTAP (N- [1- (2,3-dioleoilossi) propyl] -N, N, N-trimetilammonio methyl-sulfate) (Mangiapia et a., 2013; Vitiello et al., 2015). The evaluation of the biological activity of Ru-based complexes is achieved by means of *in vitro* experimental models of human tumours and metastases of different histological origin. As well, the *in vitro* bioactivity profile toward healthy cells will be also assessed in order to establish the biocompatibility of the compounds under testing. The used human tumour cell lines - characterized by different metastatic potential and cultured according to the ATCC (American Type Culture Collection) procedures - are included in the cellular lines panel of the National Cancer Institute (USA) for the bioscreening of the antitumour and antimetastatic effects.

Many different ruthenium compounds have been recently tested for their anticancer properties, without enough investigations into both their mode of action at cellular level and their mechanism of action at the molecular level. In this frame, given that the identification of the exact mode of action is critical not only for drug classification but also for the rational design of new compounds with enhanced properties, an important goal of this work is to deeper elucidate the molecular mechanisms of action of ruthenium in cancer cells, giving

more insights about the activated cell death pathways as well as the main molecular biological targets involved through a series of *in vitro* bioscreens. In particular, by focusing on well-established breast cancer cell lines as *in vitro* models for human mammary tumours (such as the endocrine-responsive (ER) breast adenocarcinoma MCF-7 and the triple-negative breast adenocarcinoma (TNBC) MDA-MB-231 cell models, together with their variants CG5, MDA-MB-436 and MDA-MB-468), we report *via* preclinical bioscreens how ruthenium complexes administration can activate specific molecular cell death pathways, thereby interfering with cancer cells growth and proliferation.

In addition, given the importance of tumour microenvironment for the efficacy of the most common anticancer therapy, as for the Ru(III) complexes (because of their "activation by reduction"), and considering that the microenvironment is rich in immune adaptive cells, a further study of this work, realized in collaboration with the clinical immunology laboratory at the faculty of Pharmacy in Paris, concerns the role of EPO on extra-erythroid components - such as immune system cells - and the evaluation of exogenous EPO administration impact on tumour intake/growth and on tumour immune environment in the 4T1 mouse mammary carcinoma cells transplanted into Balb/c female mice. In this respect, some studies have shown that EPO might promote tumour proliferation both *in vitro* on primary or cell lines and *in vivo* models, whereas other show an absence of a direct action on tumours. Otherwise, EPO's action on tumorigenesis might be mediated, at least in part, by EPO's role in angiogenesis as demonstrated in mouse models, through activation of endothelial cells, which is also a matter of debate.

Furthermore, recent studies have explored in depth the impact of EPO-delivery on the immune system. EPO receptors expression at the mRNA level has already been demonstrated in T cells, B cells and macrophages in several species, including human. Despite huge efforts and years of research spent on both clinical and experimental model

development, neither mechanisms underlying the increase in tumour progression nor the markers of susceptibility have been identified. However, the individual EPO susceptibility might modulate immunity and impact tumour surveillance.

Giving that $CD11b^{+}Ly6G^{+}$ tumour-infiltrating lymphocytes population is decreased in EPO-treated mice, as described before, in order to evaluate the gene expression profiles by RT-qPCR on FACS-sorted and to discriminate between the anti-tumourigenic (such as IL-12, TNFα, ICAM1), and the pro-tumourigenic (such as Arginase 1, iNOS, MMP9, CCL3) phenotypes, as well as to classify the different polarization of the adaptive immune cells, such as CD4 (Th1, Th2, Th17 or Treg), 4T1 breast tumour cells were intra-dermal injected nearby the mammary gland of Balb/c female mice.

In addition, a further step of this study is focused on the determination of cytokine and chemokine profiles induced by EPO in the tumour microenvironment and peripheral blood as well as in draying lymph nodes. Identifying the most relevant source of immune suppressive factors (such as TGF-β and IL-17) produced by immune cells and/or tumour cells themselves could be an important step in the characterization of the cascade of events underling the EPO tolerogenic effect. To this aim, a large panel of cytokines and chemokines has been analyzed in purified tumour-associated immune cells as well as in serum of tumour-bearing mice. In this setting, the levels of the main Th1-, Th2-, Th17- and Treg-derived cytokines as well as chemokines known for their neutrophil attraction potential has been analyzed by Cytometric Bead Array or ELISA.

MATERIALS AND METHODS

4.1 Cell cultures

Human cancer cell lines have been a useful tool for the study of the genetics, molecular biology, biology, and therapy of cancer in many tumor types, including breast cancer (Chavez et al., 2010).

Human breast adenocarcinoma cells, epithelial-like type as MCF-7, CG-5, MDA-MB-231 and MDA-MB-468 lines, and pleomorphic-like type as MDA-MB-436 line, were grown in DMEM (Invitrogen, Paisley, UK) supplemented with 10% fetal bovine serum (FBS, Cambrex, Verviers, Belgium), L-glutamine (2 mM, Sigma, Milan, Italy), penicillin (100 units/ml, Sigma) and streptomycin (100 μg/ml, Sigma), and cultured in a humidified 5% carbon dioxide atmosphere at 37°C, according to ATCC recommendations. MCF-7 and CG-5 are endocrine-responsive (ER) breast cancers; MDA-MB-231, MDA-MB-468 and MDA-MB-436 are triple-negative breast cancers (TNBC) (Lacroix et al., 2004; Holliday et al., 2011). Human HaCaT keratinocytes and rat L6 skeletal muscle cells, used as healthy control cell lines, were grown in the same experimental conditions.

- **MCF-7 cells**, (HTB-22, ATCC), human breast adenocarcinoma cells isolated from a 69-year-old Caucasian woman. Initially they are distributed in monolayer ("Cell Biology" ATCC protocol) retaining several characteristics of differentiated mammary epithelium including ability to process estradiol via cytoplasmic estrogen receptors and the capability of forming domes. Their growth is inhibited by the tumor necrosis factor alpha (TNF α). The cells express the WNT7B oncogene.
- **CG-5 cells**, derived from a casual contamination by MCF-7 cells of a primary culture from a pleural effusion of a patient with postmenopausal advanced breast cancer, a generous gift from Dr Sica (Institute of General Histology and Embryology, Catholic University “Sacro Cuore”, Rome, Italy) (Natoli et al., 1983). The characterization of this MCF-7 variant revealed chromosomal properties highly similar and alloenzyme

phenotypes identical to those of MCF-7 cells. However, CG-5 cells contain higher concentrations of steroid receptors and are more sensitive to the proliferative effect of estrogens than MCF-7 cells (Badino et al., 1996).

- **MDA-MB-231 cells**, are aneuploid female, with chromosome counts in the near-triploid range. Normal chromosomes N8 and N15 were absent. Eleven stable rearranged marker chromosomes are noted as well as unassignable chromosomes in addition to the majority of autosomes that are trisomic (ATCC HTB-26). Many of the marker chromosomes are identical to those shown in the karyotype reported by Satya-Prakash and coworkers (Satya-Prakash et al., 1981). MDA-MB-231 cells present a precise spectrum of proteolytic activities; they are also characterized by a relatively rare steroid receptor status (two of them are estrogen receptor-negative (ER−)/progesterone receptor-positive (PgR+), the third is ER+/PgR−) (Lacroix et al., 2004).
- **MDA-MB-468 cells**, were isolated in 1977 by Cailleau et al., from a 51-year-old female patient with metastatic adenocarcinoma of the breast, and is commonly used in cancer research (Cailleau et al., 1978). These cells were extracted from pleural effusion of mammary gland and breast tissue, and have proven useful for the study of metastasis, migration and invasion of breast cancer (ATCC HTB-132). MDA-468, is a breast cancer cell line with a very high number of EGF receptors and is growth-inhibited at EGF concentrations, that stimulate most other cells **(**Filmus et al., 1985).
- **MDA-MB-436**, breast cancer cell line was first derived from pleural fluid obtained from a 43-year-old breast cancer Caucasian patient in 1976. MDA-MB-436 is pleomorphic with multinucleated component cells and reacts intensely with anti-tubulin antibody. *In vitro*, the MDA-MB-436 cell line has abundant activity in both the Boyden chamber chemo invasion and chemotaxis assay (ATCC HTB-130).

4.2 Synthesis of the ruthenium complexes ToThyRu, HoThyRu and DoHuRu and preparation of the lipid-based nanoaggregates

The ruthenium complexes investigated, ToThyRu, HoThyRu and DoHuRu were prepared by reacting in stoichiometric amounts the starting nucleolipids, named ToThy, HoThy or DoHu (Simeone et al, 2011) with the Ru complex [*trans*-RuCl4(DMSO)2]$^{-}$Na^{+} following a previously described procedure (Mangiapia et al., 2012). All the synthetic intermediates and the final nucleolipidic Ru(III) complexes were obtained in a pure form and characterized by ESI-MS and NMR analysis in order to confirm their identity. Remarkably, the signals in the 1H NMR spectra of the nucleolipid-based Ru(III) complexes are particularly diagnostic of the effective complex formation (Velders et al., 2004). Detailed microstructural characterization of these nucleolipidic complexes was carried out in pure water and in a pseudo-physiological solution, through an experimental strategy combining small-angle neutron scattering (SANS) to analyze the aggregate morphology as well as to determine their geometrical characteristics, dynamic light scattering (DLS) to estimate aggregate dimensions and electron paramagnetic resonance (EPR) to provide information on the dynamics of the lipid hydrophobic tail in the bilayer. Furthermore, biological validation of these nanocarriers was carried out by studying their cytotoxicity profiles on a panel of different human and non-human cell lines (Riccardi et al., 2017).

4.3 *In vitro* bioscreens

The anticancer activity of ruthenium-containing nucleolipidic nanoparticles and of AziRu was investigated through the estimation of a “cell survival index”, arising from the combination of cell viability evaluation with cell counting (Mangiapia et al., 2012). More

specifically, the cell survival index is calculated as the arithmetic mean between the percentage values derived from the MTT assay and the automated cell count, providing a more accurate parameter of the concrete number of cells that survive after a preclinical *in vitro* study (Irace et al., 2017). Cells were inoculated in 96-microwell culture plates at a density of 10^4 cells/well, and allowed to grow for 24 h. The medium was then replaced with fresh medium and cells were treated for further 48 h with a range of concentrations (1 → 1000 μM) of AziRu, and of ToThyRu and DoHuRu complexes lodged either in POPC or DOTAP liposomes (ToThyRu/POPC and ToThyRu/DOTAP, DoHuRu/POPC and DoHuRu/DOTAP, respectively). Using the same experimental procedure, cell cultures were also incubated with ruthenium-free ToThy/POPC, ToThy/DOTAP, DoHu/POPC and DoHu/DOTAP liposomes as negative controls, as well as with cisplatin (*c*DDP) - a positive control for cytotoxic effects. Cell viability was evaluated using the MTT assay procedure, which measures the level of mitochondrial dehydrogenase activity using the yellow 3-(4,5-dimethyl-2-thiazolyl)-2,5-diphenyl-2H-tetrazolium bromide (MTT, Sigma) as substrate. The assay is based on the redox ability of living mitochondria to convert dissolved MTT into insoluble purple formazan. Briefly, after the treatments, the medium was removed and the cells were incubated with 20 μl/well of a MTT solution (5 mg/ml) for 1 h in a humidified 5% CO2 incubator at 37 °C. The incubation was stopped by removing the MTT solution and by adding 100 μl/well of DMSO to solubilize the obtained formazan. Finally, the absorbance was monitored at 550 nm using a microplate reader (iMark microplate reader, Bio-Rad, Milan, Italy). Cell number was determined by TC10 automated cell counter (Bio-Rad, Milan, Italy), providing an accurate and reproducible total count of cells and a live/dead ratio in one step by a specific dye (trypan blue) exclusion assay. Bio-Rad's TC10 automated cell counter uses disposable slides, TC10 trypan blue dye (0.4% trypan blue dye w/v in 0.81% sodium chloride and 0.06% potassium phosphate dibasic solution) and a CCD camera to count cells

based on the analyses of captured images. Once the loaded slide is inserted into the slide port, the TC10 automatically focuses on the cells, detects the presence of trypan blue dye and provides the count. When cells are damaged or dead, trypan blue can enter the cell allowing living cells to be counted. Operationally, after treatments in 96-microwell culture plates, the medium was removed and the cells were collected. Ten microliters of cell suspension, mixed with 0.4% trypan blue solution at 1:1 ratio, were loaded into the chambers of disposable slides. The results are expressed in terms of total cell count (number of cells per ml). If trypan blue is detected, the instrument also accounts for the dilution and shows live cell count and percent viability. Total counts and live/dead ratio from random samples for each cell line were subjected to comparisons with manual hemocytometers in control experiments. The calculation of the concentration required to inhibit the net increase in the cell number and viability by 50% (IC_{50}) is based on plots of data ($n = 6$ for each experiment) and repeated five times (total $n = 30$). IC_{50} values were obtained by means of a concentration response curve by nonlinear regression using a curve fitting program, GraphPad Prism 5.0, and are expressed as mean values ± SEM ($n = 30$) of five independent experiments.

4.4 Cell morphology

Human breast cancer cell lines were grown on 60 mm culture dishes by plating 5×10^5 cells. After reaching the subconfluence, cells were incubated for 48 h with IC_{50} concentrations of the ruthenium-containing liposomes (DoHuRu/POPC and DoHuRu/DOTAP) under the same *in vitro* experimental conditions described above and were then morphologically examined by a phase-contrast microscope (Labovert microscope, Leizt) for autophagic

vacuoles and apoptotic markers. Microphotographs at a 200 × total magnification (20 × objective and 10 × eyepiece) were taken with a standard VCR camera (Nikon).

4.5 Fluorescence microscopy and fluorescent probes

To evaluate the cellular uptake of the liposome, rhodamine B lipid derivative, 1,2- dioleoyl-sn-glycero-3-phosphoethanolamine-N-(lissamine rhodamine B sulfonyl) ammonium salt (λex 560 - λem 583 nm) (Figure 19), was used as a fluorescent probe by adding 2% mol during the synthesis of DoHuRu/DOTAP liposome. Sterile coverslips were placed in twenty-four-well plates. MCF-7 cells were seeded at a concentration of 5×10^4/ml in the same twenty-four-well plates. Following a growth period of 24 h at 37°C in RPMI 1640 medium containing 10% FBS, the medium was replaced with serum-free RPMI 1640 medium, which was followed by the addition of fluorescent liposomes at final concentration 100 μM or free PBS saline solution to each well. The cells were incubated for additional times (30 min, 1, 3 and 6 h) with liposomes and washed with PBS three times to remove unassociated liposomes. The cells were then fixed at room temperature in 4% paraformaldehyde for 20 min. After washing with PBS three times, the cells were treated with diaminophenylindole (DAPI) (Sigma) to stain the cell nuclei. The coverslip from each well was mounted onto a glass microslide with 80% fluorescence-free glycerol mounting medium. Finally, the interaction of liposomes with MCF-7 cells and the cellular uptake was monitored using a fluorescent microscope (Leica Microsystems GmbH, Wetzlar, Germany) to visualize DAPI (345/661 nm) and fluorescent liposomes (557/571 nm). Images were taken using an AxioCam HRc video-camera (Zeiss) connected to an Axioplan fluorescence microscope (Zeiss) using the AxioVision 3.1 software.

Furthermore, a fluorescently labeled nucleolipid has been designed using HoThyRu as the model compound. The dansyl group (λex 370 - λem 450 - 550 nm) has been here selected to provide the fluorescent tag because it offers several advantages, for example, high chemical stability, limited steric hindrance compared to other commonly used fluorescent dyes, and simple installation protocols. In addition, dansyl derivatives are very sensitive to the solvent polarity conditions, thus providing relevant information on the local environment in which they are found. The dansyl-labeled nucleolipid Ru(III) complex (here indicated as HoThyDansRu) and depicted in Figure 19 thus contains the following moieties:

• one pyridine-methyl arm at the N-3 position, as the privileged

ligand for the ruthenium complexation;

• a dansyl group attached via a sulfate bridge at the 2′position;

• one oleic acid residue at the 3′ position;

• one hexa(ethylene glycol) chain, capped with a benzyl group, in 5′ position.

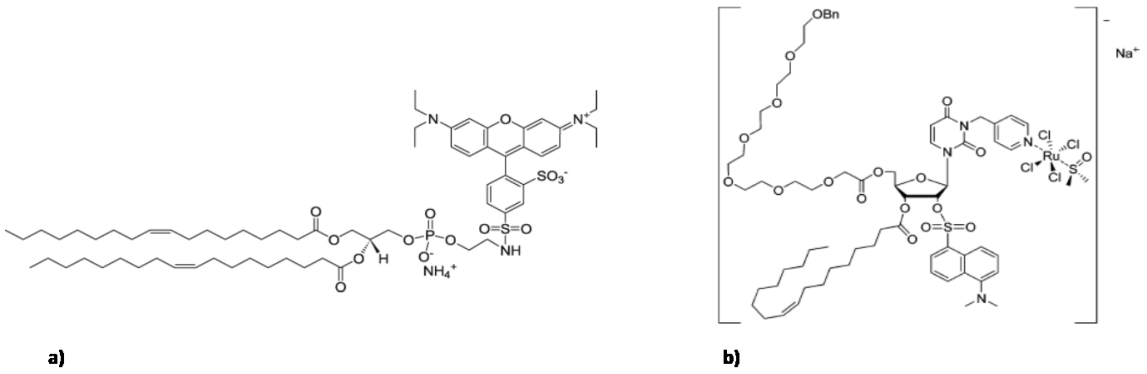

Figure 19. Molecular structure of **a)** Rhodamine-based fluorescent probe and **b)** HoThyDansRu (Mangiapia et al., 2013).

4.6 Immunostaining and confocal microscopy

For a detailed investigation of the cellular mechanism of action of the synthesized Ru(III) complexes, aiming at a deeper comprehension of their cell internalization process and metabolic fate, the fluorescent dansyl- labeled nucleolipidic complex HoThyDansRu (above described) has been used. Hence, human MCF-7 breast adenocarcinoma cells were exposed or not to 100 μM of the cationic dansylated HoThyDansRu/DOTAP nanoaggregate for 30 min, 1, 2, 3, and 4 hours, in the same experimental condition described for bioscreen *in vitro*. After treatments, cells were fixed for 20 minutes with a 3% (w/v) paraformaldehyde (PFA) solution and permeabilized for 10 minutes with 0.1% (w/v) Triton X-100 in phosphate-buffered saline (PBS) at room temperature. To prevent nonspecific interactions of antibodies, cells were treated for 2 h in 5% bovine albumin serum (BSA) in PBS. Immunostaining was carried out by incubation with Alexa Fluor 647 Anti-Human CD324 (E-Cadherin) Antibody (BIOLEGEND) (Shamran et al., 2017); DAPI/Moviol Pro Long Diamond Antifade Mountant with Dapi (Invitrogen) was used as nuclear stain. The slides were mounted on microscope slides by Mowiol. The analyses were performed with a Zeiss LSM 510 microscope equipped with a plan-apochromat objective X 63 (NA 1.4) in oil immersion.

4.7 Subcellular fractionation and ICP-MS analysis for ruthenium intracellular localization

Breast cancer cells, such as MCF-7 and MDA-MB-231 cells, were grown on standard plastic 100 mm culture dishes by plating 8×10^5 cells. After 24 h of growth, the cells were incubated with IC_{50} doses of the “naked” AziRu and DoHuRu/DOTAP liposome for 48 h under the

same experimental conditions described for bioscreens. At the end of the treatment, the culture medium was collected and the cells were enzymatically harvested by trypsin, then centrifuged at RT for 3 min at 1300 × *g*. The cell pellets obtained were, then, resuspended in 500 µl of a solution I (10 mM HEPES pH 7.9, 10 mM KCl, 0.1 mM $MgCl_2$, 0.1 mM EDTA, 0.1 mM DTT, Protease Inhibitor Cocktail) and centrifuged at 2000 × *g* for 10 min at 4°C. The supernatant, representing the cytosolic f raction, was separated from the pellets which instead contained the nuclear and mitochondrial fraction. Furthermore, the pellets were washed 3 times with the solution I and 200 µl of lysis buffer (10mM HEPES, 3 mM MgCl2, 40 mM KCl, 5% glycerol, 1 mM DTT, 0.2% NP40) was added and incubated for 30 min in ice. After centrifugation at 4°C for 30 min at 1300 ×*g*, the pellets containing the nuclear fraction were obtained.

Furthermore, to obtain the purified DNA fraction, the pellets were suspended in DNA lysis buffer (50 mM Tris-HCl, pH 8.0, 5 mM EDTA, 100 mM NaCl, 1% SDS, 0.5 mg/mL Proteinase K) and incubated at 50 °C for 1 h. After incubation, 10 mg/ml RNase was added to the lysates and incubated for 1 h at 50°C. DNA was precipitated with NaOAc pH 5.2 and ice cold 100% EtOH and centrifuged at 14000 × *g* for 10 min. Pellets were dissolved in TE buffer (10 mM Tris-HCl, pH 8.0, 1 mM EDTA). Aliquots of culture medium, cellular pellet, cytosolic fraction, nuclear fraction and DNA sample were analyzed by inductively coupled plasma-mass spectrometry **(**ICP-MS) to determine the ruthenium amounts.

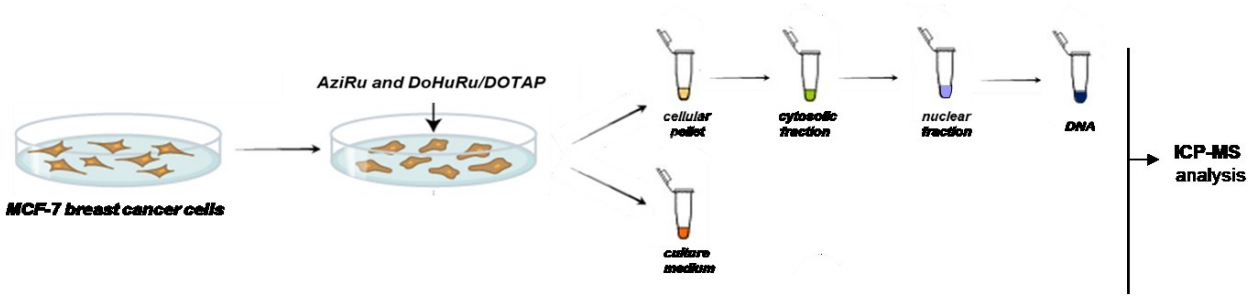

Figure 20. Schematic representation of subcellular fractionation coupled to ICP-MSS spectrometry.

4.8 DNA fragmentation assay

MCF-7 and MDA-MB-231 cells were grown on standard plastic 60 mm culture dishes by plating 5×10^5 cells. After 24 h of growth the cells were treated for 48 h with IC_{50} doses of DoHuRu/ POPC and DoHuRu/DOTAP liposomes under the same experimental conditions described for bioscreens, as well as with IC_{50} doses of cisplatin (*c*DDP) - a positive control for *in vitro* apoptosis (Okamura et al., 2004). The DNA fragmentation assay was carried out as previously reported (Vitiello et al., 2015). After treatments, cells were collected and the pellets were suspended in lysis buffer (50 mM Tris-HCl, pH 8.0, 5 mM EDTA, 100 mM NaCl, 1% SDS, 0.5 mg/mL Proteinase K) and incubated at 50°C. After 1 h incubation, 10 mg/ml RNase was added to the lysates and incubated for 1 h at 50 °C. DNA was precipitated with NaOAc pH 5.2 and ice cold 100% EtOH and centrifuged at 14000 × *g* for 10 min. Pellets were dissolved in TE buffer (10 mM Tris-HCl, pH 8.0, 1 mM EDTA). A 20 µl aliquot of each DNA sample was analyzed on a 1.5% agarose gel stained with ethidium bromide and visualized under UV light.

4.9 FACS analysis

Annexin V-FITC (fluorescein isothiocyanate) was used in conjunction with a vital dye, propidium iodide (PI), to differentiate apoptotic (Annexin V-FITC positive, PI negative) from necrotic (Annexin V-FITC positive, propidium iodide positive) cells (Misso et al., 2013). Briefly, cells were incubated with Annexin V–FITC (MedSystems Diagnostics, Vienna, Austria) and propidium iodide (Sigma, St. Louis, MO, USA) in a binding buffer (10 mM HEPES, pH 7.4, 150 mM NaCl, 5 mM KCl, 1 mM MgCl2, 2.5 mM CaCl2) for 10 min at room temperature, washed and resuspended in the same buffer. Analysis of apoptotic cells was performed by flow cytometry (FACScan, Becton 4 Dickinson) (Esposito et al., 2009). For each sample, 2×10^4 events were acquired. The study was carried out by triplicate determination on at least three separate experiments (Figure 21).

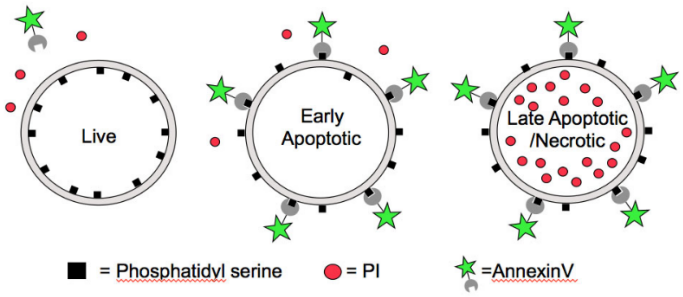

Figure 21. Double method of PI and Annexin V detection of apoptosis by FACS analysis (www.lifesci.dundee.ac.uk).

4.10 Labeling of autophagic vacuoles with monodansylcadaverine (MDC)

To quantify the induction of the autophagic process, MCF-7 and MDA-MB-231 cells, treated with IC_{50} concentrations of the DoHuRu/POPC and DoHuRu/DOTAP formulations, were stained with the autofluorescent agent monodansylcadaverine (MDC), a selective

marker for autophagic vacuoles (AVOs), especially for autolysosomes (Grimaldi et al., 2015). Treated cells were incubated with 50 μM MDC in PBS at 37°C for 15 min. After incubation, cells were washed twice with PBS, and immediately analyzed by flow cytometry with a FACScalibur flow cytometer (Becton Dickinson). The fluorescent emissions were collected through a 530 nm band pass filter (FL1 channel). At least 104 events were acquired in log mode. For the quantitative evaluation of MDC, CellQuest software (Becton Dickinson) was used to calculate mean fluorescence intensities (MFIs) (Figure 22). The MFIs were calculated by the formula (MFI treated/MFI control), where MFI treated is the fluorescence intensity of cells treated with the various compounds and MFI control is the fluorescence intensity of untreated and unstained cells.

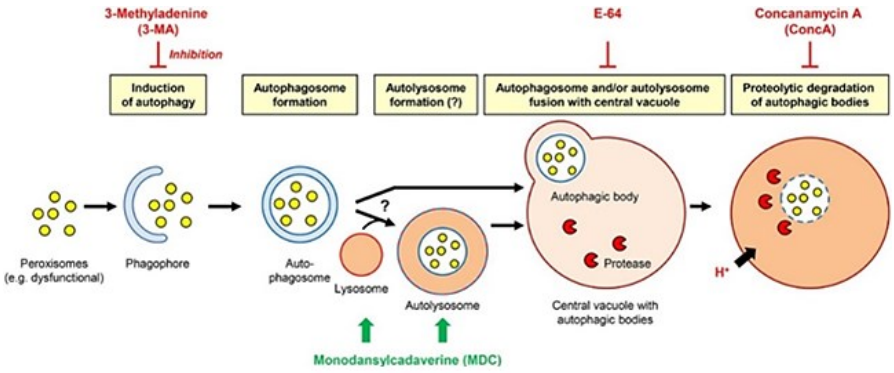

Figure 22. Schematic representation of the autophagic phases (www.frontiersin.org).

4.11 Preparation of cellular extracts

MCF-7 and MDA-MB-231 cells were cultured in standard plastic 60 mm culture dishes by plating 5×10^5 cells. Behind reaching the subconfluence, cells were incubated for 48 and 72

h with IC_{50} concentrations of the ruthenium-containing liposomes (DoHuRu/POPC and DoHuRu/DOTAP) under the same experimental conditions described above. After treatments, cells were washed and collected by scraping with PBS containing 1 mM EDTA and low-speed centrifugation. Cell pellets were then lysed at 4°C for 30 min in a buffer containing 20 mM Tris–HCl, pH 7.4, 150 mM NaCl, 5 mM EDTA, 5% (v/v) glycerol, 10 mM NP-40 and protease inhibitor tablets (Roche) (Miniaci et al., 2016). The supernatant fraction was obtained by centrifugation at 15,000 × g for 10 min at 4°C and then stored at −80°C. Protein concentration was determined by the Bio-Rad protein assay (Bio-Rad, Milan, Italy).

4.12 Western blot analysis

For Western blot analysis, samples containing 30–50 μg of proteins were loaded on 10% SDS–PAGE and transferred to nitrocellulose membranes (Fiorito et al., 2013; Marra et al., 2013). After blocking at room temperature in milk buffer [1 × PBS, 5–10% (w/v) non-fat dry milk, 0.2% (v/v) Tween-20], the membranes were incubated at 4°C overnight with: 1:500 rabbit polyclonal antibody to human caspase-8 (Santa Cruz Biotechnology, Santa Cruz, CA); 1:500 mouse monoclonal antibody to human caspase-9 (Santa Cruz Biotechnology); 1:500 rabbit polyclonal antibody to human caspase-3 (Santa Cruz Biotechnology); 1:500 rabbit polyclonal antibody to human Bcl-2 (26 kDa) (Santa Cruz Biotechnology); 1:250 rabbit polyclonal antibody to human Bax (Santa Cruz Biotechnology, Santa Cruz); 1:1000 rabbit polyclonal antibody to human LC3B (Novus Biologicals); 1:100 mouse monoclonal antibody to human BECN1(E-8) (Santa Cruz Biotechnology, Santa Cruz). Subsequently, the membranes were incubated with peroxidase-conjugated goat anti-

rabbit IgG, or with peroxidase-conjugated goat anti-mouse IgG+IgM (all the secondary antibodies were purchased from Jackson ImmunoResearch Laboratories). The resulting immunocomplexes were visualized by the ECL chemoluminescence method (ECL, Amersham Biosciences Little Chalfont, Buckinghamshire, UK) and analyzed byan imaging system (ImageQuantTM400, GE Healthcare Life Sciences) (Russo et al., 2016). Densitometric analysis was conducted using the GS-800 imaging densitometer (Bio-Rad). Normalization of results was ensured by incubating the nitrocellulose membranes in parallel with the tubulin antibody.

4.13 Analysis of CD4 T helper polarization in draining lymph nodes

$CD4^+$ T helper (TH) cells play a central role in the adaptive immune system. Indeed, according to the type of pathogens (extracellular-, intracellular pathogens), $CD4^+$ Th cells will polarize either into Th1, Th2, Th9 or Th17. Thus CD4+ T cells secreting Th1 cytokines help macrophages and cytotoxic CD8 T cells to kill cancer or infected cells. Th2 cells secrete cytokine necessary for B cell differentiation into plasmocytes secreting antibodies. This type of adaptive immunity is necessary to eliminate extracellular pathogens. Finally, Th17 cells are mainly observed at the epithelial barriers where they help B and epithelial cells to block entrance of pathogens. Another type of CD4 T cells, named T regulators (Treg) are important in the tolerance. They secrete cytokine leading to the inhibition of immune cells. In order to study the polarization of CD4 helper T cells and the balance T effector/Treg, we choose to study gene expression of specific transcription factors or cytokines. The selected genes are represented in the Table 5.

CD4 populations	Transcription factors	cytokines
Th1	Tbet/Eomes	IFN-γ
Th2	GATA-3	IL-4 ; IL-10
Th17	RORγt	IL-17 ; IL-22
Treg	FoxP3	TGF-β; IL-10

Table 5. Main transcription factors and cytokines produced by the different populations of CD4 T cells. In bold appear the genes of which I analyzed expression.

4.14 FACS and cell sorting

Before analyzing the expression of these different genes, we need to purify CD4 T cells in the draining lymph nodes. To do that, the total cell population is stained with α-CD4 and α-CD8 antibodies coupled to fluorochromes and isolated thanks to the FACS (Fluorescence-activated Cell Sorting) (Figure 23). After isolation the CD4 T cells are lyzed and the total RNA are isolated according to the manufacturer's instruction (Qiagen).

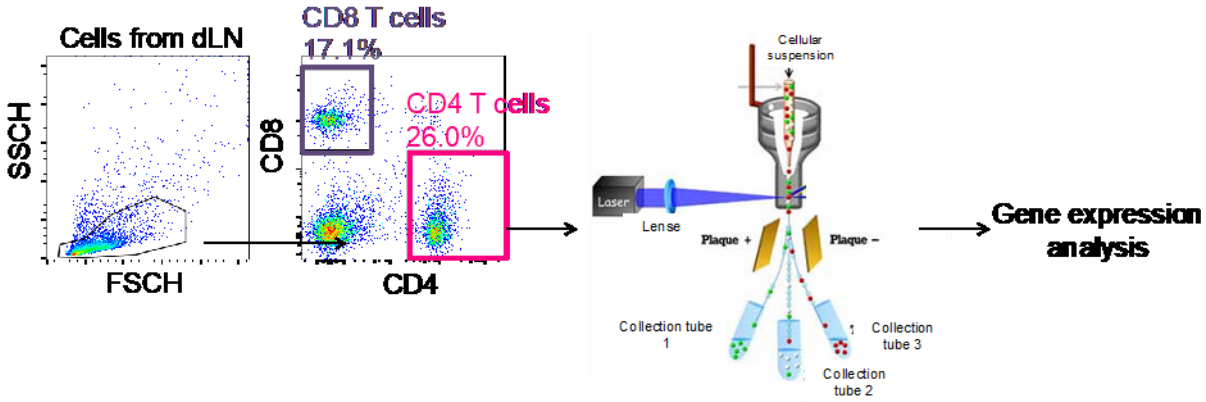

Figure 23. Protocol of CD4 T cell isolation and RNA extraction. Cells obtained from the draining lymph node were stained with specific antibodies α-CD16-32, α -CD4-BV421, α -CD8 α -AF700, during 30 min at 4°C. One experiment is representative of 7. The CD4 were then isolated thanks to the FACS technology (ARIA) and the total RNA was extracted and analyzed.

4.15 RT-qPCR

RT-qPCR can be performed in a one-step or a two-step assay. One-step assays combine reverse transcription and PCR in a single tube and buffer. In two-step assays (which we used), the reverse transcription and PCR steps are performed in separate tubes, with different optimized buffers, reaction conditions, and priming strategies.

By using this method, gene expression profiles of tumour-infiltrating immune cells have been analyzed. In particular, IFN-ɣ (Fw: GGATGCATTCATGAGTATTGC; Rv: CCTTTTCCGCTTCCTGAGG) , Tbet (Fw: GATCATCACTAAGCAAGGACGGC; Rv: AGACCACATCCACAAACATCCTG), IL-4 (Fw: TCGGCATTTTGAACGAGGTC; Rv: GAAAAGCCCGAAAGAGTCTC), FoxP3 (Fw: CACCCAGGAAAGACAGCAACC; Rv: GCAAGAGCTCTTGTCCATTGA) were analyzed. The housekeeping genes used are: GADPH (Fw: TGCGACTTCAACAGCAACTC; Rv: ATGTAGGCCATGAGGTCCAC); Rpl13 (Fw: ACAGCCACTCTGGAGGAGAA; Rv: GAGTCCGTTGGTCTTGAGGA); PPIA (Fw: TGGAGAGAAAGGATTTGGCTA; Rv: AAAACTGGGAACCGTTTGTG); b2m (Fw: ACTGATACATACGCCTGCAGAGTT; Rv; TCACATGTCTCGATCCCAGTAGA) and SDHA (Fw: ACACAGACCTGGTGGAGACC; Rv: GGATGGGCTTGGAGTAATCA).

4.16 Statistical analysis

All data were presented as mean values ± SEM. The statistical analysis was performed using Graph-Pad Prism (Graph-Pad software Inc., San Diego, CA) and ANOVA test for multiple comparisons was performed followed by Bonferroni's test.

RESULTS

5.1 *In vitro* bioscreens for anticancer activity

The antiproliferative properties of the liposomes containing the Ru(III)-nucleolipids were screened on human breast cancer models by means of selected mammary malignant cells endowed with different phenotypic and/or genotypic features and different replicative and/or invasive potential (MCF-7, CG-5, MDA-MB-231, MDA-MB-468 and MDA-MB-436 cell lines). The concentration-effect curves (Figure 24) - here reported in terms of a "cell survival index" (CSI) which combines the measurements of cell number and viability - show a typical concentration-dependent sigmoid trend yielding IC_{50} values in the low micromolar range. In particular, CSI is an adimensional value calculated by the arithmetic mean between the percentage values emerging from the MTT assay (a functional assay to evaluate cell viability) and the automated cell count (to determine the live/dead cells ratio). The simultaneous evaluation of cell survival by means of both a functional parameter and the actual number of live/dead cells allows for a more accurate information about cellular response to treatments during preclinical *in vitro* testing. According to the IC_{50} values (Table 6), the ToThyRu/DOTAP and DoHuRu/DOTAP formulations are the most effective in reducing the proliferation of all the used cell lines. This result, consistent with our previous reports, is likely associated to the positive charge of DOTAP formulations which can promote the interaction with the plasma membranes allowing a faster and quantitative drug cellular uptake (Mangiapia et al., 2013). Moreover, in relation to their effectiveness *in vitro*, there are no significant differences between the ToThyRu and DoHuRu nucleolipidic Ru(III) complexes used in our liposomial formulations, consistently with the rationale that the ruthenium center is the bioactive species, and the nucleolipids are simply carrier molecules (Riccardi et al., 2017). IC_{50} data normalization in favour of the actual ruthenium content enclosed in ToThyRu/DOTAP and DoHuRu/DOTAP liposomes (15% mol/mol), leads up to values of IC_{50} of about 3–4 μM in CG-5 cells and of about 10 μM in MCF-7 cells, suggestive

of a marked antiproliferative bioactivity *in vitro*. Overall, the calculated ruthenium IC_{50} values for DOTAP liposomes are in the low micromolar range (≤ 20 μM), similar or lower than those measured for cisplatin used in the same experimental conditions as a reference drug. All the breast cancer cells used in this screening are therefore sensitive to the action of metal-based drugs. The ruthenium IC_{50} values relative to cell growth inhibition in the presence of ToThyRu/POPC and DoHuRu/POPC formulations are also relevant, reaching values below 20 μM as in the case of MDA-MB-468, MCF-7 and CG-5 cancer cells. Looking further at IC_{50} values, the "naked" low molecular weight Ru(III) complex AziRu exhibits a milder antiproliferative activity on the same breast cancer cells, showing IC_{50} values constantly greater than 250 μM. These values are generally in agreement with those reported in the literature for the antimetastatic NAMI-A (Groessl et al., 2007), and once more highlight the critical importance of the delivery strategy to ensure the drug stability in the extra-cellular environment, a quantitative transport across the membranes and the bioavailability at the biological targets. Noteworthy, the bioactivity potentiating factors calculated as the ratio of IC_{50} values of the Ru(III)-containing liposomes with respect to the IC_{50} of AziRu, reach values of more than 20 in terms of antiproliferative ability (Vitiello et al., 2015).

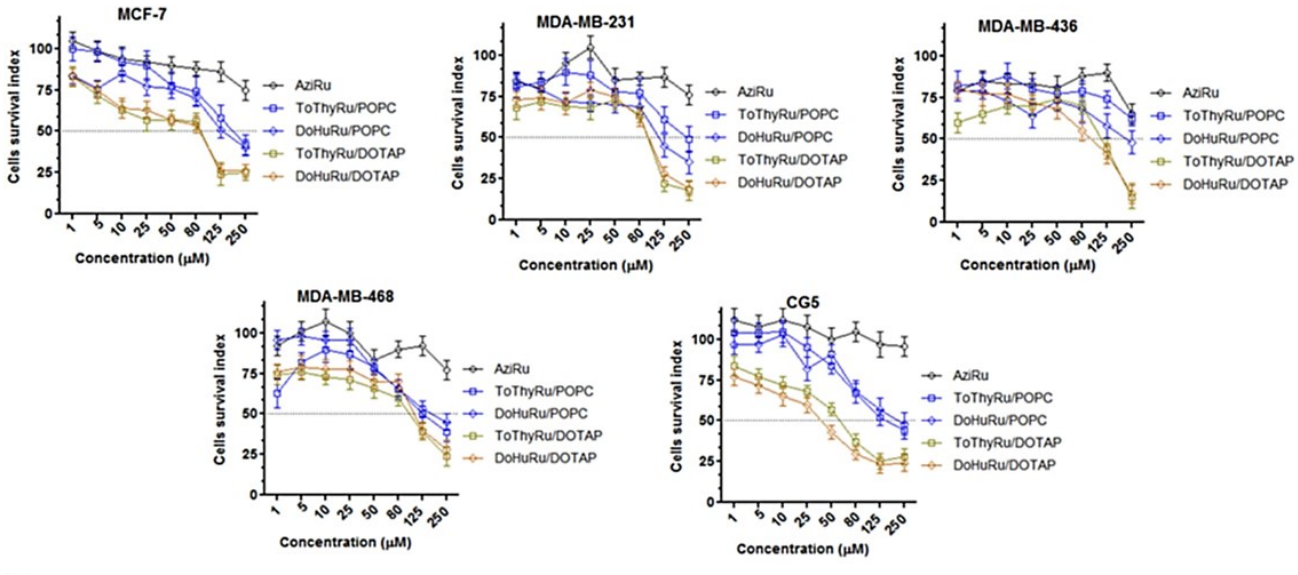

Figure 24. Cell survival index, evaluated by the MTT assay and monitoring of live/dead cell ratio for MCF-7, MDA-MB-231, MDA-MB-436, MDA-MB-468, and CG-5 cell lines following 48 h of incubation with the indicated concentration (the range 1 → 1000 μM has been explored, the one 1 → 250 μM is shown) of AziRu, and of the ruthenium-containing (15% mol/ mol) POPC formulations (ToThyRu/POPC and DoHuRu/POPC) and DOTAP formulations (ToThyRu/DOTAP and DoHuRu/DOTAP), as indicated in the legend. Data are expressed as percentage of untreated control cells and are reported as mean of five independent experiments ± SEM (n = 30).

Cell lines	IC$_{50}$(μM±SEM)									
	ToThyRu/POPC		DoHuRu/POPC		ToThyRu/DOTAP		DoHuRu/DOTAP		AziRu	*c*DDP
	Total liposome	Ru	Total liposome	Ru	Total liposome	Ru	Total liposome	Ru		
MCF-7	185 ± 0.1	27.8 ± 0.1	126 ± 0.1	18.9 ± 0.1	74.6 ± 0.1	10.1 ± 0.1	67.3 ± 0.2	10.3 ± 0.2	>250	17 ± 1
MDA-MB-231	239 ± 3	35.8 ± 3	98 ± 1	14.7 ± 1	79.5 ± 0.2	10.8 ± 0.2	81 ± 0.3	12.1 ± 0.3	>250	19 ± 1.5
MDA-MB-436	>250	>37.5	245 ± 1	36.7 ± 1	110 ± 0.2	15.0 ± 0.2	130.9 ± 0.2	20.0 ± 0.2	>250	NA
MDA-MB-468	111.1 ± 0.1	15.7 ± 0.1	136 ± 0.8	20.4 ± 0.8	107.8 ± 0.1	14.7 ± 0.1	95 ± 0.1	14.2 ± 0.1	>250	24 ± 1
CG-5	138 ± 0.2	19.4 ± 0.2	204 ± 0.8	30.6 ± 0.8	30.1 ± 0.2	4.1 ± 0.2	21.5 ± 0.2	3.3 ± 0.2	>250	NA

Table 6. IC$_{50}$ values (μM) relative to the specified POPC and DOTAP ruthenium-containing liposomes, and to cisplatin (*c*DDP), used as cytotoxic reference drug, and to the naked Azi-Ru complex in the listed breast cancer cell lines following 48 h of incubation. The ruthenium IC$_{50}$ values corresponding to the effective metal concentration (15% mol/mol) carried by each nanoaggregate are reported as mean values ± SEM (n = 30). (NA = not assessed).

5.2 Cellular morphological changes

Monitoring the cellular morphological changes over time can provide an additional support to the antiproliferative effects produced by ruthenium-based nanoaggregates. Throughout the *in vitro* trials, imaging end-points were collected by light microscopy from cells to assess cellular morphological changes induced by drug administration. Microphotographs in Figure 25a of MCF-7 and MDA-MB-231 breast adenocarcinoma cells, nowadays among the most reliable *in vitro* models of breast cancer, in the presence of DoHuRu/POPC and DoHuRu/DOTAP (at their IC_{50} concentrations for 48 and 72 h) are suggestive of the characteristic cell shrinkage as well as loss of cell-cell contact that accompanies apoptosis occurrence. Moreover, after *in vitro* treatments cells were morphologically examined at a higher magnification by a phase-contrast microscope for autophagic vacuoles formation. As shown in Figure 25b, in addition to apoptotic hallmarks, autophagic vacuoles clearly appear when MCF-7 cells were treated with the DoHuRu/DOTAP liposomes for 48 h at IC_{50} concentration, providing a morphological support of autophagy activation. These observations were further confirmed by FACS analysis, discussed below. Thus, the AziRu *in vitro* treatment by the DoHuRu/POPC liposome seems to trigger exclusively apoptosis, whereas the one with the cationic DoHuRu/DOTAP seems to simultaneously activate apoptosis and autophagy.

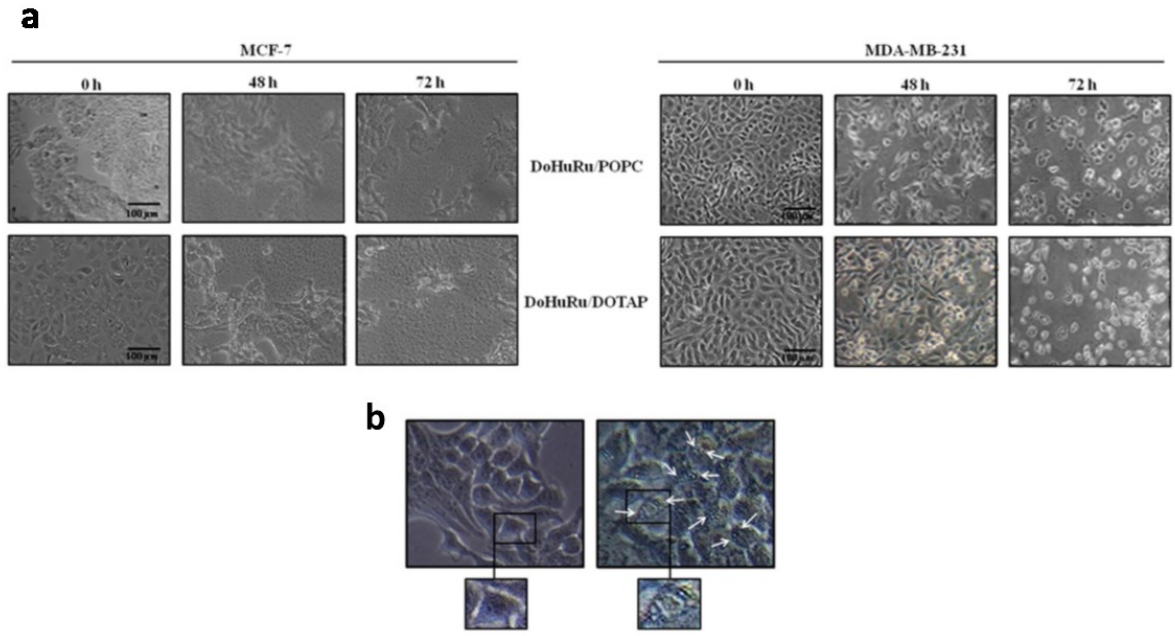

Figure 25. Cytomorphological alterations on cell monolayers **(a)** Representative microphotographs at a 200 × magnification (20 × objective and a 10 × eyepiece) by phase-contrast light microscopy of MCF-7 (left panels) and MDA-MB-231 (right panels) breast cancer cells treated for 48 and 72 h with ruthenium IC50 micromolar concentrations of DoHuRu/POPC (18.9 and 14.7 μ M, respectively) and DoHuRu/DOTAP liposomes (10.3 and 12.1 μM, respectively), showing the cellular morphological changes and the cytotoxic effects on cell monolayers. The shown images are representative of three independent experiments. **(b)** Representative microphotographs of untreated (left panel) and 48 h DoHuRu/DOTAP treated (right panel) MCF-7 cells by phase-contrast light microscopy at a 600 × magnification (30 × objective and a 20 × eyepiece). DoHuRu/DOTAP (at IC_{50} concentration) induces the formation of autophagic vacuoles detectable in cell cytoplasm. Inset: higher magnifications of MCF-7 cells before and after treatment.

5.3 Pro-apoptotic effects in breast cancer cells

Changes both in the cell morphology and in the monolayers appearance suggest that liposomes containing the nucleolipidic Ru(III)-complexes might have chemotherapeutic effects in human breast cancer initiating cells towards specific cell death pathways. The evaluation of apoptosis induction *via* FACS analysis has revealed that both DoHuRu/POPC and DoHuRu/DOTAP formulations are able to induce remarkable pro-apoptotic effects on MCF-7 cells and MDA-MB-231. In fact, as depicted in Figure 26a,c with reference to MCF-7 cells, the 46% of total cell population is in advanced stage of apoptosis following 48 h of exposure to IC_{50} concentrations of DoHuRu/DOTAP; further 24 h of treatment results in the

82% of cell population in late apoptosis phase. Milder pro-apoptotic effects, but nonetheless of significance, are detected in the case of DoHuRu/POPC treatment, leading after 48 h to about 36% of total MCF-7 cell population in early apoptosis and to a 37% in late apoptosis after 72 h. As a further validation of these data, no significant signals of apoptosis perturbation, such as an increased necrosis, were detectable by FACS analysis. A similar distribution of cell population among the different apoptotic stages has been observed by investigating the effects of liposomes containing nucleolipidic Ru(III)-complexes on MDA-MB-231 cells (Figure 26b,d), confirming the increased *in vitro* efficacy - especially as a trend over time - of the cationic nanoaggregates (*i.e.*, the DoHuRu/DOTAP ones) with respect to the zwitterionic POPC ones. This scenario is fully consistent with our previous studies (Mangiapia et al., 2013;Vitiello et al., 2015). As a result of different cellular uptake kinetics, ruthenium-containing cationic liposomes (DoHuRu/DOTAP) induce faster biological effects by way of cellular apoptosis activation than those dependent by the neutral liposomes (DoHuRu/POPC).

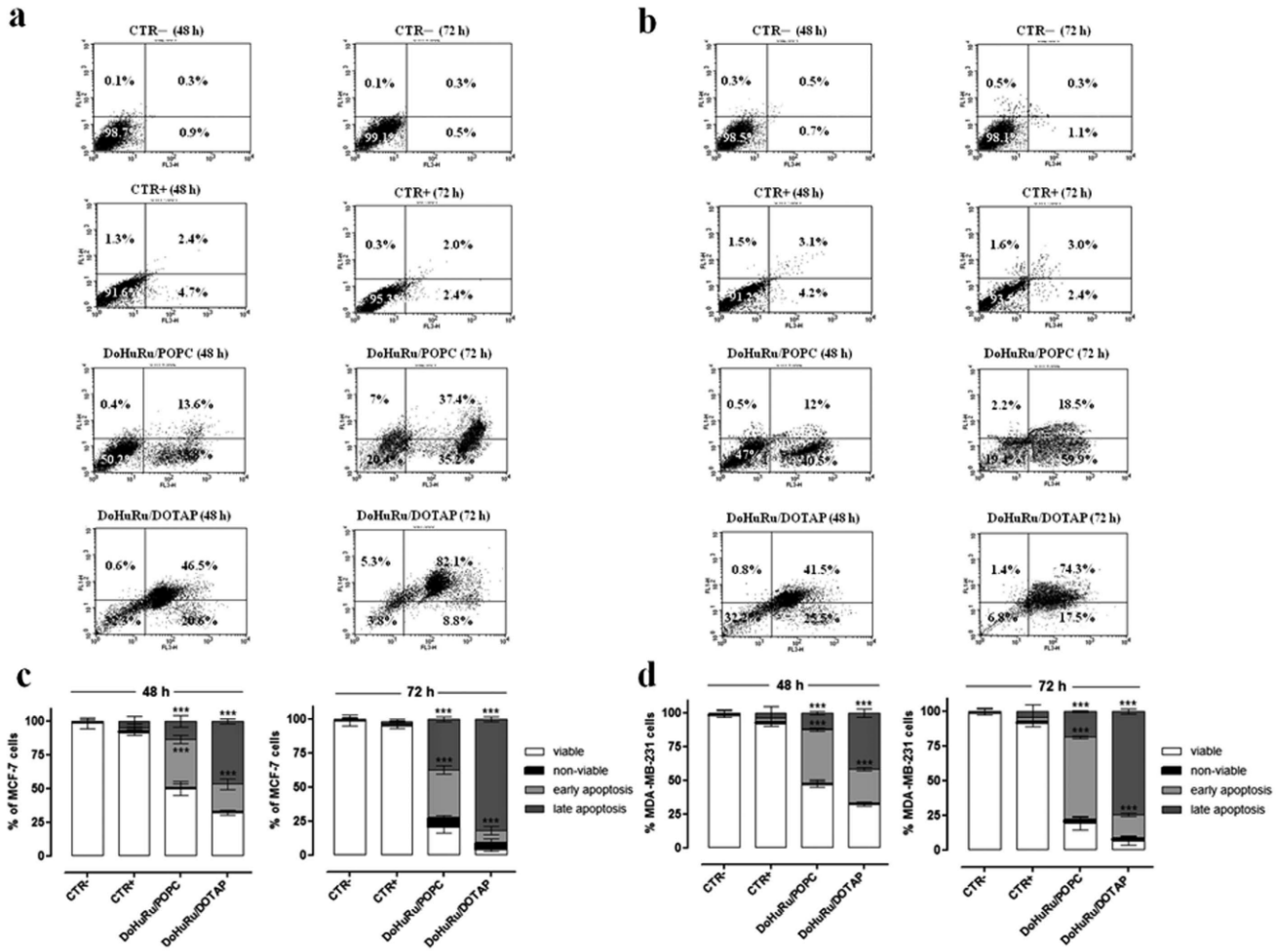

Figure 26. Induction of apoptosis in MCF-7 and MDA-MB-231 breast cancer cells. Apoptosis was evaluated by FACS analysis, after cell labeling with propidium iodide (PI) and FITC-Annexin V. MCF-7 **(a)** and MDA-MB-231 **(b)** cells were both unlabeled and untreated (CTR−), labeled and not treated (CTR +), treated with DoHuRu/POPC or with DoHuRu/DOTAP for 48 and 72 h using IC_{50} concentrations, as indicated. The lower left quadrants of each panels show the viable cells, which exclude PI and are negative for FITC-Annexin V binding. The upper left quadrants contain the non-viable, necrotic cells, negative for FITC-Annexin V binding and positive for PI uptake. The lower right quadrants represent the cells in early apoptosis, that are FITC Annexin V positive and PI negative. The upper right quadrants represent the cells in late apoptosis, positive for both FITC-Annexin V binding and for PI uptake. The experiments were performed at least three times with similar results. Quantitative analysis of viable, non-viable (necrotic), early and late apoptotic MCF-7 **(c)** and MDA-MB-231 **(d)** cells after 48 and 72 h of treatments are shown. Data are expressed as percentage of untreated control cells and are reported as mean of four independent experiments ± SEM (n = 24); ***p < 0.001 *vs.* control (untreated cells).

5.4 DNA fragmentation in MCF-7 and MDA-MB-231 breast cancer cells

It is generally accepted that DNA damage and subsequent induction of apoptosis is the primary cytotoxic mode of action of cisplatin and other metal-based antiproliferative drugs. In addition to shrinkage and fragmentation of the cells and nuclei, the apoptotic process is

accompanied by degradation of the chromosomal DNA into nucleosomal units. Indeed, late events of apoptosis typically lead to DNA cleavage, resulting in a “ladder” formation detectable by agarose gel electrophoresis. To verify apoptosis induction in breast cancer cells in a direct manner, we analyzed DNA degradation on genomic DNA samples obtained from treated cells. As depicted in Figure 27, though with a non-canonical nuclear fragmentation pattern in MCF-7 due to inherent caspase-3 expression deficiency, the DNA damage markedly increased in cells exposed to both DoHuRu/POPC and DoHuRu/DOTAP for 48 h at IC_{50} doses. Moreover, the typical internucleosomal DNA laddering of cell undergoing apoptosis clearly appeared in MDA-MB-231 cells, with a fragmentation pattern similar to that induced by IC_{50} doses of cisplatin *in vitro*, herein used as positive control (Okamura et al., 2004).

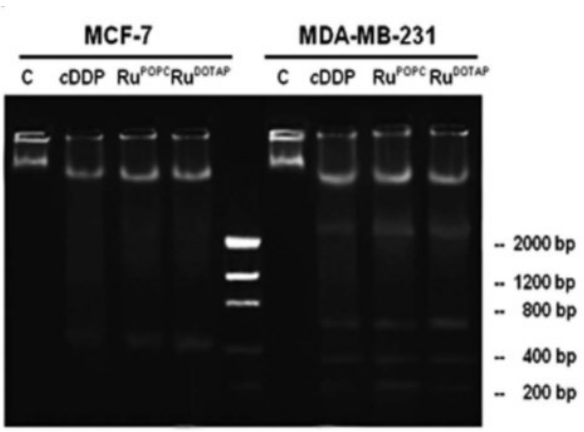

Figure 27. DNA fragmentation assay on MCF-7 and MDA-MB-231 cells treated or not (C) with IC_{50} concentrations of DoHuRu/POPC (RuPOPC) and DoHuRu/DOTAP (RuDOTAP) for 48 h, and with IC_{50} doses (17 and 19 μM, respectively) of cisplatin (*c*DDP) as the positive control for DNA fragmentation. After incubation, the DNA was extracted and visualized on 1.5% agarose gel as detailed in the Methods section. The lane in the middle corresponds to the molecular weight markers. The agarose gel is representative of three independent experiments.

5.5 Apoptotic-related proteins in MCF-7 and MDA-MB-231 breast cancer cells

Given that the expression profile of pro-apoptotic proteins is a central determinant for the death mode induced by ruthenium-based drugs, we analyzed the expression of proteins linked to the two main pathways that control mammalian apoptosis, *i.e.* the extrinsic (or death receptor) and intrinsic (or mitochondrial) apoptotic pathways. As determined by Western blot analysis reported in Figure 28a,c,e, protein extracts from MCF-7 exposed for 48 and 72 h to IC_{50} concentrations of DoHuRu/POPC and DoHuRu/DOTAP showed a remarkable increase in caspase-9 activity compared with control, whereas in the same experimental conditions no caspase-8 activation was detectable. Indeed, the activation of pro-caspase-9 involves intrinsic proteolytic processing, resulting in the production of an active p35 subunit. Moreover, as clearly detectable by immunoblot, an additional cleavage occurred producing a large p37 subunit which is known to amplify the apoptotic response. On the other hand, full length pro-caspase-8 expression was not affected by *in vitro* treatments. Taken together, these results suggest a ruthenium-dependent activation of the apoptotic mitochondrial pathway, wherein Bax and Bid are key cell death factors increasing mitochondrial permeability and release of cytochrome *c*. Conversely, cell survival factor Bcl-2 inhibits actions of Bax and Bid on mitochondria (Zheng et al., 2016). In MCF-7 cells Bax was significantly increased and Bcl-2 decreased upon DoHuRu/POPC and DoHuRu/DOTAP treatment - a cellular response predisposing to apoptosis activation. These biological effects were time-dependent and more evident following *in vitro* treatment with the cationic DoHuRu/ DOTAP liposomes. In the same way, ruthenium treatment in MDA-MB-231 breast cancer cells *via* DoHuRu/POPC and DoHuRu/ DOTAP *in vitro* administration at IC_{50} concentrations elicited caspase-9 activation after 48 h, and this anew was coupled to the simultaneous Bax and Bcl-2 up-regulation and down-regulation, respectively (Figure 28b,d,f). Furthermore, in this breast cancer cell line DoHuRu/DOTAP

seemed able to promote full length pro-caspase-8 cleavage, as evidenced by the formation of the active p10 and p18 fragments. In turn, activated initiator caspases further process other caspase members, including caspase-3 and caspase-7, to initiate a caspase cascade, which generally leads to complete the programmed cell death process. In fact, the immunoblotting analysis performed on MDA-MB-231 cells exposed to Ru(III)-containing liposomes further revealed a marked proteolytic cleavage of the inactive proenzyme to activate caspase-3. Hence, the evaluation of apoptosis regulatory proteins in breast cancer models for the *in vitro* preclinical evaluation of ruthenium biological effects suggests the invariable induction of the mitochondrial apoptotic cell death pathway, but also the cell-specific activation of the extrinsic death pathway particularly in the case of the cationic nanoaggregate. Interestingly, the treatment with either DoHuRu/POPC or DoHuRu/DOTAP alters the expression profile of Bax and Bcl-2 proteins with respect to basal amounts, radically changing the Bax/Bcl-2 ratio. The Bax up-regulation and Bcl-2 down-regulation observed in concert following ruthenium action may predispose cells to apoptosis (Zheng et al., 2016).

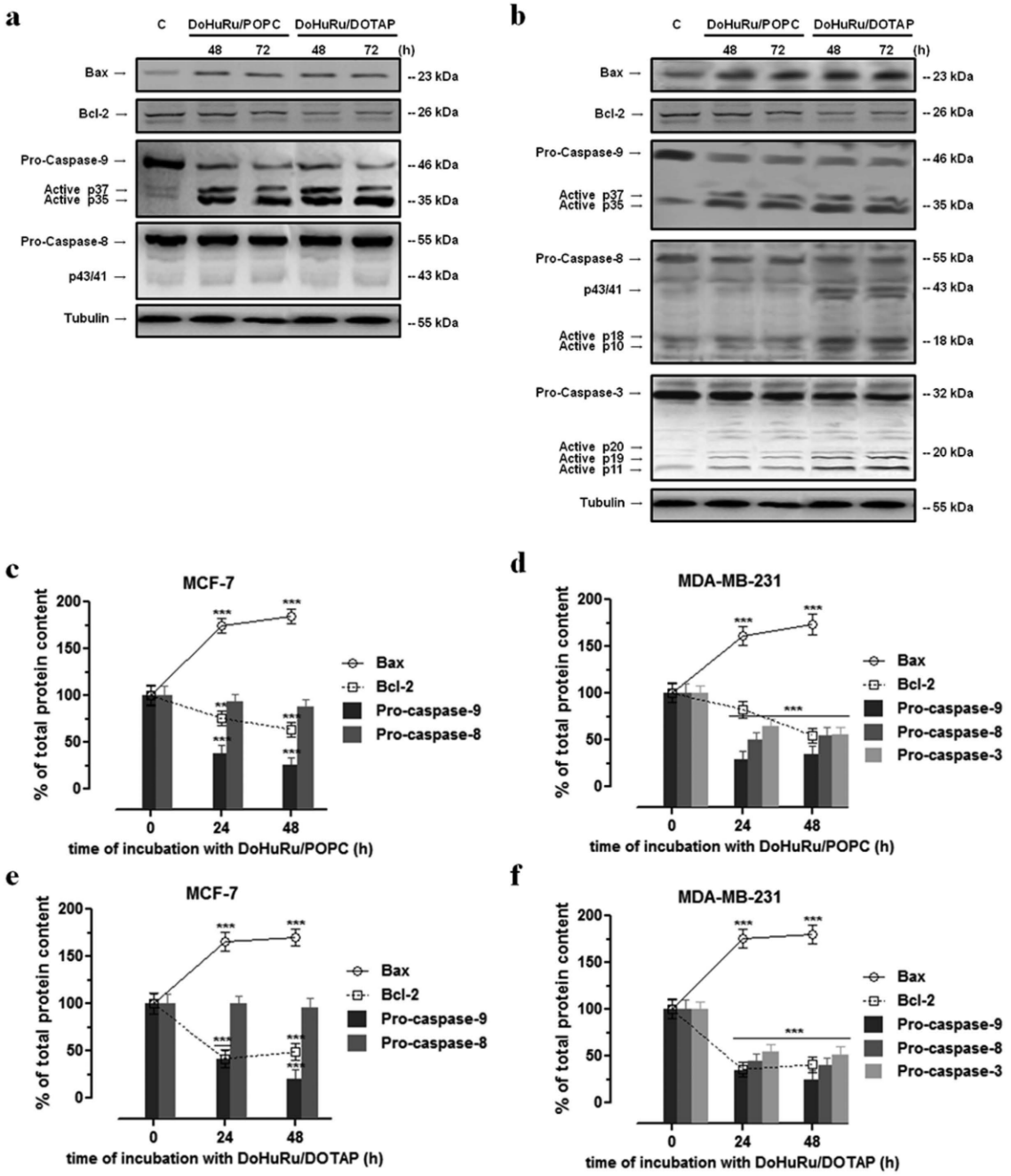

Figure 28. Apoptotic regulatory proteins in MCF-7 and MDA-MB-231 cells. Western blot analysis showing the effects of IC_{50} concentrations of DoHuRu/POPC and DoHuRu/DOTAP following 48 and 72 h of incubations in MCF-7 **(a)** and MDA-MB-231 **(b)** cells on caspases-3, -8 and -9 expression and activation, and on Bax and Bcl-2 expression, to characterize the apoptotic response. Shown are blots representative of four independent experiments. After chemoluminescence, the bands resulting from MCF-7 **(c, e)** and MDA-MB-231 **(d, f)** cell extracts were quantified by densitometric analysis and plotted in line (solid and dotted line for Bax and Bcl-2 proteins, respectively) and bar (caspases-3, -8 and -9) graphs as percentage of control in relation to the used ruthenium-containing nanoaggregate, as indicated. Shown are the average ± SEM values of four independent experiments. The anti-tubulin antibody was used to standardize the amounts of proteins in each lane. **p < 0.01 *vs.* control cells; ***p < 0.001 *vs.* control cells.

5.6 Autophagy activation in MCF-7 and MDA-MB-231 breast cancer cells

In addition to apoptosis, cellular suicide can also be executed *via* non-apoptotic forms of programmed death such as autophagy. The simultaneous evaluation of apoptosis and autophagy by means of the herein used methods is not mutually exclusive, *i.e.* it is possible to ascertain the degree of autophagy independently from that of apoptosis. Thus, to investigate whether DoHuRu/POPC and DoHuRu/DOTAP can also induce autophagy in MCF-7 and MDA-MB-231 cells, we have examined the formation of autophagic vacuoles using monodansylcadaverine (MDC), a selective autofluorescent dye for autolysosomes detection. Autolysosomes occurrence, which results from lysosomes-autophagosomes fusion, exclusively characterizes late steps in the autophagic cell death process. In order to verify this circumstance, cells were exposed for 48 and 72 h to ruthenium IC_{50} concentrations enclosed within DoHuRu/POPC and DoHuRu/DOTAP nanoaggregates (18.9 and 10.3 μM, respectively for MCF-7, 14.7 and 12.1 μM, respectively for MDA-MB-231) and the quantitative evaluation of MDC staining by means of FACS analysis was performed (Figure 29). As a result of MDC accumulation and consistently with phase contrast cell imaging, the cationic DoHuRu/DOTAP formulation induced an evident increase in the Mean Fluorescence Intensity (MFI), in particular 4.3 and 5.8-fold higher at 48 and 72 h for MCF-7, and 3.9 and 5.3-fold higher for MDA-MB-231 than untreated control cells. These results indicate an increased formation of the MDC-labeled vacuoles after ruthenium treatment *via* DoHuRu/DOTAP cationic liposomes and suggest the activation of autophagy in presence of apoptosis. Conversely, by using the zwitterionic DoHuRu/POPC liposomes, no significant autolysosomes formation was detected, at least up to 72 h.

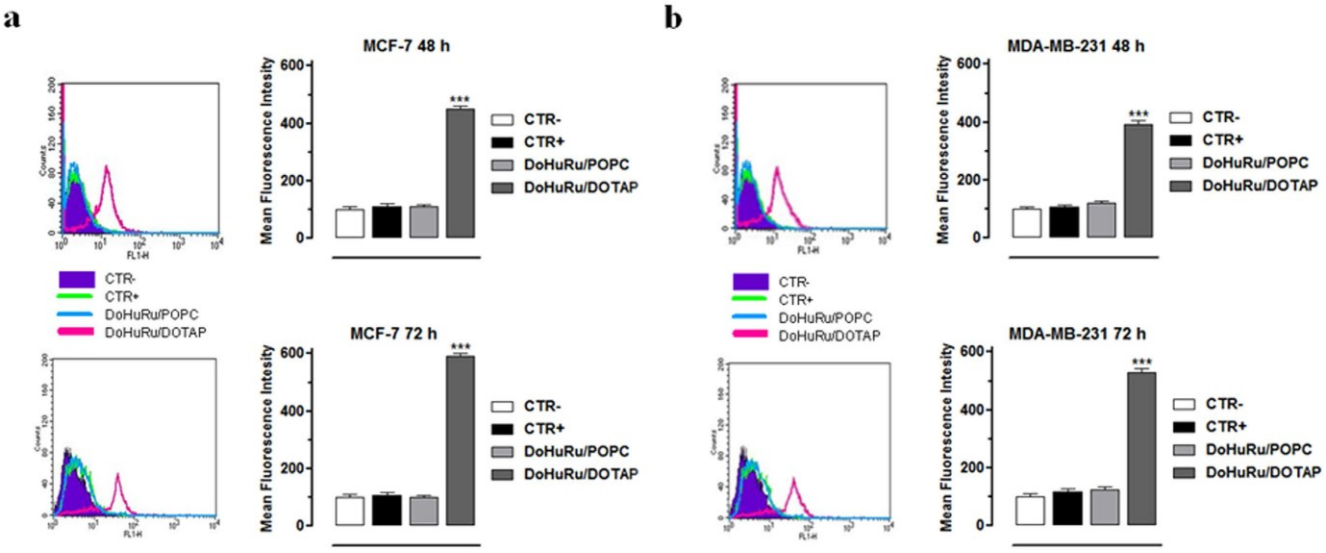

Figure 29. Autophagy activation in MCF-7 and MDA-MD-231 breast cancer cells.
Quantitative flow cytometric analysis of autophagosomes formation (MDC incorporation) in MCF-7 **(a)** and MDA-MB-231 **(b)** breast cancer cells, unlabeled and untreated (CTR−), labeled and untreated (CTR+), treated with IC_{50} concentrations of DoHuRu/POPC or with DoHuRu/DOTAP for 48 and 72 h, as indicated. The main fluorescence intensities (MFIs) were calculated, as described in 'Materials and Methods'. In the corresponding bar graphs, values are expressed as percentage of control cells and are reported as mean of four independent experiments ± SEM (n = 24); ***$p < 0.001$ *vs.* control (untreated cells).

5.7 Evaluation of the expression of the main autophagy-related proteins

Autophagy is bulk degradation of cytoplasmic components during which double-membrane vesicles, called autophagosomes, carry unwanted cell components to the lysosomes within an inner autophagic membrane. They then fuse liberating the autophagic body and its contents into the lumen of the vacuole for degradation. This is a complex process involving at least 16 proteins (Divac et al., 2017). However, LC3 is the only one known to form a stable association with the membrane of autophagosomes. It is known to exist in two forms: LC3-I, which is found in the cytoplasm and LC3-II, which is membrane-bound and is converted from LC3-I, to initiate formation and lengthening of the autophagosome (Ngabire and Kim, 2017). In this frame, detection of LC3 expression by immunoblot analysis is a useful biomarker to detect possible autophagy activation.

As can be evidently observed in Figure 30, protein samples from MCF-7 and MDA-MB-231 show evidence of a significant increase in both forms of LC3 protein following exposure *in vitro* to DoHuRu/DOTAP cationic Ru(III)-containing liposomes. Antibody for LC3 detection recognizes both the forms: LC3-II differs from LC3-I only in the fact it is covalently modified with lipid extensions and has undergone removal of a short amino acid sequence (Romao et al., 2014). This scenario is consistent with the previous reported detection of autophagic vacuoles in the same experimental conditions, as well as of autolysosomes occurrence in late steps of autophagic cell death process. Hence, allowing for the role of LC3 within the autophagic pathway and in the light of all the obtained data, DoHuRu/DOTAP is able to induce autophagy activation in addition to apoptosis, the main pathways of programmed cell death inhibiting the uncontrolled proliferation of cancer cells *in vitro*. On the other hand but still in accordance with the results shown above, the treatment with the zwitterionic DoHuRu/POPC formulation results in a non-significant increase in LC3 protein, thus suggestive of no autophagy activation.

These data were further substantiated by the study of the expression of the regulatory protein Beclin 1 throughout preclinical *in vitro* evaluations. Beclin 1 - a Bcl2 interacting protein - is the first identified mammalian gene to mediate autophagy and also has tumour suppressor and antiviral function (Ngabire and Kim, 2017). As already mentioned, autophagy is important for differentiation, survival during nutrient deprivation, and normal growth control, and is often defective in tumour cells. Indeed, expression of the Beclin 1 protein is frequently decreased in malignant breast epithelial cells (Packer et al., 2015). Based upon these observations, it is speculated that Beclin 1 may work through induction of autophagy to negatively regulate tumorigenesis and to control viral infections. Indeed, the autophagy-promoting activity of Beclin 1 in MCF-7 cells is associated with inhibition of cellular proliferation (Gong et al., 2013). Whilst not disposing of the healthy counterpart of MCF-7

cells as appropriate control to actually detect Beclin 1 down-regulation in cancer cell models, immunoblot experiments here show there are not neither significant changes following exposure to both neutral and cationic nucleolipidic Ru(III)-containing liposomes, nor further decrease in protein content with respect to untreated cells. This invariable basal amount of Beclin 1 we have detected in treated or not MCF-7 and MDA-MB-231 adenocarcinoma cells would be essential to enable the possible activation and execution of autophagic pathways following the administration of ruthenium-based drugs *in vitro*, as demonstrated by previous experiments. Certainly, some recent experimental evidences have shown a lack of autophagy pathways following total Beclin 1 depletion induced by different conditions.

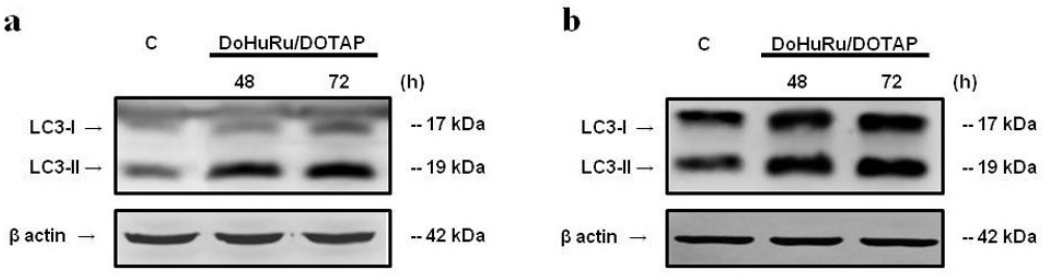

Figure 30. LC3 protein expression in MCF-7 and MDA-MB-231 cells. Western blot analysis showing the effects of IC_{50} concentrations of DoHuRu/DOTAP following 48 and 72 h of incubations in MCF-7 **(a)** and MDA-MB-231 **(b)** cells on LC3-I and LC3-II, to characterize the autophagic response. Shown are blots representative of four independent experiments. The anti-β-actin antibody was used to standardize the amounts of proteins in each lane.

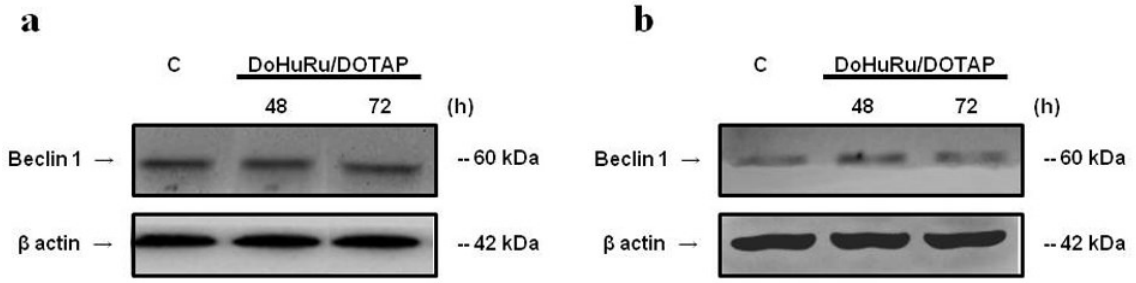

Figure 31. Beclin 1 protein expression in MCF-7 and MDA-MB-231 cells. Western blot analysis showing the effects of IC_{50} concentrations of DoHuRu/DOTAP following 48 and 72 h of incubations in MCF-7 **(a)** and MDA-MB-231 **(b)** cells on Beclin1, to characterize the autophagic response. Shown are blots representative of four independent experiments. The anti-β-actin antibody was used to standardize the amounts of proteins in each lane.

5.8 Sub-cellular compartmentalization and localization of Ru complexes

The internalization and accumulation of metal-based drugs into cancer cells is crucial for the therapeutic effect against tumours (McQuitty, 2014). For this reason, as already described in the introduction, we have previously investigated nucleolipidic Ru-containing liposomes interactions with cell membranes, along with the cell internalization processes (Mangiapia et al., 2012). To this aim, standardized protocol based on a rhodamine B fluorescent probe loaded into POPC and DOTAP liposomes has been used to evaluate their uptake in human carcinoma cells. Furthermore, additional *in vitro* fluorescence experiments have been performed by dansyl-labeled ruthenium complex loaded into nucleolipidic liposomes in order to assess the fate of the active ruthenium complex once inside target cancer cells. In this way we have demonstrated that nucleolipidic nanoaggregates rapidly interact with biological membranes allowing a massive cellular uptake, even after short incubation times such as 30 min and 1 h, in a process of cell internalization probably occurring by nonspecific patterns *via* membrane fusion and/or endocytosis. Therefore, once the ability of our nanovectors to transport the active ruthenium to cancer cells has been established, to give an

insight into the action mechanism of the AziRu complex so as to suppose possible interactions with specific biomolecular targets, new and more targeted experiments have been carried out to determine the accurate subcellular location of the active ruthenium. In particular, using *ad hoc* designed fluorescent formulations and confocal microscopy approaches, coupled to subcellular fractionation and inductively coupled plasma-mass spectrometry (ICP-MS), we have now further confirmed that Ru-nanovectors have a high propensity to cross cell membranes, and to massively accumulate within both cytoplasm and nuclear compartment, thus allowing ruthenium to interact with mitochondrial and nuclear molecular targets.

As far as confocal microscopy is concerned, aiming at a deeper comprehension of their cell internalization process and metabolic fate, a fluorescently labeled nucleolipid has been designed using HoThyRu as the model compound, as detailed in the experimental section. The dansyl group has been here selected to provide the fluorescent tag because it offers several advantages, *e.g.* high chemical stability, limited steric hindrance compared to other commonly used fluorescent dyes, and simple installation protocols. In addition, dansyl derivatives are very sensitive to the solvent polarity conditions, thus providing relevant information on the local environment in which they are found (Giordano et al., 1985). The dansyl-labeled nucleolipid Ru(III) complex - here indicated as HoThyDansRu - has been co-aggregated with DOTAP under the same conditions used for HoThyRu, ToThyRu, and DoHuRu (Mangiapia et al., 2013). In this way, the fate of the active ruthenium complex can be directly assessed, thereby examining its location after nanocarriers application to cells monolayers. Consistently with our previous results, fluorescently labeled HoThyDansRu/DOTAP localizes rapidly within MCF-7 cells, and microphotographs in Figure 32 clearly show a time course accumulation as the duration of incubations increased. The dansyl-dependent fluorescence occurs after very short contact times, and following 2

hours from the start of the treatment the fluorescent maximum diffusion is reached. Accordingly, the analysis of fluorescent emission also suggests that the complexes lodged in DOTAP liposomes enter the cytoplasm, spreading then to the whole cell including the perinuclear compartment; moreover, although attenuated by DAPI nuclear staining, dansyl-dependent fluorescence emission is also detectable in the nuclei area. After 4 hours of contact, cytotoxic effects induced on MCF-7 by ruthenium-containing liposomes begin to be detectable, *e.g.* altered adherens-junctions to bind cells together, as it is evident by the appraisal of the red E-cadherine-associated fluorescence. Cadherins are a class of type-1 transmembrane proteins which play important roles in cell adhesion, forming adherens junctions. They are dependent on calcium (Ca^{2+}) ions to function, hence their name. Cell-cell adhesion is mediated by extracellular cadherin domains, whereas the intracellular cytoplasmic tail associates with a large number of adaptor and signaling proteins, collectively referred to as the cadherin adhesome (Shamran et al., 2017). Overall, in addition to demonstrating an effective process of cellular uptake, the fluorescent patterns seem to suggest an intracellular liposome degradation coupled with the release of the pharmacologically active agent within the cytoplasm. This would explain the widespread dansyl-associated fluorescence and the concomitant generation of discrete dansyl-associated spots following cellular uptake and disaggregation of nanocarriers.

All these data on AziRu intracellular and metabolic fate following nucleolipidic liposomes application to cells were further confirmed by subcellular fractionation protocols performed on MCF-7 adenocarcinoma cells, coupled with subsequent analysis by inductively coupled plasma-mass spectrometry (ICP-MS). As shown in bar graph in Figure 33 and in comparison to the naked Azi-Ru complex, ruthenium assessment and localization in breast cancer cells after treatments *in vitro* firstly prove that cellular uptake is considerably increased by suitable nanovehiculation: although sufficiently lipophilic, much of Azi-Ru remains in the culture

medium, whereas large amounts of ruthenium are found at cellular level after treatment with DoHuRu/DOTAP liposome. Moreover, ICP-MS analysis performed on the isolated subcellular fractions indicate that the liposomial ruthenium entering the cells is widely distributed amongst the intracellular compartments, but above all at the nuclear level, as evidenced by the high metal content bound to nuclear DNA.

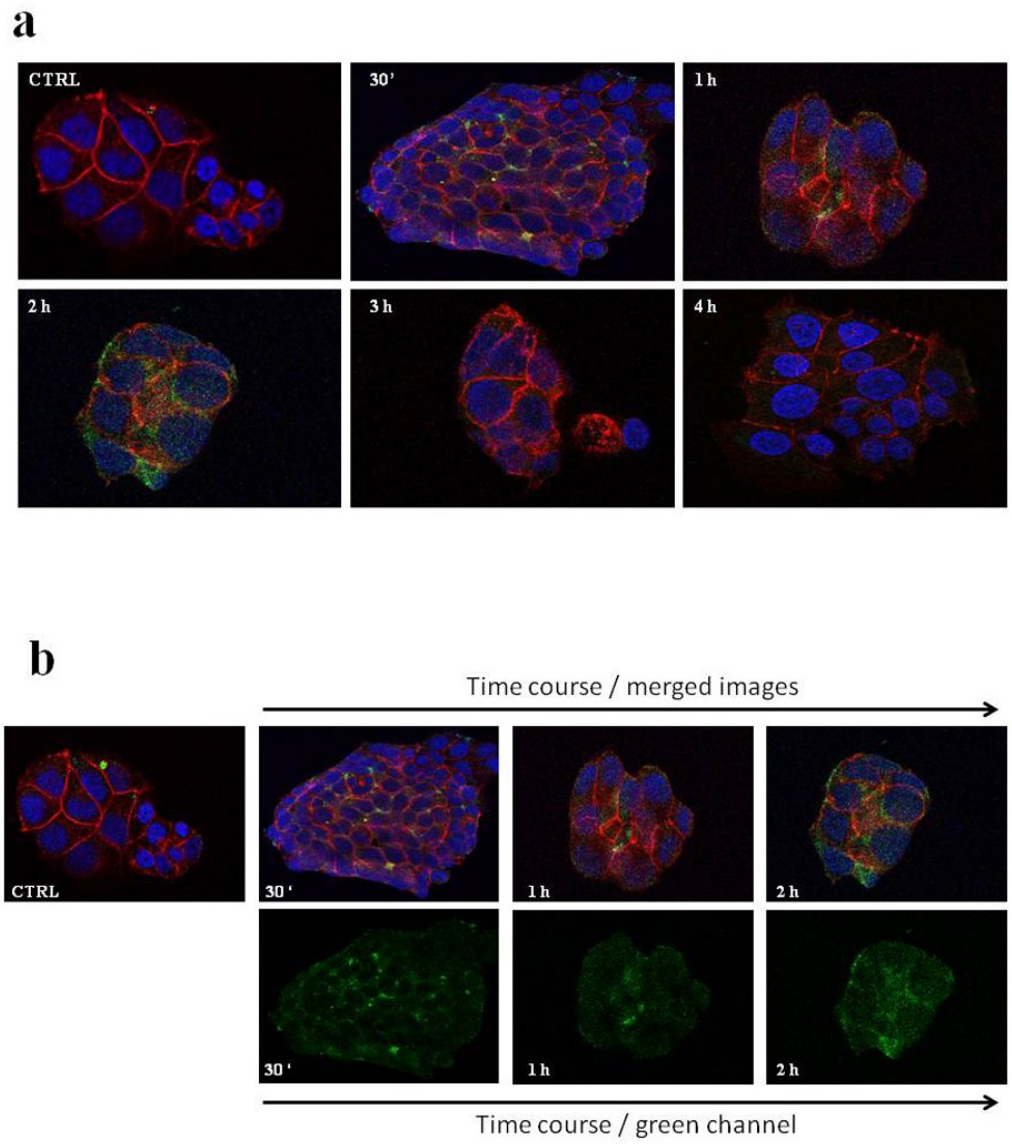

Figure 32. Fluorescent microphotographs by confocal microscopy of cell monolayers showing the intracellular localization of dansylated-HoThyDansRu complex into human MCF-7 breast adenocarcinoma cells subsequent to nanocarriers application. MCF-7 were incubated with 100 μM of the intrinsically fluorescent HoThyDansRu/DOTAP liposome solution for 30 min, 1, 2, 3, and 4 h. DAPI is used as a nuclear stain (shown in blue); fluorescent immunostaining of E-cadherine is used to highlight cell membranes (shown in red); dansyl-dependent fluorescence in HoThyDansRu/DOTAP liposomes is used to label the AziRu complex (shown in green). (a) In merged images of the time course experiment, the three fluorescent emissions are overlapped. The images shown are representative of three independent experiments. (b) Merged images and green channel imaging during the time course experiments to analyze the intracellular distribution of AziRu following 100 μM HoThyDansRu/DOTAP administration to MCF-7 for the indicated times.

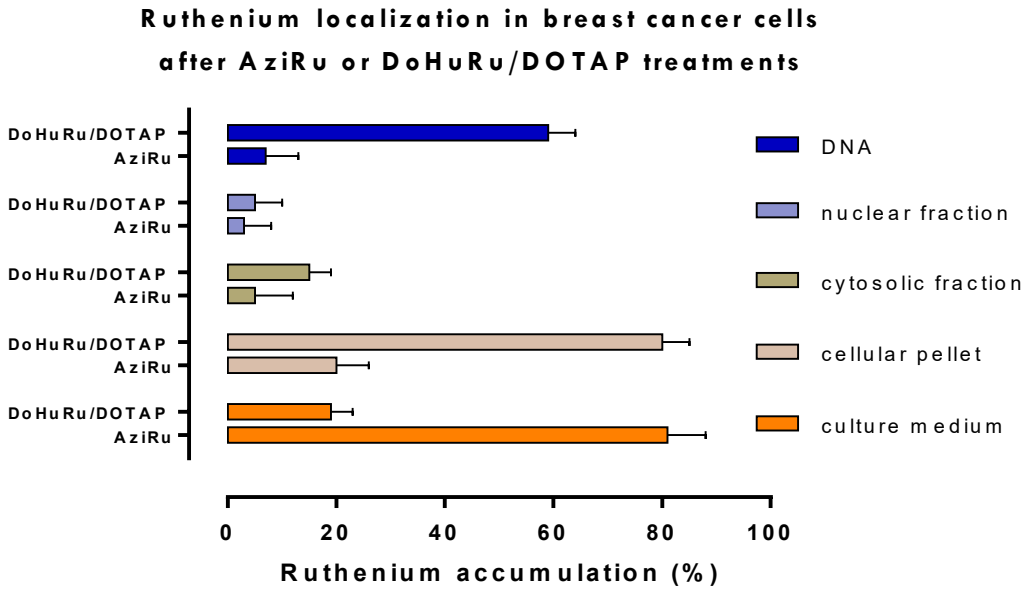

Figure 33. Localization and ruthenium accumulation by Inductively Coupled Plasma-Mass **S**pectrometry (ICP-MS) analysis following AziRu and DoHuRu/DOTAP application to MCF-7 cells and subcellular fractionation protocols, as deeply described in the experimental section. As shown in bar graph, and in comparison to the naked AziRu complex, the ruthenium assessment and localization in breast cancer cells after treatments with the cationic DoHuRu/DOTAP liposome is investigated, making an allowance for culture medium and cellular pellets, and for the subcellular cytosolic and nuclear compartments, as well as for DNA fraction.

5.9 Analysis of Th1 and Th2 related gene expression and EPO impact on Treg population

The data obtained show that gene expression of IFN-ɣ and Tbet is higher in PBS mice compared to EPO one at D14 after 4T1 engraftment (Figure 34, left and middle panel). At D16 and D20, expression of these genes is low in PBS and EPO groups (data not shown). Thus, EPO decreases the differentiation of CD4 T cells into Th1 profile. Surprisingly, whereas it is well known that Th1/Th17 cytokines inhibit Th2 development and vice and versa, we observed that at days 16 and 20, the gene expression level of IL-4 is also reduced in EPO mice (Figure 34, right panel). This last result needs to be confirmed, as the number

of experiment is low. Moreover, the analysis of IL-10 and GATA-3 gene expression will increment these preliminary results on EPO's effect on Th2 polarization.

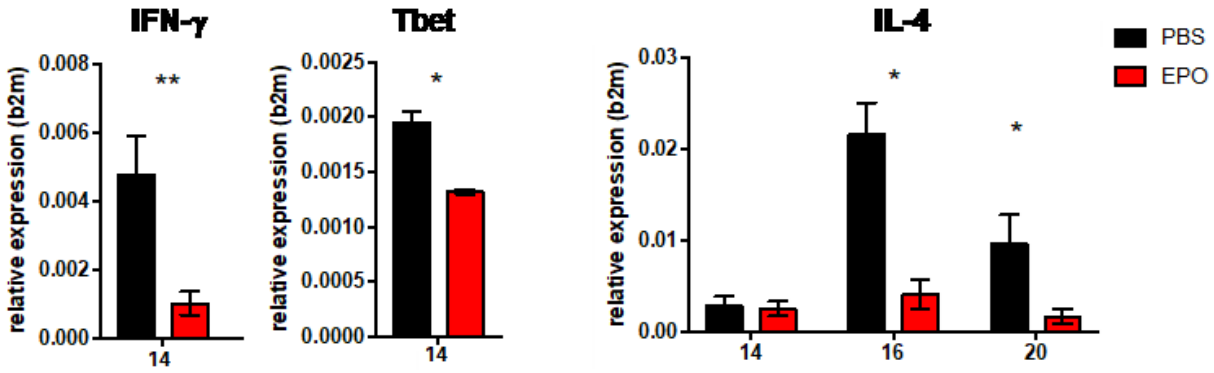

Figure 34. Analysis of Th1 and Th2 related gene expression. Gene expression of CD4 T cells from draining lymph node was analyzed on Light Cycler 480 (Roche) according to the manufacturer's instructions. At d14 n=4, D16 n=1, D20 n=2. Statistics: unpaired t test, *p<0.05, **p<0.01, ***<0.001.

As Treg suppress immune response, we also analyze effect of EPO on this population. To do so, we studied their specific transcription factor FoxP3 by RT-qPCR and evaluated the Treg number in the dLN. There is neither difference in the expression of FoxP3 gene in the CD4 population (Figure 35, left panel), nor difference in the absolute number of Treg in the dLN (Figure 35, right panel). In order to confirm this result, we will also analyzed the expression of TGF-β gene.

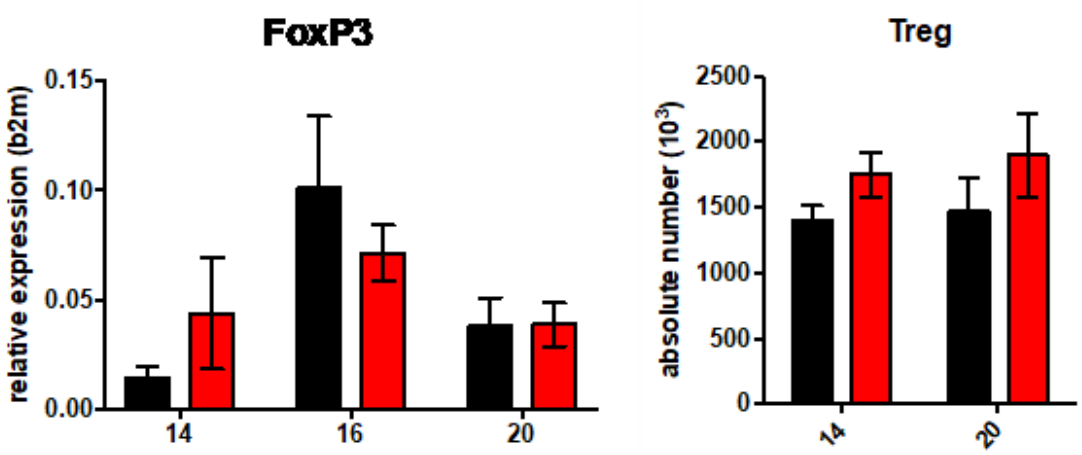

Figure 35. Analysis of EPO impact on Treg population. Left panel: gene expression of CD4 T cells from draining lymph node was analyzed on Light Cycler 480 (Roche) according to the manufacturer's instructions. At d14 n=4, D16 n=1, D20 n=2. Right panel: Treg population was analyzed by FACS and their count was calculated by multiplying the percentage of FoxP3+ CD4+ CD3+ cells among alive cells by the number found when we count cells at the microscope. At day 14-20 n=5. Statistics: unpaired t test, *p<0.05, **p<0.01, ***<0.001.

Finally, the team is also interested to look at the impact of EPO on Th17 polarization. The analysis of RORγt and IL-17 gene expression is ongoing.

5.10 Analysis TIL cells in tumour

In order to analyze the consequence of changes in Th polarization in dLN due to EPO treatment, we made the same analysis on Tumour-infiltrating lymphocytes. Unfortunately, no difference in the expression of genes specific for Th1, Th2 or Treg was found in the tumour (data not shown).

However, the proportion of CD8 T cells was already found to be decreased after EPO treatment. By analyzing gene expression of these cytotoxic CD8 T cells, we found a decrease of Tbet et IFN-γ gene expression at D14 after tumour engraftment in EPO-treated mice

compared to controls (Figure 36). A slight expression of Tbet in CD8 correlates with an exhaustion phenotype of CD8, that may explain the decrease of IFN-γ gene expression. Further studies need to be done to confirm this preliminary result (n=1). Moreover, the analysis of Eomes and KLRG1 gene expression as well as protein presence in CD8 TIL, is needed to conclude on EPO impact on CD8 effector T cells.

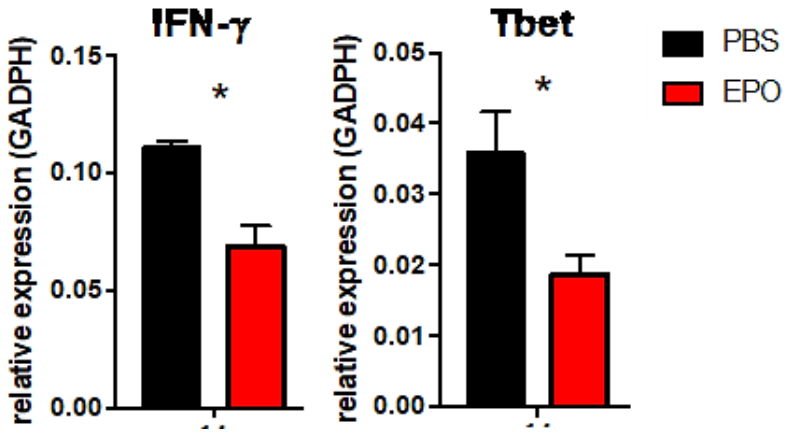

Figure 36. Analysis of EPO impact on CD8 TIL. Gene expression of CD8 T cells from tumour was analyzed on Light Cycler 480 (Roche) according to the manufacturer's instructions. At d14 n=1. Statistics: unpaired t test, *p<0.05, **p<0.01, ***<0.001.

DISCUSSION

Innovative anticancer drugs with new molecular mechanisms of action are essential in chemotherapeutic treatment to kill specific cancer types, and to overcome toxic side effects as well as chemoresistance (Hutchinson et al., 2010). Current research efforts are focused on a deeper understanding of the cellular response and/or resistance to anticancer treatments, including the role of cell death pathways activation, such as apoptosis and autophagy, by using chemotherapeutics (Holohan et al., 2013). Recently, we have developed new biocompatible ruthenium-based nanosystems, proved to be particularly effective against specific cell lines derived from human solid tumours (Mangiapia et al., 2013; Simeone et al., 2012; Riccardi et al., 2017). Starting from these encouraging data, we have first confirmed their efficacy focusing on a panel of human tumour cells arising from breast cancer. At the moment, the endocrine-responsive (ER) breast adenocarcinoma MCF-7 and the triple-negative breast adenocarcinoma (TNBC) MDA-MB-231 cell models account for the great majority of investigations on breast cancer cells and are considered the most reliable *in vitro* models of breast cancer together with their variants CG5, and MDA-MB-436 and MDA-MB-468, respectively (Lacroix et al., 2004; Holliday et al., 2011). All these cells are sensitive to cisplatin *in vitro*, so that cisplatin is currently the drug-based option in the therapeutic armamentarium. Although new types of ruthenium complexes with bigger anticancer activity *in vitro* have been meanwhile reported (Koceva-Chyła et al., 2016), the induction of comparable or even greater cytotoxic effects than cisplatin have been herein confirmed for nucleolipidic Ru(III) formulations. Then, aiming at an in-depth investigation of their mode of action, we have shown that amphiphilic ruthenium complexes, properly delivered by suitable nano-systems, are able to kill cancer cells by activating specific apoptotic processes, coupled in some cases to cellular autophagy. Indeed, in the last decade many different ruthenium compounds have been tested for their anticancer properties. However, all the reported studies have not clearly evidenced a unique mode of action at

cellular level, nor unambiguously defined a specific mechanism of action at molecular level (Alessio et al., 2016; Riccardi et al., 2017). In-depth bioanalytical studies have been so far performed especially for cisplatin, which have validated nuclear DNA as the main final drug target causing adducts formation and DNA damage, leading to cell division inhibition and cytotoxicity. In analogy with cisplatin, some of us have recently demonstrated that also AziRu and NAMI-A can interact with DNA model systems, with Ru(III) ions being incorporated into oligonucleotide structures *via* stable linkages (Musumeci et al., 2015). However, since an increasing number of evidences demonstrate that both ruthenium(II) and (III)-based drugs are able to interact with both intra- and extra-cellular protein targets, currently other molecular mechanisms of action cannot be excluded. Beyond molecular targeting, we have observed an invariable activation of programmed cell death pathways which confirms that the primary mode of action in breast cancer models of AziRu *via* DoHuRu/POPC and DoHuRu/DOTAP formulations is the induction of apoptosis. These data are largely in accordance with several reports highlighting the occurrence of distinct hallmarks of apoptosis after ruthenium administration *in vitro*. Cellular morphological changes and DNA fragmentation provided additional evidence of an apoptosis-inducing activity at the basis of the anticancer properties of AziRu. The regulation of apoptotic cell death orchestrated by intracellular caspases plays a fundamental role in the response to chemotherapeutics, as evasion of apoptosis is one of the central features of malignant progression as well as of drug resistance. Indeed, survival of malignant mammary cells is a key event in disease occurrence and progression, but also in therapy failure and chemoresistance development. Physiological mammary cells growth is controlled by a balance between cell proliferation and apoptosis. A large body of evidence has clarified that tumour growth is not just a result of uncontrolled proliferation but also of reduced apoptosis, so that the balance between proliferation and apoptosis is crucial in determining the overall

growth or regression of the tumour in response to chemotherapy. Two main pathways of caspase activation have been described in mammalian cells, which result in final control of apoptosis. In the intrinsic pathway, typically activated by intracellular stress signals, pro-apoptotic cell death factors belonging to the Bcl-2 family increase mitochondrial permeability and release of cytochrome *c*, as well as of other proteins from the intermembrane space of mitochondria. Apaf-1, a downstream mediator of apoptosis, along with cytochrome *c*, associates with caspase-9 in cytoplasm and leads to its activation. The resulting apoptosome initiates a cascade of effector caspases, which include caspases-3, -6, and -7. In turn, the active caspase-3 triggers DNA fragmentation factor (Caspase-Activated DNase, CAD) and promotes DNA internucleosomal cleavage. All the formulations containing nucleolipidic Ru(III)-complexes we have tested activate the mitochondrial apoptotic cell death pathway in breast cancer cells, as highlighted by a remarkable activation of caspase-9. Interestingly, this occurs independently of the cell ability to complete apoptosis process *via* the executioner caspase-3, as demonstrated by Ru-dependent activation of apoptosis in MCF-7. This adenocarcinoma model is known to be resistant to some chemotherapeutics due to a deletion in the CASP-3 gene that leads to an inherited deficiency of caspase-3. Caspase-3 - commonly turned on by numerous death signals - cleaves a variety of important cellular proteins and is ultimately responsible for apoptotic DNA fragmentation. Despite the lack of caspase-3 expression, liposomes containing nucleolipidic Ru(III)-complexes have hitherto shown to be particularly effective on this *in vitro* model. It has been also reported that MCF-7 undergoes cell death by apoptotic stimuli in the absence of the typical DNA fragmentation, and recent observations further suggest that large and small DNA fragments coupled to even single-strand cleavage events occur during apoptotic death. Consistently with our results, these observations have raised relevant questions on the degradation pattern of nuclear DNA in agarose gel electrophoresis detection, which remains

controversial. However, morphological changes and MCF-7 cell death were independent of caspase-3 and may correlate with the activation of different apoptotic pathways and other effector caspases, such as caspase-6 or -7. As far as the activation of programmed cell death pathways is concerned, DoHuRu/DOTAP formulation seems capable to concurrently activate the two major pathways of apoptosis in a cell-specific mode. In fact, MDA-MB-231 cells, undergoing the apoptotic mitochondrial pathway after exposure to DoHuRu/DOTAP, show an apparent proteolytic processing of pro-caspase-8 to form various fragments, including the active p18 and p10. The extrinsic pathway is activated by extracellular ligands able to bind to death receptors on the cell surface, which leads to the formation of the death-inducing signaling complex (DISC). This death receptor pathway is triggered by members of the death receptor superfamily such as CD95 and tumour necrosis factor receptor. Formation of a death-inducing signaling complex induces caspase-8 activation and thereby the downstream caspase cascade (Kiraz et al., 2016). We hypothesize that the cationic DOTAP nanoaggregate, by means of its inherent surface charge, can interact in peculiar manner with the external surface of cell membranes, as suggested by the faster cellular uptake kinetics compared to POPC formulations observed in a previous study. Although a hypothesis, exclusive molecular interactions coupled to local drug release could stimulate specific surface receptors involved in the activation of the extrinsic pathway. Indeed, not infrequently the killing of tumour cells by anticancer chemotherapeutics has been linked to activation of extrinsic apoptosis pathways. These outcomes are consistent with former investigations and demonstrate that some ruthenium(II) and (III) complexes can simultaneously trigger intrinsic and extrinsic apoptosis pathways. As far as the Bcl-2 family proteins are concerned, we believe that some central aspects closely linked to ruthenotherapy have emerged. Members of this family are regulatory proteins involved in the control of cell death, by either inducing (pro-apoptotic factors) or inhibiting (anti-apoptotic factors)

apoptosis. Bcl-2 is a crucial anti-apoptotic protein to be regarded as an oncogene, playing an important role in promoting cellular survival by inhibition of pro-apoptotic proteins. On the other hand, the pro-apoptotic effectors of the Bcl-2 family, including Bax, normally act on the mitochondrial membrane to promote permeabilization coupled to the release of both cytochrome *c* and ROS as important signals in the apoptosis cascade. Several clinical studies have provided support for an overexpression of the antiapoptotic Bcl-2 protein as a negative prognostic marker in various tumours. Alternatively, decreased Bax levels have been found in correlation with shorter survival in patients with breast cancer and colorectal cancer (Sturm et al., 2000). In MCF-7 and MDA-MB-231 we found an important effect induced by both DoHuRu/POPC and DoHuRu/DOTAP treatment on the cellular content of Bcl-2 and Bax, which could be correlated to the induction of the mitochondrial cell death pathway. The significant increase in Bax/Bcl-2 ratio detected in treated cells with respect to untreated cells could have an important impact in the regulation of cell fate by interfering with breast cancer cell survival. Indeed, in accordance with experimental and clinical investigations, tumours dependent on Bcl-2 family members are likely sensitive to Bcl-2 modulation in order to survive; in turn high Bax expression has been associated with a better response to chemotherapy in many cancers forms. Consistently with our results, it should be possible to circumvent the inherent apoptosis deficiency of malignant cells by directly affecting the mitochondrial function. In this way, following mechanisms yet to be clarified, the ruthenium complexes may interact with mitochondrial targets, possibly *via* selective accumulation and ROS generation. At the same time, dysfunction of mitochondria might be responsible for autophagic cell death. More and more studies underline the important interplay between apoptosis and autophagy, and suggest that apoptosis activation is often related to increased autophagy processes. As in the case of apoptosis, autophagy plays a vital role in cellular proliferation and survival, and dysregulated autophagy activation has been described in

many pathologies, including cancer. Although the role of the autophagic programmed cell death in neoplastic development remains to be clarified *in vivo*, cancer cells with up-regulated autophagy exhibit a less aggressive behavior as well as an increased susceptibility to chemotherapy. Autophagic degradation of cellular contents is employed by eukaryotes from yeast to man in order to maintain cellular homeostasis and protect against disease. The process involves the coordinated activity of a family of autophagy-related (ATG) proteins to mediate sequestration of cargo in a double-membrane vesicle (autophagosome) that then fuses to a lysosome (autolysosome) filled with, among other components, lysosomal enzymes. Studies now suggest that multiple forms of selective autophagy are continuously active at some basal level in order to maintain cellular homeostasis, whereas specific stimuli can activate selective autophagic pathways in order to address particular stressor. Coincident with its importance in maintaining cellular homeostasis, the disruption of selective autophagy pathways has been shown to play a role in diverse disease processes including cancer. In particular, studying the role of selective autophagy pathways has in part unraveled the complex role of autophagy in cancer as tumour suppressive and pro-tumourigenic dependent on context. Importantly, understanding the precise roles of various forms of selective autophagy in maintaining tumour growth provides the opportunity to target these processes more selectively. In this frame, the molecular mechanisms of selective autophagy receptor action and regulation are complex. The autophagy core machinery consists of a set of ATG proteins. Among these, LC3 is at the core of the autophagic process. As demonstrated by an ever-growing number of evidence, it is the only essential autophagy protein that can be found in the autophagosome after its completion, and therefore is the marker *par excellence* to experimentally monitor the fate of these vesicles. As above mentioned, the role of autophagy in cancer is extremely complex, as demonstrated by a growing literature describing situations where autophagy can either promote or inhibit

tumourigenesis. The most likely explanation is that the role of autophagy in cancer is dynamic with both tumour-suppressive and pro-tumourigenic roles, which depend on multiple factors including tumour stage, cellular context, and tissue of origin. Autophagy was initially considered a mechanism by which to suppress tumour initiation. However, recent work has brought to light tumour-suppressive selective autophagy pathways that can mitigate oncogenic signals and conversely selective autophagic pathways that support tumour maintenance and progression. More direct evidence of autophagy as a tumour suppressor came from mouse genetic studies of core autophagy machinery including ATG5, ATG7, and BECN1 (Beclin 1) showing that when autophagy is impaired, there is an increase in tumour initiation. Indeed, from a mechanistic standpoint, inhibition of autophagy leads to an accumulation of reactive oxygen species, increased DNA damage, and mitochondrial defects, all implicated in tumourigenesis. Another potential mechanism for tumour suppression by autophagy is *via* its role in cellular senescence. Cellular senescence is a program of permanent arrest of the cell division cycle that can be induced by cells in response to oncogenes in order to prevent malignant transformation. For sure, while the situation is very complex *in vivo*, the activation *in vitro* of autophagic pathways represents another challenging possible molecular mechanism to inhibit uncontrolled proliferation of cancer cells. However, studying the role of autophagy pathways in cancer has in part unraveled the complex role of autophagy in cancer as tumour suppressive and pro-tumourigenic, dependent on context. Importantly, understanding the precise roles of various forms of selective autophagy in maintaining tumour growth provides the opportunity to target these processes more selectively.

Since the effectiveness of many apoptosis-inducing chemotherapies can be affected by specific mutations in genes orchestrating apoptotic regulation, the activation of alternative cell death pathways, in tandem with or in the absence of an efficient apoptotic machinery,

may represent an attractive goal for novel metal-based chemotherapeutics. In this perspective, recent evidence supports the occurrence of the simultaneous induction of apoptosis and autophagy in cancer cells as a result of specific signaling. In addition, autophagy can be also activated upon exposure to genotoxic compounds, including several metal-based drugs able to target DNA. The induction of autophagy in the case of cationic nucleolipidic formulations could be linked to the ruthenium-induced down-regulation of the prosurvival protein Bcl-2, evident in both MCF-7 and MDA-MD-231 cells. Indeed, disturbances in the interaction between Beclin 1 and Bcl-2 family proteins, by which Beclin 1 is inhibited in normal conditions, has been established to stimulate cellular autophagy. Thus Ru(III) complexes activity in inhibiting breast cancer cells proliferation *via* DoHuRu/DOTAP administration would lie in the crosstalk connecting the main molecular mechanisms involved in the regulation of apoptosis and autophagy processes. Nevertheless, the existence of other non-apoptotic nor necrotic cell death pathways, triggered upon exposure to ruthenium-containing nanoaggregates we have documented in breast cancer models, needs further and more targeted studies. According to our previous findings (Mangiapia et al., 2012) and to recent literature reports (Koceva-Chyła et al., 2016; Qian et al., 2013) it cannot be excluded that the simultaneous activation of different mechanisms of cell death can be caused by multiple potential interactions at the subcellular/molecular level, both nuclear and cytosolic. Nevertheless, the activation of multiple death pathways by metal-based chemotherapeutics in aggressive cancer diseases with limited treatment options is a largely desired goal, in order to possibly restrict the onset of chemoresistance as well as to efficiently counteract uncontrolled proliferation (Figure 37).

Furthermore, giving the great importance of the tumour microenvironment on cancer growth as well as on the efficacy of the chemotherapy, upcoming investigations on the evaluation of the Ru(III)-containing liposomes impact on the tumour-infiltrating immune system cells

are underway to strengthen knowledge in favor of future *in vivo* applications for these high potential candidate drugs.

For a long time, tumour-related investigations were focused only on cancer cells, ignoring the environment created around the tumour. Indeed, it has been known that tumours are heterogeneous organs, rich in various number of components which are very important for the cancer growth and proliferation. In this setting, given that the immune cell compartment within the tumour is recognized as major driver, directly or indirectly, of angiogenesis and vascular remodeling in addition to the tumour cell itself (Li and Zhang, 2017), one of the interests of cell laboratories is to investigate the role of tumour-infiltrating immune system cells (such as TAM, TIL, CD4 T cells) and their secreted components, as well as their possible modulation.

In particular, CD4 T cells play essential roles in the function of the immune system. They are able to regulate different functions, such as to regulate/suppress immune responses both controlling autoimmunity and adjusting the extent and persistence of responses. They are divided into two major groups, designated Th1 and Th2 cells by Mosmann and Coffman, which are distinguished by the cytokines produced and through the expression of different patterns of cell surface molecules. Other types of CD4 T cells recognized are T regulators (Treg) - important in the tolerance and so able to the inhibition of immune cells - NKT, but also into Th9 or Th17 (Zhu et al., 2010).

Moreover, recent studies have shown a possible role of EPO in regulating tumour-infiltrating immune system cells within its micro environment, since EPO receptors -endowed with critical functions - have been identified on these cells surface (Feldman et al., 2006; Um et al., 2006; Henke et al., 2006).

Erythropoietin (EPO), the most widely used erythropoiesis-stimulating agent (ESA), is largely used in the treatment of anemia associated with chronic kidney disease (CKD)

(Eschbach et al., 1987), and also in cancer-related anemia in association with conventional chemotherapy (Littlewood et al., 2002).

Although erythropoiesis-stimulating agents (ESAs) reduce anemia in patients with cancer and could improve their quality of life, these drugs have been reported to might increase mortality (Bohlius et al., 2009). Indeed, they could induce tumour progression independently of the type of cancer or the anti-cancer treatment (Henke et al., 2003; Bohlius et al., 2009), even if mechanisms underlying the role of EPO/ESA on tumour proliferation still remain unknown and highly controversial.

Interestingly immunosuppressive role of EPO in humans has already been described by decreasing T cell function (Cravedi et al., 2003). In another hand, in an auto-immune encephalomyelitis mouse model, the beneficial effect of EPO was attributed to a Th2-polarized immune response. Moreover, EPO was shown in a mouse model of infection, to inhibit macrophage activation, through NF-κB pathway inhibition, impairing antibacterial function (Nairz et al., 2011).

In particular, studies carried out by Hacein-Bey-Abina's team show that EPO decreases the differentiation of CD4 T cells into Th1 profile, which is an anti-tumourigenic profile. Moreover, whereas it is well known that Th1/Th17 cytokines inhibit Th2 development (and vice and versa), we have observed that the gene expression level of IL-4 – principal cytokine secreted by Th2 - is also reduced in EPO treated mice.

Moreover, preliminary studies on the PNM:MDSC genes expression profile would indicate an increase in the expression of cytokines with immunosuppressive action but these results cannot be confirmed and so for the time we cannot conclude on the commitment toward the N2 profil, but further experiments are ongoing.

Therefore, in agreement with literature data, these results lastly demonstrate that *in vivo* EPO administration leads to an increase in tumour growth and proliferaition, probably due to a

direct effect on the immune system cells polarization within tumour microenvironment, showing an immunosuppressive profile along with a pro-tumourigenic activity.

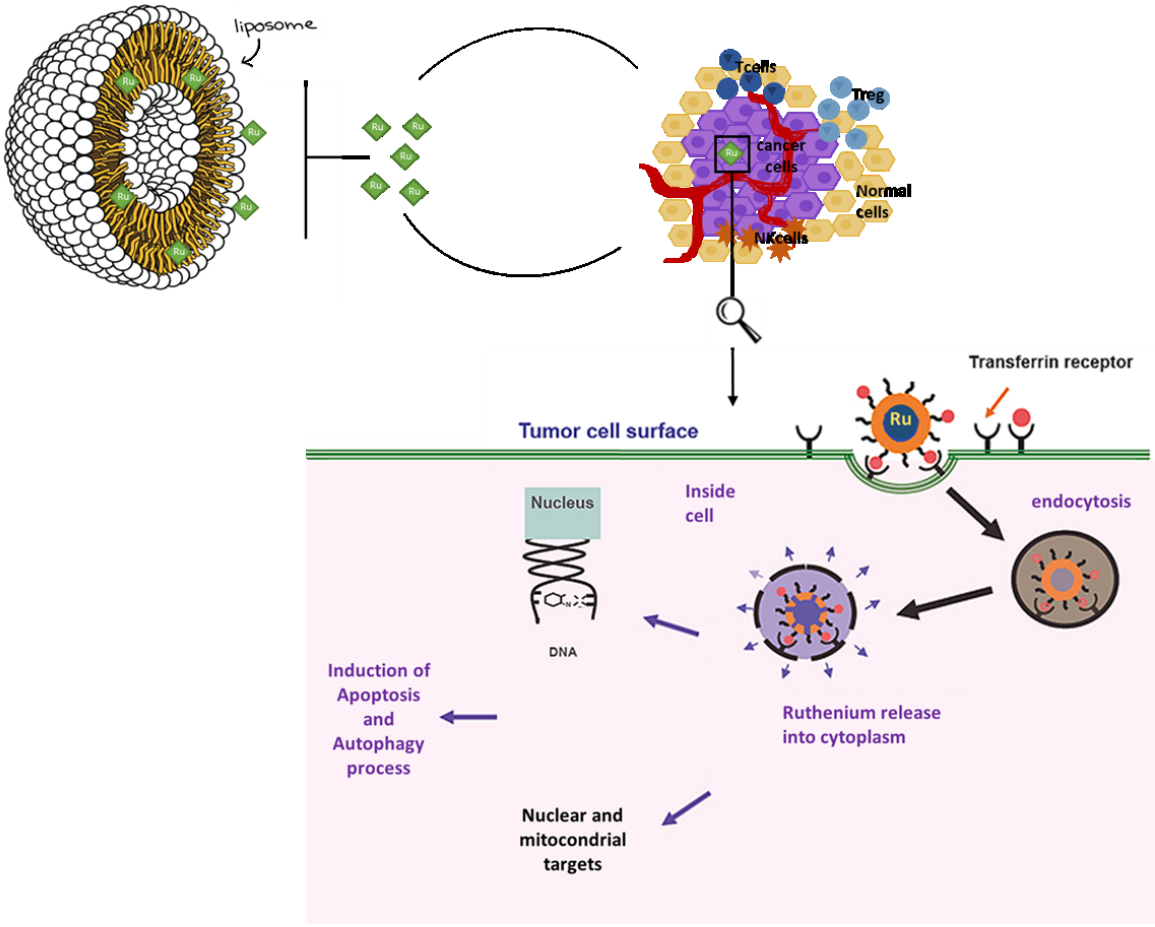

Figure 37. Mechanism of action of ruthenium-based nucleolipidic nanosystems, assumed on the basis of a series of experimental evidences. From the selective cellular uptake in the tumor microenvironment to the possible interaction with specific mitochondrial and nuclear biomolecular targets, responsible for the activation of specific programmed cell death pathways.

References

A

Alessio, E. Thirty years of the drug candidate NAMI-A and the myths in the field of ruthenium anticancer compounds: a personal perspective. Eur J Inorg Chem. 2017. 1549-1560.

Arriaga LR., Lopez-Montero I, Monroy F, Orts-Gil G, Farago B, Hellweg T. Stiffening effect of cholesterol on disordered lipid phases: a combined neutron spin echo þ dynamic light scattering analysis of the bending elasticity of large unilamellar vesicles. Biophys J 2009;96:3629e37.

B

Badino GR, Novelli A, Girardi C, Di Carlo F. Evidence for functional beta-adrenoceptor subtypes in CG-5 breast cancer cell. Pharmacol Res. 1996 Apr-May;33(4-5):255-60.

Bai L. and Wang S. Targeting apoptosis pathways for new cancer therapeutics. Annu Rev Med. 2014;65:139-55. Epub 2013 Nov 4.

Barthelemy P, C. A. H. Prata, S. F. Filocamo, C. E. Immoos, B. W. Maynor, S. A. N. Hashmi, S. J. Lee and M. W. Grinstaff, Chem. Commun. Supramulecular assemblies of DNA with neutral nucleoside amphiphiles. (Cambridge, U. K.), 2005, 1261–1263.

Barthelemy P. Nucleoside-based lipids at work: from supramolecular assemblies to biological applications. CR Chim 2009;12:171e9.

Bellocq A., Antoine M, Flahault A, Philippe C, Crestani B, Bernaudin JF, Mayaud C, Milleron B, Baud L, Cadranel J. Neutrophil alveolitis in bronchioloalveolar carcinoma: induction by tumor-derived interleukin-8 and relation to clinical outcome. Am J Pathol. 1998 Jan;152(1):83-92.

Berndsen RH, Weiss A, Abdul UK, Wong TJ, Meraldi P, Griffioen AW, Dyson PJ,No wak-Sliwinska P. Combination of ruthenium(II)-arene complex [Ru(η(6)-p-cymene)Cl(2)(pta)] (RAPTA-C) and the epidermal growth factor receptor inhibitor erlotinib results in efficient angiostatic and antitumor activity. Sci Rep. 2017 Feb 22;7:43005.

Bohlius J., Schmidlin K, Brillant C, Schwarzer G, Trelle S, Seidenfeld J, Zwahlen M, Clarke M, Weingart O, Kluge S, Piper M, Rades D, Steensma DP, Djulbegovic B, Fey MF, Ray-Coquard I, Machtay M, Moebus V, Thomas G, Untch M, Schumacher M, Egger M, Engert A. Recombinant human erythropoiesis-stimulating agents and mortality in patients with cancer: a meta-analysis of randomised trials. Lancet. 2009 May 2;373(9674):1532-42.

Brines M. and Cerami A. Emerging biological roles for erythropoietin in the nervous system. Nat Rev Neurosci. 2005 Jun;6(6):484-94. Review. PubMed PMID:15928718.

C

Cailleau R, Olivé M, Cruciger QV. Long-term human breast carcinoma cell lines of metastatic origin: preliminary characterization. In Vitro. 1978 Nov;14(11):911-5

Carlson, R.W.; Henderson, I.C. Sequential hormonal therapy for metastatic breast cancer after adjuvant tamoxifen or anastrozole. Breast Cancer Res. Treat. 2003, 80, 19–26.

Chang, M. Tamoxifen resistance in breast cancer. Biomol. Ther. 2012, 20, 256–267.

Chavez KJ, Garimella SV, Lipkowitz S. Triple negative breast cancer cell lines: one tool in the search for better treatment of triple negative breast cancer. Breast Dis. 2010;32(1-2):35-48.

Chen J., Chen, L., Liao, S., Zheng, K. & Ji, L. A theoretical study on the hydrolysis process of the antimetastatic ruthenium(III) complex NAMI-A. J Phys Chem B. 111, 7862–1869 (2007).

Cohen G. M. Caspases: the executioners of apoptosis. Biochem J 326 (Pt 1), 1–16. 1997.

Cravedi P, Remuzzi G, Ruggenenti P. Rituximab in primary membranous nephropathy: first-line therapy, why not? Nephron Clin Pract. 2014;128(3-4):261-9.

D

Dasari S. and Tchounwou, P. B. Cisplatin in cancer therapy: molecular mechanisms of action. Eur J Pharmacol. 740, 364–378 (2014).

Dawood, S. Triple-negative breast cancer: Epidemiology and management options. Drugs 2010, 70, 2247–2258.

De Maria R, Grignani F, Testa U, Valtieri M, Ziegler BL, Peschle C. Gene regulation in normal and leukaemic progenitor/stem cells. Haematologica. 1999 Jun;84 Suppl EHA-4:8-10.

Divac Rankov A, Ljujić M, Petrić M, Radojković D, Pešić M, Dinić J. Targeting autophagy to modulate cell survival: a comparative analysis in cancer, normal and embryonic cells. Histochem Cell Biol. 2017 Nov;148(5):529-544.

Dragutan I., Dragutan, V., Demonceau, A. Editorial of Special Issue Ruthenium Complex: The Expanding Chemistry of the Ruthenium Complexes. Molecules. 20, 17244–17274 (2015).

E

Elliott SJ, Wilf P, Walter RC, Merritts DJ. Subfossil leaves reveal a new upland hardwood component of the pre-European Piedmont landscape,Lancaster County, Pennsylvania. PLoS One. 2013; 8(11):e79317.

Elmore S. Apoptosis: a review of programmed cell death .Toxicol Pathol. 2007 Jun;35(4):495-516.

Eschbach JW., Egrie JC., Downing MR., Browne JK., Adamson JW. Correction of the anemia of end-stage renal disease with recombinant human erythropoietin. Results of a combined phase I and II clinical trial. N Engl J Med. 1987 Jan 8;316(2):73-8.

Esposito F., Libertini S., Franco R., Abagnale A., Marra L., Portella G., Chieffi P. Aurora B expression in post-puberal testicular germ cell tumours. J Cellular Physiology 221, 435–439 (2009).

Eva Steliarova Foucher, MarkO'Callaghan, JacquesFerlay, EricMasuyer, StefanoRosso, DavidForman, FreddieBray, HarryComber. The European Cancer Observatory: A new data resource. European Journal of cancer. https://doi.org/10.1016/j.ejca. 2014.01.027

F

Feldman L., Wang Y, Rhim JS, Bhattacharya N, Loda M, Sytkowski AJ. Erythropoietin stimulates growth and STAT5 phosphorylation in human prostate epithelial and prostate cancer cells. Prostate. 2006 Feb 1;66(2):135-45.

Fengsrud M, Roos N, Berg T, Liou W, Slot JW, Seglen PO. Ultrastructural and immunocytochemical characterization of autophagic vacuoles in isolated hepatocytes: effects of vinblastine and asparagine on vacuole distributions. Exp Cell Res. 1995 Dec;221(2):504–519.

Ferlay J., E. Steliarova-Foucher, J. Lortet-ieulent, S. Rosso, J.W.W. Coebergh, H. Comber, D. Forman, F. Bray. Cancer incidence and mortality patterns in Europe: Estimates for 40 countries in 2012. European Journal of cancer https://doi.org/10.1016/j.ejca.2012.12.027

Ferlay J., Soerjomataram I., Dikshit R., Eser S., Mathers C., Rebelo M., Parkin D.M., Forman D., Bray F. Cancer incidence and mortality worldwide: Sources, methods and major patterns in globocan 2012. Int. J. Cancer 2015, 136, E359–E386.

Filmus J, Pollak MN, Cailleau R, Buick RN. MDA-468, a human breast cancer cell line with a high number of epidermal growth factor (EGF) receptors, has an amplified EGF receptor

gene and is growth inhibited by EGF. Biochem Biophys Res Commun. 1985 Apr 30;128(2):898-905

Fimia GM and Piacentini M. Regulation of autophagy in mammals and its interplay with apoptosis. Cell Mol Life Sci. 2010 May;67(10):1581-8.

Fiorito F, Irace C., Di Pascale A., Colonna A., Iovane G., Santamaria R., De Martino L. 2,3,7,8-Tetrachlorodibenzo-p-dioxin promotes BHV-1 infection in mammalian cells by interfering with iron homeostasis regulation. PLoS One. 8, e58845 (2013).

Fortini M., Berti D, Baglioni P, Ninham BW. Specific anion effects on the aggregation properties of anionic nucleolipids. Curr Opin Colloid Interface Sci 2004;9:168e72.

Foulkes, W.D.; Smith, I.E.; Reis-Filho, J.S. Triple-negative breast cancer. N. Engl. J. Med. 2010, 363, 1938–1948.

Frasca D., Ciampa J, Emerson J, Umans RS, Clarke MJ. Effects of hypoxia and transferrin on toxicity and DNA binding of ruthenium antitumor agents in hela cells. Met Based Drugs. 1996;3(4):197-209.

Fridlender ZG., Sun J, Kim S, Kapoor V, Cheng G, Ling L, Worthen GS, Albelda SM. Polarization of tumor-associated neutrophil phenotype by TGF-beta: "N1" versus "N2" TAN. Cancer Cell. 2009 Sep 8;16(3):183-94.

G

García-Aranda M, and Redondo M. Protein Kinase Targets in Breast Cancer. Int J Mol Sci. 2017 Nov 27;18(12). pii: E2543.

Giordano PA, Wyroba E, Bottiroli G. Internalization of cycloheptaamylose-dansyl chloride complex during labelling of surface membrane in living Paramecium aurelia cells. Basic Appl Histochem. 1985;29(2):121-33.

Gong C, Bauvy C, Tonelli G, Yue W, Deloménie C, Nicolas V, Zhu Y, Domergue V, Marin-Esteban V, Tharinger H, Delbos L, Gary-Gouy H, Morel AP, Ghavami S, Song E, Codogno P, Mehrpour M. Beclin 1 and autophagy are required for the tumorigenicity of breast cancer stem-like/progenitor cells. Oncogene. 2013;32(18):2261-72, 2272e.1-11.

Gras Navarro A, Björklund AT, Chekenya M. Therapeutic potential and challenges of natural killer cells in treatment of solid tumors. Front Immunol. 2015 Apr 29;6:202. doi: 10.3389/fimmu.2015.00202. eCollection 2015.

Grimaldi A, Santini D, Zappavigna S, Lombardi A, Misso G, Boccellino M, Desiderio V, Vitiello PP, Di Lorenzo G, Zoccoli A, Pantano F, Caraglia M. Antagonistic effects of chloroquine on autophagy occurrence potentiate the anticancer effects of everolimus on renal cancer cells. Cancer Biol Ther. 2015;16(4):567-79.

Grivennikov SI., Greten FR, Karin M. Immunity, inflammation, and cancer. Cell. 2010 Mar 19;140(6):883-99.

Groessl, M. et al. Structure-activity relationships for NAMI-A-type complexes (HL)[trans-RuCl4L(S-dmso)ruthenate(III)] (L = imidazole, indazole, 1,2,4-triazole, 4-amino-1,2,4-triazole, and 1-methyl-1,2,4-triazole): aquation, redox properties, protein binding, and antiproliferative activity. J Med Chem. 50, 2185–2193 (2007).

H

Hartinger CG., Jakupec MA, Zorbas-Seifried S, Groessl M, Egger A, Berger W, Zorbas H, Dyson PJ, Keppler BK. KP1019, a new redox-active anticancer agent--preclinical development and results of a clinical phase I study in tumor patients. Chem Biodivers. 2008 Oct;5(10):2140-55.

Henke M, Mattern D, Pepe M, Bézay C, Weissenberger C, Werner M, Pajonk F. Do erythropoietin receptors on cancer cells explain unexpected clinical findings? J Clin Oncol. 2006 Oct 10;24(29):4708-13. Erratum in: J Clin Oncol. 2007 Apr 10;25(11):1457.

Henke M., Laszig R, Rübe C, Schäfer U, Haase KD, Schilcher B, Mose S, Beer KT, Burger U, Dougherty C, Frommhold H. Erythropoietin to treat head and neck cancer patients with anaemia undergoing radiotherapy: randomised, double-blind, placebo-controlled trial. Lancet. 2003 Oct 18;362(9392):1255-60.

Hodges VM., Rainey S, Lappin TR, Maxwell AP. Pathophysiology of anemia and erythrocytosis. Crit Rev Oncol Hematol. 2007 Nov;64(2):139-58. Epub 2007 Jul 25.

Holliday, D. L. and Speirs, V. Choosing the right cell line for breast cancer research. Breast Cancer Res. 13, 215 (2011).

Holohan, C., Van Schaeybroeck, S., Longley, D. B. & Johnston, P. G. Cancer drug resistance: an evolving paradigm. Nat Rev Cancer. 13, 714–726 (2013).

Hui L. and Chen Y. Tumor microenvironment: Sanctuary of the devil. Cancer Lett. 2015 Nov 1;368(1):7-13. doi: 10.1016/j.canlet.2015.07.039. Epub 2015 Aug 11.

Hutchinson L. Breast cancer: challenges, controversies, breakthroughs. Nat Rev Clin Oncol. 7, 669–670 (2010).

I

Igney FH., Krammer PH. Immune escape of tumors: apoptosis resistance and tumor counterattack. J Leukoc Biol. 2002 Jun;71(6):907-20.

Irace C., Misso G, Capuozzo A, Piccolo M, Riccardi C, Luchini A, Caraglia M, Paduano L, Montesarchio D, Santamaria R. Antiproliferative effects of ruthenium-based nucleolipidic nanoaggregates in human models of breast cancer in vitro: insights into their mode of action. Sci Rep. 2017 Mar 28;7:45236.

J

Jelkmann W. Control of erythropoietin gene expression and its use in medicine. Methods Enzymol. 2007;435:179-97.

Kang C and Avery L. To be or not to be, the level of autophagy is the question: dual roles of autophagy in the survival response to starvation. Autophagy. 2008 Jan;4(1):82-4. Epub 2007 Oct 12.

Kapitza S., Pongratz M, Jakupec MA, Heffeter P, Berger W, Lackinger L, Keppler BK, Marian B. Heterocyclic complexes of ruthenium(III) induce apoptosis in colorectal carcinoma cells. J Cancer Res Clin Oncol. 2005 Feb;131(2):101-10. Epub 2004 Oct 16.

Killar L., MacDonald G, West J, Woods A, Bottomly K. Cloned, Ia-restricted T cells that do not produce interleukin 4(IL 4)/B cell stimulatory factor 1(BSF-1) fail to help antigen-specific B cells. J. Immunol. 1987;138:1674–1679.

Kim J.; Kundu, M.; Viollet, B.; Guan, K.L. AMPK and mTOR regulate autophagy through direct. Phosphorylation of Ulk1. Nat. Cell Biol. 2011, 13, 132–141.

Kiraz, Y., Adan, A., Kartal Yandim, M. & Baran, Y. Major apoptotic mechanisms and genes involved in apoptosis. Tumour Biol. 37,471–486 (2016).

Klionsky DJ and Ohsumi Y. Vacuolar import of proteins and organelles from the cytoplasm. Annu Rev Cell Dev Biol. 1999;15:1-32.

Koceva-Chyła A., Matczak K, Hikisz MP, Durka MK, Kochel MK, Süss-Fink G, Furrer J., Kowalski K. Insights into the in vitro Anticancer Effects of Diruthenium-1. ChemMedChem. 11, 2171–2187 (2016).

Komeda S. and Casini A. Next-generation anticancer metallodrugs. Curr Top Med Chem. 12, 219–235 (2012).

Krieg M, Srichai MB, Redmond RW. Photophysical properties of 3,3'-dialkylthiacarbocyanine dyes in organized media: unilamellar liposomes and thin polymer films. Biochim Biophys Acta. 1993 Sep 19;1151(2):168-74.

Krutzfeldt J, N. Rajewsky, R. Braich, G. Rajeev Kallanthottathil, T. Tuschl,M.Manoharan andM. Stoffel, Nature, 2005, 438, 685–689.

L

Lacroix, M. and Leclercq, G. Relevance of breast cancer cell lines as models for breast tumours: an update. Breast Cancer Res Treat. 83, 249–289 (2004).

Lainé A. L. and Passirani, C. Novel metal-based anticancer drugs: a new challenge in drug delivery. Curr Opin Pharmacol. 12, 420–6 (2012).

Lambertini M, Pondé NF, Solinas C, de Azambuja E. Adjuvant trastuzumab: a 10-year overview of its benefit. Expert Rev Anticancer Ther. 2017 Jan;17(1):61-74. Epub 2016 Dec 5.

Lasic DD.; Woodle, M. C.; Martin, F. J.; Valentincic, T. Phasebehavior of stealth-lipid-lecithin mixtures. Period. Biol. 1991, 93, 287−290.

Lee MS., Dees EC, Wang AZ. Nanoparticle-Delivered Chemotherapy: Old Drugs in New Packages. Oncology (Williston Park). 2017 Mar 15;31(3):198-208.

Lelekakis M, Moseley JM, Martin TJ, Hards D, Williams E, Ho P, Lowen D, Javni J, Miller FR, Slavin J, Anderson RL. A novel orthotopic model of breast cancer metastasis to bone. Clin Exp Metastasis. 1999 Mar;17(2):163-70.

Licona C., Spaety M., Capuozzo A., Ali M., Santamaria R., Armant O., Delalande F., Van Dorsselaer A., Cianferani S., Spencer J., Pfeffer M., Mellitzer G., Gaiddon C. A ruthenium anticancer compound interacts with histones and impacts differently on epigenetic and death pathways compared to cisplatin. Oncotarget. 8, 2568–2584 (2017).

Littlewood TJ., Cella D, Nortier JW; Epoetin Alfa Study Group. Erythropoietin improves quality of life. Lancet Oncol. 2002 Aug;3(8):459-60.

Liu J. and Itoh J. Kinetic determination of cysteine on flow injection system by utilizing catalytic complexation reaction of Cu(II) with 5,10,15,20-tetrakis (4-N-trimethylammino-phenyl) porphyrin. Talanta. 2006 Nov 15;70(4):791-6.

Luo S. and Rubinsztein, D.C. Apoptosis blocks Beclin 1-dependent autophagosome synthesis: An effect rescued by Bcl-xL. Cell Death Differ. 2010, 17, 268–277.

M

Mabrey S, Mateo PL, Sturtevant JM. High-sensitivity scanning calorimetric study of mixtures of cholesterol with dimyristoyl- and dipalmitoylphosphatidylcholines. Biochemistry. 1978 Jun 13;17(12):2464-8.

Mangiapia G, D'Errico G, Simeone L, Irace C, Radulescu A, Di Pascale A, Colonna A, Montesarchio D, Paduano L. Ruthenium-based complex nanocarriers for cancer therapy. Biomaterials. 2012 May;33(14):3770-82

Mangiapia G, D'Errico G, Simeone L, Irace C, Radulescu A, Di Pascale A, Colonna A, Montesarchio D, Paduano L. Ruthenium-based complex nanocarriers for cancer therapy. Biomaterials. 2012 May;33(14):3770-82.

Mao C., T. H. LaBean, J. H. Reif and N. C. Seeman, Nature, 2000,407, 493–496.

70. Marra L, Cantile M, Scognamiglio G, Perdonà S, La Mantia E, Cerrone M,Gigantino V, Cillo C, Caraglia M, Pignata S, Facchini G, Botti G, Chieffi S, Chieffi P, Franco R . Deregulation of HOX B13 expression in urinary bladder cancer progression. Curr Med Chem. 20, 833–839 (2013).

Martinvalet D, Zhu P, Lieberman J.Granzyme A induces caspase-independent mitochondrial damage, a required first step for apoptosis. Immunity. 2005 Mar;22(3):355-70.

Mazuryk O, Kurpiewska K, Lewiński K, Stochel G, Brindell M. Interaction of apo-transferrin with anticancer ruthenium complexes NAMI-A and its reduced form. J Inorg Biochem. 2012 Nov;116:11-8.

Mazuryk O., Kurpiewska K., Lewinski K., Stochel G. and Brindell M. “Interaction of apo-transferrin with anticancer ruthenium complexes NAMI-A and its reduced form.” J Inorg Biochem. 116, 11-18, 2012.

McQuitty RJ. Metal-based drugs. Sci Prog. 2014;97(Pt 1):1-19.

Meijer AJ, Codogno P. Regulation and role of autophagy in mammalian cells. Int J Biochem Cell Biol. 2004 Dec;36(12):2445-62.

Miller, S.M.; Goulet, D.R.; Johnson, G.L. Targeting the breast cancer kinome. J. Cell, Physiol. 2017, 232, 53–60.

Miniaci MC, Irace C, Capuozzo A, Piccolo M, Di Pascale A, Russo A, Lippiello P, Lepre F, Russo G, Santamaria R Cysteine Prevents the Reduction in Keratin Synthesis Induced by Iron Deficiency in Human Keratinocytes. J Cell Biochem. 117, 402–412 (2016).

Misso G., Giuberti G, Lombardi A, Grimaldi A, Ricciardiello F, Giordano A,Tagliaferri P, Abbruzzese A, Caraglia M. Pharmacological inhibition of HSP90 and ras activity as a new strategy in the treatment of HNSCC. J Cell Physiol. 228, 130–141 (2013).

Mizushima N. and Komatsu M. Autophagy: renovation of cells and tissues. Cell 147 728–741.

Mizushima N., Yoshimori T., Ohsumi Y. (2011). The role of Atg proteins in autophagosome formation. Annu. Rev. Cell Dev. Biol. 27 107–132.

Montesarchio D, Mangiapia G, Vitiello G, Musumeci D, Irace C, Santamaria R, D'Errico G, Paduano L. A new design for nucleolipid-based Ru(III) complexes as anticancer agents. Dalton Trans. 2013 Dec 28;42(48):16697-708.

Montesarchio D., G. Mangiapia, G. Vitiello, D. Musumeci, C. Irace, R. Santamaria, G. D'Errico, L. Paduano. A new design for nucleolipid-based Ru(III) complexes as anticancer agents. Dalton Transactions 2013; 42(48), 16697-16708.

Mosmann TR, Cherwinski H, Bond MW, Giedlin MA, Coffman RL. Two types of murine helper T cell clone. I. Definition according to profiles of lymphokine activities and secreted proteins. J. Immunol. 1986;136:2348–2357.

Mühlgassner G., Bartel C., Schmid W. F., Jakupec M. A., Arion V. B. and Keppler B. K. Biological activity of ruthenium and osmium arene complexes with modified paullones in human cancer cells. J Inorg Biochem. 116, 180-187, 2012.

Musumeci D, Rozza L, Merlino A, Paduano L, Marzo T, Massai L, Messori L, Montesarchio D. Interaction of anticancer Ru(III) complexes with single stranded and duplex DNA model systems. Dalton Trans. 44, 13914–13925 (2015).

N

Nairz M, Haschka D, Dichtl S, Sonnweber T, Schroll A, Aßhoff M, Mindur JE, Moser PL, Wolf D, Swirski FK, Theurl I, Cerami A, Brines M, Weiss G. Cibinetide dampens innate immune cell functions thus ameliorating the course of experimental colitis. Sci Rep. 2017 Oct 12;7(1):13012.

Nairz M, Schroll A, Moschen AR, Sonnweber T, Theurl M, Theurl I, Taub N, Jamnig C, Neurauter D, Huber LA, Tilg H, Moser PL, Weiss G. Erythropoietin contrastingly affects bacterial infection and experimental colitis by inhibiting nuclear factor-κB-inducible immune pathways. Immunity. 2011 Jan 28;34(1):61-74.

Natoli C, Sica G, Natoli V, Serra A, Iacobelli S. Two new estrogen-supersensitive variants of the MCF-7 human breast cancer cell line. Breast Cancer Res Treat. 1983;3:23–32

Ngabire D, Kim GD. Autophagy and Inflammatory Response in the Tumor Microenvironment. Int J Mol Sci. 2017 Sep 20;18(9). pii: E2016.

Nowak-Sliwinska P., J. R. van Beijnum, A. Casini, A. A. Nazarov, G. Wagnières, H. van den Bergh, P. J. Dyson and A. W. Griffioen, J. Med. Chem., 2011, 54, 3895–3902

O

Okamura M., Hashimoto, K., Shimada, J. & Sakagami, H. Apoptosis-inducing activity of cisplatin (cDDP) against human hepatoma and oral squamous cell carcinoma cell lines. Anticancer Res. 24, 655–661 (2004).

Okazaki T, Ebihara S, Asada M, Yamanda S, Niu K, Arai H. Erythropoietin promotes the growth of tumors lacking its receptor and decreases survival of tumor-bearing mice by enhancing angiogenesis. Neoplasia. 2008 Sep;10(9):932-9.

Olivier Renier, Connor Deacon-Price, Joannes E. B. Peters, Kunsulu Nurekeyeva, Catherine Russon, Simba Dyson, Siyabonga Ngubane, Judith Baumgartner, Paul J. Dyson, Tina

Riedel, Haleden Chiririwa and Burgert Blom. Synthesis and In Vitro (Anticancer) Evaluation of η6-Arene Ruthenium Complexes Bearing Stannyl Ligands. Inorganics 2017.

Onda M, K. Yoshihara, H. Koyano, K. Ariga and T. Kunitake, J. Am. Chem. Soc., 1996, 118, 8524–8530.

P

Packer M, Xie Y, Levine B. Decreased BECN1 mRNA Expression in Human Breast Cancer is Associated with Estrogen Receptor-Negative Subtypes and Poor Prognosis. EBioMedicine. 2015 Mar;2(3):255-263.

Palermo G., Magistrato A., Riedel T., von Erlach T., Davey C., Dyson P., Rothlisberger U. Fighting Cancer with Transition Metal Complexes: From Naked DNA to Protein and Chromatin Targeting Strategies. ChemMedChem. 11, 1199–1210 (2016).

Pessoa J. C. and Tomaz, I. Transport of therapeutic vanadium and ruthenium complexes by blood plasma components. Curr Med Chem. 17, 3701–3738 (2010).

Petitjean A., R. G. Khoury, N. Kyritsakas and J.-M. Lehn, J. Am. Chem. Soc., 2004, 126, 6637–6647.

Petrelli F., Barni, S., Bregni, G., de Braud, F. & Di Cosimo, S. Platinum salts in advanced breast cancer: a systematic review and metaanalysis of randomized clinical trials. Breast Cancer Res Treat. 160, 425–437 (2016).

Prove, A.; Dirix, L. Neratinib for the treatment of breast cancer. Expert Opin. Pharmacother. 2016, 17, 2243–2248.

Q

Qian C., Wang JQ, Song CL, Wang LL, Ji LN, Chao H al. The induction of mitochondria-mediated apoptosis in cancer cells by ruthenium(II) asymmetric complexes. Metallomics. 5, 844–854 (2013).

R

Rademaker-Lakhai JM, van den Bongard D, Pluim D, Beijnen JH, Schellens JHClin. A Phase I and pharmacological study with imidazolium-trans-DMSO-imidazole-tetrachlororuthenate, a novel ruthenium anticancer agent. Cancer Res. 2004 Jun 1;10(11):3717-27.

Rai N. K., Tripathi, K., Sharma, D., and Shukla, V. K. Apoptosis: a basic physiologic process in wound healing. Int J Low Extrem Wounds 4, 138–44. 2005.

Ravera, M., Baracco, S., Cassino, C., Zanello, P. & Osella, D. Appraisal of the redox behaviour of the antimetastatic ruthenium(III) complex [ImH][RuCl(4)(DMSO)(Im)], NAMI-A. Dalton Trans. 15, 2347–51. 2004.

Riccardi C., Musumeci, D., Irace, C., Paduano, L. & Montesarchio, D. Ru(III) complexes for anticancer therapy: the importance of being nucleolipidic. Eur. J. Org. Chem. 7, 1100–1119. 2017.

Romao S, Münz C. LC3-associated phagocytosis. Autophagy. 2014 Mar;10(3):526-8.

Rosemeyer H., Chem. Biodiversity, 2005, 2, 977–1062.

Russo, A. et al. Regulatory role of rpL3 in cell response to nucleolar stress induced by Act D in tumor cells lacking functional p53. Cell Cycle 15, 41–51 (2016).

S

Sanna B., M. Debidda, G. Pintus, B. Tadolini, A. M. Posadino, F. Bennardini, G. Sava and C. Ventura, Arch. Biochem. Biophys., 2002, 403, 209–218.

Satya-Prakash, K.L., Pathak, S., Hsu, T.C., Olive, M. and Cailleau, R. Cytogenetic analysis on eight human breast tumor cell lines: high frequencies of 1q, 11q and HeLa-like marker chromosomes. Cancer Genet Cytogenet. 1981:3, 61-73.

Sava G., and Bergamo A. Drug control of solid tumour metastases: a critical view. Anticancer Res. 19, 1117-1124, 1999.

Sava G., Bergamo A., Zorzet S., Gava B., Casarsa C., Cocchietto M., et al. Influence of chemical stability on the activity of the antimetastasis ruthenium compound NAMI-A. Eur J Cancer. 38, 427-35, 2002.

Shamran H, Ali SH, Ali M, Al-Mayah Q, Jasim EA. E-Cadherin Gene Polymorphisms and Susceptibility to Urolithiasis in Iraqi Children. Nephrology (Carlton). 2017 Oct 20.

Segovia-Mendoza, M.; Gonzalez-Gonzalez, M.E.; Barrera, D.; Diaz, L.; Garcia-Becerra, R. Efficacy and mechanism of action of the tyrosine kinase inhibitors gefitinib, lapatinib and neratinib in the treatment of HER2-positive breast cancer: Preclinical and clinical evidence. Am. J. Cancer Res. 2015, 5, 2531–2561. 20.

Simeone L, Mangiapia G, Vitiello G, Irace C, Colonna A, Ortona O, Montesarchio D, Paduano L. Cholesterol-based nucleolipid-ruthenium complex stabilized by lipid aggregates for antineoplastic therapy. Bioconjug Chem. 2012 Apr 18;23(4):758-70.

Simeone L., Mangiapia G., Irace C., Di Pascale A., Colonna A., Ortona O., De Napoli L., Montesarchio D. and Paduano L. Nucleolipid nanovectors as molecular carriers for potential applications in drug delivery. Mol Biosyst. 7(11), 3075-86, 2011.

Sinclair AM, Coxon A, McCaffery I, Kaufman S, Paweletz K, Liu L, Busse L, Swift S, Elliott S, Begley CG. Functional erythropoietin receptor is undetectable in endothelial, cardiac, neuronal, and renal cells. Blood. 2010 May 27;115(21):4264-72.

Solinas C, Gombos A, Latifyan S, Piccart-Gebhart M, Kok M, Buisseret L. Targeting immune checkpoints in breast cancer: an update of early results. ESMO Open. 2017 Nov 14;2(5):e000255.

Stockmann C, Schadendorf D, Klose R, Helfrich I. The impact of the immune system on tumor: angiogenesis and vascular remodeling. Front Oncol. 2014 Apr 8;4:69.

Sturm I., Papadopoulos S, Hillebrand T, Benter T, Lück HJ, Wolff G, Dörken B,Daniel PT. Impaired BAX protein expression in breast cancer: mutational analysis of the BAX and the p53 gene. Int J Cancer. 87,517–521 (2000).

T

Tamimi, R.M.; Colditz, G.A.; Hazra, A.; Baer, H.J.; Hankinson, S.E.; Rosner, B.; Marotti, J.; Connolly, J.L.; Schnitt, S.J.; Collins, L.C. Traditional breast cancer risk factors in relation to molecular subtypes of breast cancer. Breast Cancer Res. Treat. 2012, 131, 159–167.

Tang H, Sebti S, Titone R, Zhou Y, Isidoro C, Ross TS, Hibshoosh H, Xiao G,

Tanida I, Ueno T, Kominami E. LC3 and Autophagy. Methods Mol Biol. 2008;445:77-88.

Towers CG, Thorburn A. Therapeutic Targeting of Autophagy. EBioMedicine. 2016 Dec; 14:15-23.

U

Um M, Gross AW, Lodish HF. A "classical" homodimeric erythropoietin receptor is essential for the antiapoptotic effects of erythropoietin on differentiated neuroblastoma SH-SY5Y and pheochromocytoma PC-12 cells. Cell Signal. 2007 Mar;19(3):634-45

V

Vaccaro M, Del Litto R, Mangiapia G, Carnerup AM, D'Errico G, Ruffo F, Paduano L. Lipid based nanovectors containing ruthenium complexes: a potential route in cancer therapy. Chem Commun (Camb). 2009 Mar 21;(11):1404-6.

Velders A. H., A. Bergamo, E. Alessio, E. Zangrando, J. G. Haasnoot, C. Casarsa, M. Cocchietto, S. Zorzet, G. Sava, J. Med. Chem. 2004, 47, 1110–1121.

Vitiello G., Luchini, A., D'Errico, G., Santamaria, R., Capuozzo, A., Irace, C., Montesarchio, D., Paduano, L. Cationic liposomes as efficient nanocarriers for the drug delivery of an anticancer cholesterol-based ruthenium complex. Journal of Materials Chemistry B. 2015. 3; 3011-3023.

Vitlic A, Lord JM, Phillips AC. Stress, ageing and their influence on functional, cellular and molecular aspects of the immune system. Age (Dordr). 2014 Jun;36(3):9631.

W

Webb MI, Chard RA, Al-Jobory YM, Jones MR, Wong EW, Walsby CJ. Pyridine analogues of the antimetastatic Ru(III) complex NAMI-A targeting non-covalent interactions with albumin. Inorg Chem. 2012 Jan 16;51(2):954-66.

Weiss A., Robert H. Berndsen , Maxime Dubois , Cristina Müller , Roger Schibli , Arjan W. Griffioen , Paul J. Dyson and Patrycja Nowak-Sliwinska In vivo anti-tumor activity of the organometallic ruthenium(II)-arene complex [Ru(η6-p-cymene)Cl2(pta)] (RAPTA-C) in human ovarian and colorectal carcinomas. Chem. Sci., 2014, 5, 4742-4748

Wiethoff CM, Smith JG, Koe GS, Middaugh CR. The potential role of proteoglycans in cationic lipid-mediated gene delivery. Studies of the interaction of cationic lipid-DNA complexes with model glycosaminoglycans. J Biol Chem. 2001 Aug 31;276(35):32806-13.

Y

Yang L. and Zhang Y. Tumor-associated macrophages: from basic research to clinical application. J Hematol Oncol. 2017 Feb 28;10(1):58.

Yuan J. and Kroemer G. Alternative cell death mechanisms in development and beyond. Genes Dev. 2010 Dec 1;24(23):2592-602.

Zheng, J. H., Viacava Follis, A., Kriwacki, R. W. & Moldoveanu, T. Discoveries and controversies in BCL-2 protein-mediated apoptosis. FEBS J. 283, 2690–2700 (2016).

Z

Zhang, X.; Munster, P.N. New protein kinase inhibitors in breast cancer: Afatinib and neratinib. Expert Opin. Pharmacother. 2014, 15, 1277–1288.

Zhang, X.; Zhang, B.; Liu, J.; Liu, J.; Li, C.; Dong,W.; Fang, S.; Li, M.; Song, B.; Tang, B.; et al. Mechanisms of gefitinib-mediated reversal of tamoxifen resistance in MCF-7 breast cancer cells by inducing ER_re-expression. Sci. Rep. 2015, 5, 7835.

Zhu J, Yamane H, Paul WE. Differentiation of effector CD4 T cell populations. Annu Rev Immunol. 2010; 28:445-89.